

# Synthesis and Characterization of Conducting Polymer Actuators

by

Nathan A. Vandesteeg

B.S. Chemical Engineering  
Rice University, 2001

Submitted to the Department of Materials Science and Engineering  
in Partial Fulfillment of the Requirements for the Degree of

Doctor of Philosophy in Materials Science and Engineering

at the

MASSACHUSETTS INSTITUTE OF TECHNOLOGY

FEBRUARY 2007

© 2007 Massachusetts Institute of Technology. All rights reserved.

Signature of Author.....  
Department of Materials Science and Engineering  
September 29, 2006

Certified by .....  
Timothy M. Swager  
John D. MacArthur Professor of Chemistry  
Thesis Supervisor

Certified by .....  
Ian W. Hunter  
Hatsopoulos Professor of Mechanical Engineering  
Thesis Supervisor

Accepted by.....  
Samuel M. Allen  
Professor of Materials Science and Engineering  
Chairman, Department Committee on Graduate Students

# Synthesis and Characterization of Conducting Polymer Actuators

by

Nathan A. Vandesteeg

Submitted to the Department of Materials Science and Engineering on September 29<sup>th</sup>, 2006, in Partial Fulfillment of the Requirements for the Degree of Doctor of Philosophy in Materials Science and Engineering

## **ABSTRACT**

Conducting polymers are known to mechanically respond to electrochemical stimuli and have been utilized as linear actuators. To date, the most successful mechanism for actuation is ionic ingress and egress, though mechanisms based on conformational changes and molecular interactions have also been proposed. In the pursuit of new conducting polymer actuators it is necessary to design, synthesize, and characterize new materials, spanning scientific disciplines from synthetic chemistry to materials and mechanical engineering. As such, the topics of synthesis and characterization of new conducting polymers are discussed, highlighting developments in techniques and instrumentation. Actuation in poly(3,4-ethylenedioxythiophene), or PEDOT, and composites of PEDOT and carbon nanotubes is presented, demonstrating strains of 4.5% and strain rates of 0.2% per second with faster responses generated in carbon nanotube composites. Actuation in poly(3-hexylthiophene) is presented, demonstrating the observation of a novel actuation mechanism relating the potential of the polymer to the mechanical response. Further study of the actuation of polypyrrole at temperatures above 25°C is also discussed, in which response times decrease and magnitudes increase with temperature. Discrete time models of equivalent circuits and diffusion are utilized to predict conducting polymer actuator performance.

Thesis Supervisor: Timothy M. Swager  
Title: John D. MacArthur Professor of Chemistry

Thesis Supervisor: Ian W. Hunter  
Title: Hatsopoulos Professor of Mechanical Engineering

## Acknowledgements

The opportunities to thank the people who have helped me get to this point have been too few and far between. The daunting nature of the task, of getting it right, and the awkwardness and one-sidedness of the thanking usually requires a beer or two before I even try it. Unfortunately, after a few more beers, I'm more inclined to thank people, but it seems that the recipients sometimes find it less sincere or perhaps excessive. Nonetheless, I have mountains of people to thank and I'll try to list as many as I can here.

First off, I am indebted to Professors Tim Swager and Ian Hunter who have supported me, my research, and provided the laboratories of which many people dream and in which few have the opportunity to work. Second, to the numerous friends and colleagues who have helped along the way, I owe many thanks. Some, like John and Peter Madden, Patrick Anquetil, and Bruce Yu paved the way to make my research possible, though it took me plenty of time to understand what they had done just to take a few more steps. Others, like Rachel Pytel, Jocelyn Nadeau, Tim Fofonoff, and Angela Chen have had the arduous task of working with me and their help and discussions certainly fortified my knowledge and enriched my experience. A few others, like Bryan Schmid, Mike Del Zio, and Derek Rinderknecht know more about the excessive thanking I noted earlier and surely know already how much I have appreciated their help and friendship. And a very unfortunate few like Changsik Song, Hongwei Gu, Ivory Hills, Brad Holliday, and Professor Ali Shaikh had to patiently wait for my results after finally achieving their own synthetic successes. In addition, the entire casts of the Swager and Hunter groups during my stay have been enjoyable company and friendly colleagues with whom it has been my pleasure to work.

On a personal level, I have to thank my parents, Gregg and Marcia, who first stimulated my interest in science and math and taught me so much, including how to learn and to never stop. I also have to thank my sister, Michelle, whose support and friendship have helped me grow up ever since the day she left for college. I have been incredibly fortunate to have supportive grandparents throughout my time here though the distance between me and my family has made it harder for us to spend time together. And I have been fortunate to have so many friends in Boston, like Joe and Vanessa Bullard, and Jim and Julie Sullivan that it has become difficult to leave a place that feels so much like home.

And finally, I have to thank Lisa Buckey, who in her short time in my life has given me the motivation to graduate and helped set the goals that have become important in my life now that this last and most selfish goal is complete.

# Table of Contents

<b>Abstract.....</b>	<b>2</b>
<b>Acknowledgements .....</b>	<b>3</b>
<b>Preface.....</b>	<b>6</b>
<b>1. Introduction.....</b>	<b>7</b>
1.1 Conducting Polymers.....	7
1.2 Actuators .....	9
1.3 Synthesis .....	12
1.4 Characterization .....	14
1.5 Modeling.....	14
1.6 Outline.....	15
1.7 References.....	16
<b>2. Synthesis of Conducting Polymers .....</b>	<b>18</b>
2.1 Monomer Synthesis .....	19
2.2 Chemical Polymerization.....	22
2.3 Electrochemical Polymerization .....	23
2.3.1 Potentiostatic Polymerization .....	24
2.3.2 Galvanostatic Polymerization .....	27
2.3.3 Potentiodynamic Polymerization .....	28
2.3.4 Galvanodynamic Polymerization.....	34
2.4 Summary .....	35
2.5 Experimental.....	36
2.6 References.....	39
<b>3. Characterization of Conducting Polymers .....</b>	<b>40</b>
3.1 Electrical Characterization.....	40
3.2 Mechanical Characterization .....	45
3.3 Electrochemical Characterization .....	46
3.3.1 Cyclic Voltammetry.....	47
3.3.2 In-Situ Testing .....	48
3.3.3 Electrochemical Quartz Microbalance.....	51
3.3.4 Frequency Modulation Techniques.....	51
3.4 Summary .....	53
3.5 References.....	54
<b>4. Characterization of Conducting Polymer Actuators.....</b>	<b>55</b>
4.1 Systematic View .....	56
4.2 Isometric Testing .....	59
4.3 Isotonic Testing.....	61
4.4 Other Electrochemical Mechanical Tests .....	63
4.5 Summary .....	64
4.6 References.....	66
<b>5. Poly(3,4-ethylenedioxythiophene) Actuation.....</b>	<b>67</b>
5.1 Synthesis .....	67
5.2 Active Characterization .....	68
5.2.1 Actuation in Propylene Carbonate .....	68
5.2.2 Electrolyte Effects.....	71

5.3	Ionic Liquids as Salt and Solvent.....	72
5.4	Summary .....	75
5.5	References.....	76
<b>6.</b>	<b>Poly(3,4-ethylenedioxythiophene) and Carbon Nanotube Composites.....</b>	<b>78</b>
6.1	Synthesis .....	78
6.2	Passive Characterization .....	80
6.3	Actuation.....	82
6.3.1	Potential Triangle Wave Response .....	82
6.3.2	Potential Square Wave Response.....	84
6.4	Summary .....	86
6.5	References.....	88
<b>7.</b>	<b>Poly(3-hexylthiophene) Actuation .....</b>	<b>89</b>
7.1	Synthesis .....	90
7.2	Passive Characterization .....	91
7.3	Isotonic Characterization .....	92
7.4	Isometric Characterization .....	94
7.5	Potential Dependant Modulus.....	98
7.6	Unblended P3HT .....	99
7.7	Summary .....	101
7.8	References.....	102
<b>8.</b>	<b>Polypyrrole Actuation at Elevated Temperatures .....</b>	<b>103</b>
8.1	Experimental Techniques.....	104
8.2	Observations .....	105
8.3	Equivalent Circuit Modeling.....	109
8.4	Frequency Response Analysis .....	112
8.5	Summary .....	113
8.6	References.....	114
<b>9.</b>	<b>Conclusions.....</b>	<b>115</b>
9.1	The Design Cycle.....	115
9.1.1	Synthesis .....	116
9.1.2	Characterization .....	118
9.1.3	Actuation Testing.....	119
9.2	Contributions.....	121
9.3	Recommendations for Further Research.....	123
9.4	References.....	125
	<b>Appendix A .....</b>	<b>126</b>

## Preface

It is difficult to anticipate the types of questions that you will field upon brief acquaintance as a Materials Scientist until you try to be one. Being prepared for the obligatory, “What’s that?” is just a beginning. In my short time as a member of the community, I feel that my research has come to define what Materials Science is, at least to me, and certainly as representative in the case of polymer research. Working jointly in the Chemistry and Mechanical Engineering departments, it becomes clear that brilliant people can see the world very differently. And to some disappointment, they sometimes feel uncomfortable venturing across such academically defined boundaries. In the case of conducting polymer actuator research, it is paramount that a chemist has someone to test his materials and an engineer, someone to make hers. Yet, making and testing materials alone leaves much room for asking why one thing works or what if it were made a different way. These questions can be, and are, asked by successful researchers, but with understandably less enthusiasm considering the difficult challenges in meeting the initial collaborative goals. It would be easy to say that my job has been to ask these questions, and I have tried to do so. But, it has also been my job to help others ask them and realize that they *will* understand the answers.

As with much of my research, then, I write this to multiple audiences. In doing so, it becomes clear that some parts or chapters may frustrate people in communities that pride themselves on certain techniques and analysis. It is my hope in those circumstances that a patient reader will find more interesting information in a different section and that an impatient reader will jump to those sections directly. And it is my hope above all, that no one finds that all of the sections are uninformative.

Lastly, it is often said that new materials research is slow and I can’t think of a single colleague who would disagree. But saying that it cannot be done because it cannot be done today is more than cynicism. In conducting polymer actuator research, much of the inspiration comes from nature, specifically muscle tissue. And though we cannot make all of the materials and structures present in muscle tissue today, our very presence is all the proof that we need that it can be done. A scientist who says that progress is too slow to amount to anything will miss out on all of the leaps and bounds that have defined the discipline thus far. And a scientist who doesn’t ask questions for fear of not understanding the answer, should probably ask why he is a scientist in the first place.

# 1. Introduction

A tremendous number of articles, reviews, books, and theses have been written on conducting polymers, often incorporating different perspectives from Chemistry and Physics to Materials Science and Engineering as exemplified by the two lengthy handbooks of conducting polymers.<sup>1</sup> Although the various authors seek to describe essentially the same class of materials, a reading of all the literature would hardly give the reader that perspective. A closer look at one Faraday discussion section of the Chemical Society on charge transfer in polymeric systems from nearly two decades ago suggests that often from group to group and even within one research group two materials of the same composition rarely behave precisely the same way.<sup>2</sup> This observation has been made throughout my own research and in working with my colleagues. The difficulties posed by these variations should not be seen as insurmountable, however, since it is the goal of current research to improve repeatability and understanding. As is often done in this field, a look to nature for inspiration indicates that complexity, rather than simplicity, is often the evolutionary result. Indeed, had initial conducting polymer scientists sought to make something as complex as neurons rather than wires it is hard to imagine what progress would have been made in the short time since the first discovery. The same observation can be made in the case of muscle tissue, which demonstrates layers of complexity at length scales from nanometers to millimeters. If our objectives centered on synthetic muscle tissue rather than a performing replacement, current research might still be focused on the precise folding mechanism of actin and myosin. Instead, artificial muscle research has taken inspiration from nature and pursued a human invention, starting simple and finding materials difficult to characterize and understand. A better understanding of current materials and mechanisms will enable the addition of complexities that will be required to outperform nature's ubiquitous actuator.

## 1.1 Conducting Polymers

As a class of materials, conducting polymers share several characteristics, including macromolecular character and electrical transport properties. As is the case

with polyacetylene, the simplest conducting polymer structure, the electrical transport characteristics are obtained by placing the alternating carbon-carbon double bond structure directly on the backbone of the polymer. The subsequent electrical conductivity is often mistakenly visualized from resonance structures and the mobility of  $\pi$  electrons as depicted for polyacetylene in Figure 1.1a.

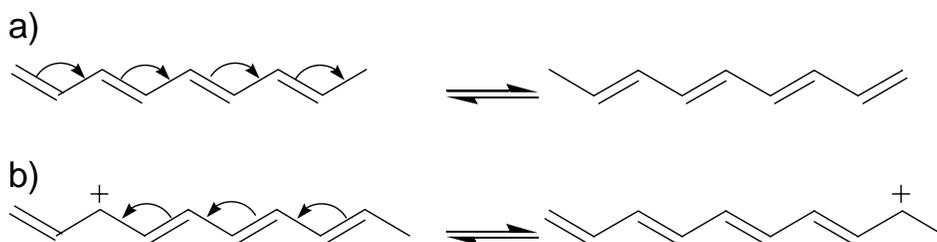


**Figure 1.1.** a) Polyacetylene structure and resonance of electronic states mistakenly attributed to conductivity. b) Polyacetylene showing the effect of dopant in conductivity. Compared to the structure in (a), the doped structure successfully transports charge across the polymer chain.

Conjugation alone, however, is not sufficient for conductivity. A dopant is required to alter the band structure of the semi-conducting polymer backbone. The defects caused by the dopant allow electrical transport either by hole or electron mobility, depicted in Figure 1.1b.<sup>3</sup> Furthermore, electrical conductivity measured in a laboratory requires a sample large enough to be manipulated and more than single chain electron transport. Thus, to be appreciated as a conducting polymer, a material must be made into a film or at least a coating. Indeed this subtlety delayed the advent of conducting polymer research by decades until a stable polyacetylene film could be obtained.<sup>3</sup> Despite the high conductivity of polyacetylene, stability issues have plagued its use and led to the development of conducting polymers based on five-member conjugated heterocycles. A sample of common conducting polymers is provided in Figure 1.2 with each polymer notably containing the alternating double bond structure inherent in conducting polymers. Other common conducting polymers can be based on six-member rings such as polyaniline and poly(para-phenylene) while synthetic organic techniques have broadened the library of possibilities to the limits of the imagination.



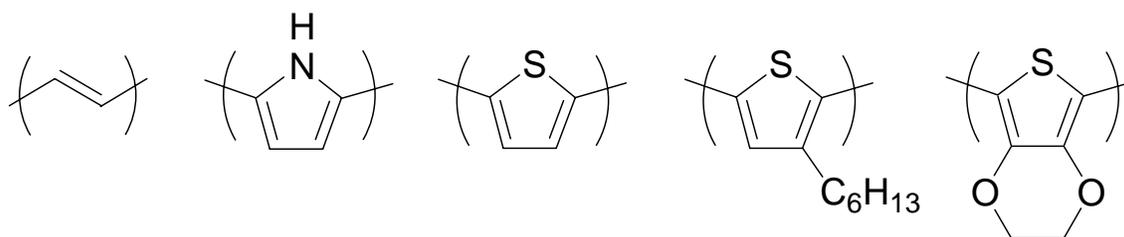


**Figure 1.2.** Common conducting polymers listed in order: polyacetylene, polypyrrole, polythiophene, poly(3-hexylthiophene), and poly(3,4-ethylenedioxythiophene).

While the difficulty of development of characterizeable samples hindered initial research in conducting polymers, the application of conducting polymers to linear actuation has placed an even more challenging demand on conducting polymer researchers. For actuation studies, the material must stand freely as a bulk material with measurable mechanical properties. The additional mechanical stability allows for testing of the polymer in a linear mechanical configuration to observe changes from electrochemical inputs (described in the next section). Actuation properties can also be derived from coated flexible electrodes that bend rather than elongate during activation as was instrumental in the initial development of conducting polymer actuation.<sup>4</sup> Bending actuators do not require the same mechanical robustness of the conducting polymer film, though the properties of the bulk film are readily applied in the bending configuration. As many of the biomimetic applications will require linear actuators, an emphasis is placed on actuation in freestanding films.

## 1.2 Actuators

By definition, actuators perform mechanical work, transformed from an input energy source. Numerous materials and mechanistic approaches are in development, encompassing a wide range of input energies.<sup>5</sup> Mechanical work is also a broad description of actuation that can be narrowed significantly by geometric constraint. For linear actuators, work is performed against a known load on a single axis and principally characterized by stress, strain, and strain rate. In nature, no actuating material is as ubiquitous as muscle tissue, and no actuating material is as familiar to us as mammalian skeletal muscle. For the sake of example, a look at skeletal muscle performance

demonstrates the important metrics in actuation and highlights many of the targets for actuator researchers. Skeletal muscle is capable of producing strains of 20%, strain rates greater than 50% per second and stresses of 0.1 MPa.<sup>6</sup> It also demonstrates a cycle life greater than  $10^9$  and the ability to heal and grow in response to injury or conditioning.

While skeletal muscle can be surpassed in the key actuation metrics by some materials, none of these replacements present the combination of capabilities in a similarly small package or requiring similarly low input energies. Furthermore, as opposed to many artificial replacements, skeletal muscle uses a complex nutrient transport system that refreshes the individual muscle cells with fuel for activation.<sup>7</sup> A synthetic replacement would also require a readily available input energy source such as the low voltage electrical signal used in conducting polymer actuators. The requirements for muscle-like actuators are low weight, large stroke, high cycle life, and high work density. Throughout this work, discussion of characterization and characterization techniques will highlight these metrics and describe them in greater detail.

For the majority of conducting polymers, actuation is achieved by ingress and egress of ions contained in an electrolyte bath. This swelling mechanism can be driven electrochemically with a polymer as working electrode and suitable non-reactive counter electrode. Figure 1.3 depicts the operation of such an actuator elongated by the application of a potential. Polypyrrole successfully actuates by this mechanism and has been the focal point of numerous conducting polymer actuator researchers<sup>5</sup>. Poly(3,4-ethylenedioxythiophene), or PEDOT, also actuates by this mechanism and will be the topic of Chapter 5.

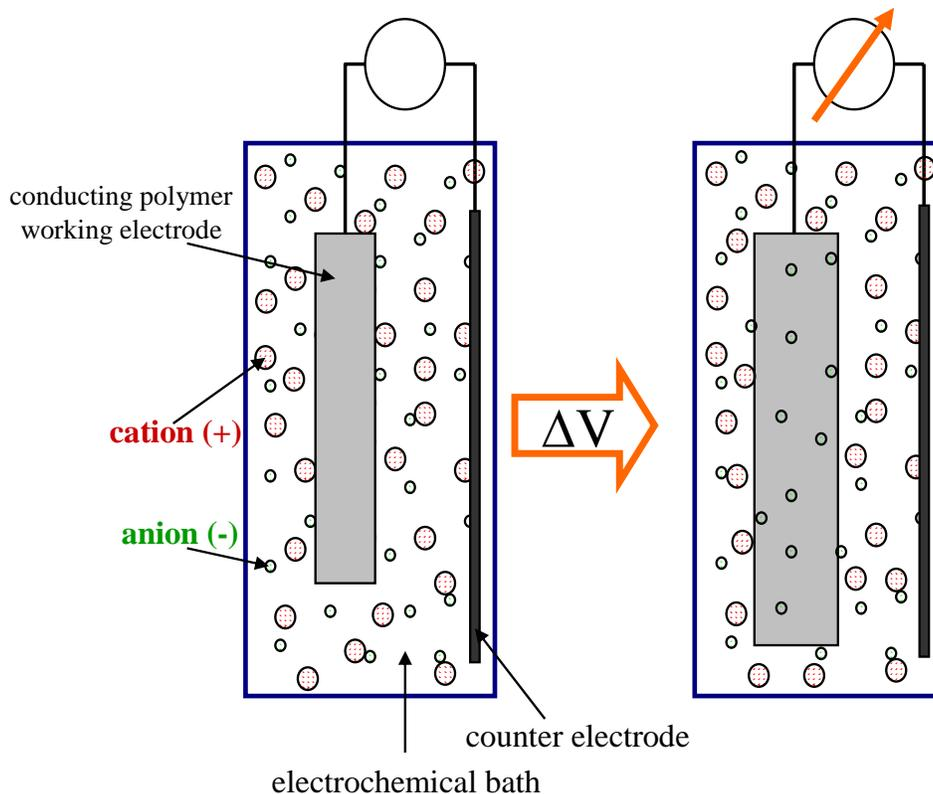


**Figure 1.3.** Schematic diagram of conducting polymer actuation in an electrolyte. Once a potential is applied between working and counter electrode, the film elongates with one ionic species and can be reversibly contracted by applying an opposing potential.

A recent step toward the further complexity exhibited by natural muscle tissue was proposed with materials that undergo conformational changes based on oxidation and reduction. This type of molecular mechanism is depicted in Figure 1.4, in which a monomer at suitable oxidation state undergoes a transformation from a bent to planar structure. Such transformations are observed in small molecules, typically by restoring aromaticity in the oxidized state, as in the case of the depicted thiepin.

The mobility of double bonds in conjugated polymers may also lead to conformational changes in the polymer. Actuation independent of the charge and discharge of ion swelling has been observed in the conducting polymer poly(3-hexylthiophene) and will be discussed in Chapter 7. A conformational mechanism has also been proposed in polymers already believed to actuate primarily via the swelling mechanism, such as polypyrrole.<sup>10</sup>

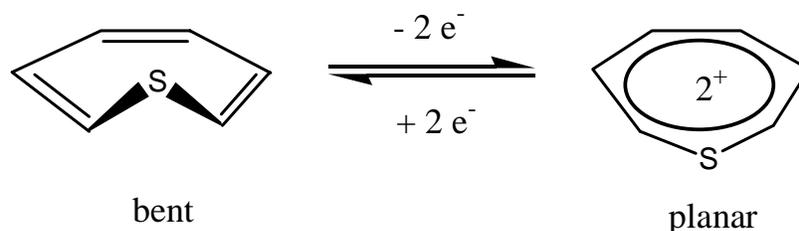


**Figure 1.4.** Conformational change of thiophene structure during oxidation and reduction.

One final proposed mechanism for conducting polymer actuation is based on interchain interactions. It has been demonstrated in short thiophene chains that a favorable interaction in the molecular orbital between two neighboring tetramers is generated upon oxidation.<sup>11</sup> The subsequent  $\pi$ - $\pi$  interaction of the oligomers can also be reversibly controlled via oxidation and reduction, as depicted in Figure 1.5. This mechanism has been proposed for actuation in polythiophenes as well as conducting polymers containing short oligomeric polythiophene moieties.<sup>12</sup> Simulations based on this mechanism have also been published,<sup>13</sup> though the comparative actuation data is limited and obscured by the swelling mechanism described above. Mechanisms that depend on complex interchain interactions more closely mimic the actual mechanism in skeletal muscle and remain attractive synthetic goals. In pursuing these new paradigms of actuation, it is clear that we have only made first steps in that direction and that much work is needed as we approach actuation similar to that observed in natural muscle tissue. Challenges in material properties and processing must be addressed to enable the development of complex mechanisms and structures.

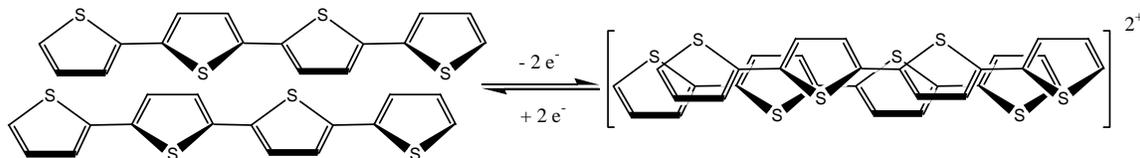


**Figure 1.5.**  $\pi$ - $\pi$  interaction between oxidized tetramers of thiophene.

### 1.3 Synthesis

There are numerous synthetic techniques used on conventional small molecules that are relevant to the conjugated bonds of conducting polymers. Of particular interest are those reactions which bond  $sp$  and  $sp^2$  carbon, for example Suzuki, Sonagashira, and

Stille couplings. Once the monomer is made, the critical step of obtaining conducting polymer requires a polymerization similarly suited to conjugated materials. Chemical techniques, including the couplings listed above may be utilized to synthesize undoped conducting polymers. Other syntheses utilize oxidation, either chemical or electrochemical, to link monomers via coupling of radical cations. The selectivity of radical cations to react at certain positions, like the  $\alpha$  carbons (2 and 5 positions) in the pyrrole monomer, enable polymers to be synthesized by successive coupling of monomers, oligomers, and polymers. In an electrochemical synthesis the proximity of cations near the anode allows for quick coupling and often results in a polymer coating on the electrode once a sufficient molecular weight is established for the loss of solubility. Maintaining control of the selective chemistry with these conditions is a complex objective, discussed in Chapter 2.

The amount of work done in studying electrochemical synthesis is extensive but small when compared to the possibilities for systematic variations. The chemical parameters that must be chosen include solvent and solvent mixtures, electrolyte, and concentrations of monomer, electrolyte, and electrode material. Subsequent electrochemical parameters include current or potential control, limits, experiment duration, and environment. On a quest for the perfect conducting polymer, most researchers are forced down a tortuous path of wide-ranging conditions and results. There is often little opportunity to systematically vary sufficient parameters before the monomer supply is exhausted. To arrive at the end of such a search with a material that may not be identical to another material synthesized the same way by a colleague can be disheartening indeed. While chemical methods may offer more control of the individual polymerization reactions, the competing goals of high conductivity and solubility generally force polymerizations to a solid-liquid interface. Obtaining a film from a suitable interface in such systems is equally as difficult as the electrochemical case (with the notable exception of poly(alkylthiophenes)).

Regardless of these difficulties, typical conducting polymer syntheses in which suitable materials for actuation are obtained often follow a pattern. The monomer is

dissolved at low concentration along with an electrolyte of greater concentration in the solvent of choice. The electrochemical cell is configured with working, reference, and counter electrodes immersed in the solution. The working electrode is usually held either at constant potential or current for a period of time, allowing for a buildup of insoluble polymer at the electrode.

## **1.4 Characterization**

Once a material is synthesized, it must be characterized for further development and insight for subsequent revisions of design. The characterization methods for such materials are numerous, though the most relevant to conducting polymer actuators focus on mechanical, electrical, and electrochemical properties. Direct measurement of actuation is also critical when possible and can be achieved in numerous ways. Nondestructive tests that completely predict actuation performance have not been developed, making direct observation paramount to actuator development. Instruments for measuring active stress and strain in conducting polymers are not commercially available and must be developed, often as a right of passage for the actuator researcher.<sup>9,12a,14</sup> Once the material and instrument are available, no concrete set of experiments predict the full actuation properties. Variations in technique from researcher to researcher are often based solely on experience and feel. The desire to improve repeatability in the material and characterization methods is a driving force for much work with conducting polymer actuators. Repeatability in these two areas is also a necessity for a successful transition from scientific curiosity to commercial material.

## **1.5 Modeling**

Modeling the performance of conducting polymer actuators serves two purposes. In the first, the successful use of electrical inputs may require a model to achieve the desired mechanical output. A model of this type is less concerned with the underlying physical and chemical phenomena but is useful for implementation of the actuator into a device as examined recently by Bowers.<sup>15</sup> The second type of model seeks a predictive capability of the polymer to verify assumptions of the underlying mechanisms, as

demonstrated by Madden.<sup>9a</sup> The success of Madden's model for polypyrrole suggested that actuation by ion ingress and egress is dominated by ion diffusion through an elastic, metallic polymer matrix, termed the Diffusive Elastic Metal. In addition, this model highlighted the relationship between strain and charge. The ratio of strain to charge, normalized by the volume of polymer has been termed  $\alpha$ , which has the units  $\text{m}^3/\text{C}$ . Furthermore, the model defined three time constants pertinent to polypyrrole actuation,  $\tau_{\text{RC}}$ ,  $\tau_{\text{D}}$ , and  $\tau_{\delta}$ , corresponding to the capacitive charging time of the polymer, the diffusion time into the polymer, and the diffusion time across the interfacial double layer respectively. The model has been applied to larger films by P. Madden<sup>9b</sup> and will also be discussed in Chapter 8.

## 1.6 Outline

The work described here is arranged in chapters relating to the topics already introduced. Chapter 2 discusses the synthetic techniques used in novel conducting polymer systems. Chapters 3 and 4 relate characterization methods first for material properties and second for techniques specific to actuators. In these three chapters, examples are taken from monomer systems studied for actuation purposes. The focus of the chapters is the discussion of each technique and its application, solidifying the experimental techniques used in conducting polymer actuator development. Chapter 5 highlights the successful conducting polymer poly(3,4-ethylenedioxythiophene), or PEDOT, while Chapter 6 examines the enhancement of PEDOT actuation in layered composites of PEDOT and carbon nanotubes. Chapter 7 introduces actuation in poly(3-hexylthiophene) and discusses the dependence of actuation on potential rather than charge. Chapter 8 presents the improvements in polypyrrole actuation speed upon increasing the temperature of actuation up to 100 °C. This data is modeled utilizing the diffusive elastic metal model developed by Madden<sup>9a</sup> for discrete time simulation.

## 1.7 References

1. a) *Handbook of Conducting Polymers*. Skotheim, T.A., Ed.; Marcel Dekker: New York, 1986. b) *Handbook of Conducting Polymers*. Skotheim, T.A; Elsenbaumer, R. L.; and Reynolds, J.R. Eds.; Marcel Dekker: New York, 1998; 2<sup>nd</sup> Ed.
2. Doblhofer, K.; Lyons, M. E. G.; Albery, W.J.; Bartlett, P.N.; Lewis, T.J.; Pickup, P.G.; Zambonin, P.G.; Hillman, A.R.; Wang, X-B.; Armand, M.; Haas, O.; Smith, A.L.; Murray, R. W.; Girault, H. H.; Mount, A.R.; D'Silva C.; Peter, L.M. General Discussion. *Faraday Discuss. Chem. Soc.* **1989**, 88, 177-187.
3. Roth, S. *One-Dimensional Metals*; VCH: New York, 1995.
4. a) Pei, Q.; Inganas, O.; Electrochemical Applications of the Bending Beam Method. 1. Mass Transport and Volume Changes in Polypyrrole during Redox. *J. Phys. Chem* **1992**, 96, 10507-10514. b) Baughman, R. H.; Conducting polymer artificial muscles. *Synth. Met.* **1996**, 78, 339-353.
5. Madden, J. D. W.; Vandesteeg, N. A.; Anquetil, P. A.; Madden, P. G. A.; Takshi, A.; Pytel, R. Z.; Lafontaine, S. R.; Wieringa, P. A.; Hunter, I. W. Artificial Muscle Technology: Physical Principles and Naval Prospects. *IEEE J. Oceanic Eng.* **2004**, 29, 706-728.
6. Hunter, I.; Lafontaine, S. A comparison of muscle with artificial actuators. In *Tech. Dig. IEEE Solid State Sensors Actuators Workshop* **1992**, 178-185.
7. Ebron, V. H.; Yang, Z. W.; Seyer, D. J.; Kozlov, M. E.; Oh, J. Y.; Xie, H.; Razal, J.; Hall, L. J.; Ferraris, J. P.; MacDiarmid, A. G.; Baughman, R. H. Fuel-powered artificial muscles. *Science* **2006** 311, 1580-1583.
8. Pollack, G. H.; Blyakhman, F. A.; Reitz, F. B.; Yakovenko, O. V.; Dunaway, D. L. Natural Muscle as a Biological System. In *Electroactive Polymer (EAP) Actuators as Artificial Muscles: Reality, Potential, and Challenges*; Bark-Coehn, Y., Ed.; SPIE Press: Bellingham, WA, 2001, 47-66.
9. a) Madden, J. D. W. Conducting Polymer Actuators. Ph.D. Thesis, Massachusetts Institute of Technology, Cambridge, MA, 2000. b) Madden, P. G. A. Development and Modeling of Conducting Polymer Actuators and the Fabrication of a Conducting Polymer Based Feedback Loop. Ph.D. Thesis, Massachusetts Institute of Technology, Cambridge, MA, 2003.
10. a) Otero, T. F.; Grande, H.; Rodriguez, J.; Conformational Relaxation During Polypyrrole Oxidation: From Experiment to Theory. *Electrochimica Acta.* **1996**, 41, 1863-1869. b) Otero, T. F.; Grade, H.; Rodriguez, J. Role of conformational relaxation on the voltammetric behavior of polypyrrole. Experiments and mathematical model. *J. Phys. Chem. B* **2006**, 101, 8525-8533.

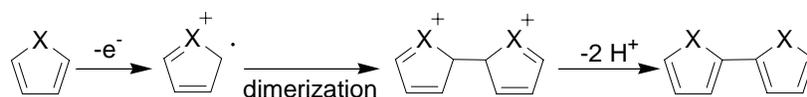


11. Kingsborough, R. P.; Swager, T. M. Polythiophene hybrids of transition-metal bis(salicylideneimine)s: Correlation between structure and electronic properties. *J. Am. Chem. Soc.* **1999**, *121*, 8825-8834.
12. a) Anquetil, P. A. Large contraction conducting polymer molecular actuators. Ph.D. Thesis, Massachusetts Institute of Technology, Cambridge, MA, 2005. b) Yu, H.-H. Molecular Actuators: Design, Syntheses and Applications toward Actuation and Sensory Materials. Ph.D. Thesis, Massachusetts Institute of Technology, Cambridge, MA, 2003.
13. Sherlis, D. A.; Marzari, N.  $\pi$  r-stacking in thiophene oligomers as the driving force for electroactive materials and devices. *J. Am. Chem. Soc.* **2005**, *127*, 3207-3212.
14. Schmid, B. Characterization of Macro-Length Conducting Polymers and the Development of a Conducting Polymer Rotary Motor. M.S. Thesis, Massachusetts Institute of Technology, Cambridge, MA, 2005.
15. Bowers, T. Modeling, simulation, and control of a polypyrrole-based conducting polymer actuator. M.S. Thesis, Massachusetts Institute of Technology, Cambridge, MA 2004.

## 2. Synthesis of Conducting Polymers

The key requirement in the synthesis of conducting polymers is that the conjugated nature of the monomer is conserved in the synthesis process. This limits both the choice of monomer and the choice of polymerization process. Monomers of great complexity have been synthesized with this careful goal in mind. Furthermore, the development of novel monomers must also target the appropriate functionality for polymerization. As such, most conducting polymer monomers are electron-rich molecules with pendant groups containing pyrroles, thiophenes, or 3,4-ethylenedioxythiophenes. These three well known conducting polymer monomers are excellent additions to conjugated systems as they typically enable electrochemical polymerization and direct the polymerizations toward linear polymers.

Polymerization of a given monomer, however can be attempted in many ways. Several of the synthetic coupling techniques can be used on highly electron-rich systems, and these often serve for the polymerizations of poly (para-phenylene vinylene)s or poly (para-phenylene ethynylene)s. The monomer and polymer in such systems must be soluble for complete polymerization reactions and synthesis of high molecular weight material. Phenylene-containing monomers are popular, since solubility can be enhanced by the addition of pendant alkyl groups, though electrical interchain interactions may be inhibited by the steric bulk of such additions. In poly (para-phenylene vinylene), conductivity is high, though the stability limits potential applications.<sup>1</sup> More often, highly conductive polymers are synthesized by oxidative polymerization. The highly electron-rich monomers are easily oxidized, leaving the cation radical as depicted in Scheme 2.1. Two such radicals may join to form a new carbon-carbon bond. This bond is stabilized by the elimination of the protons and return of aromaticity.



**Scheme 2.1.** Coupling reaction producing dimer by sequence of oxidation, radical coupling, and proton elimination.

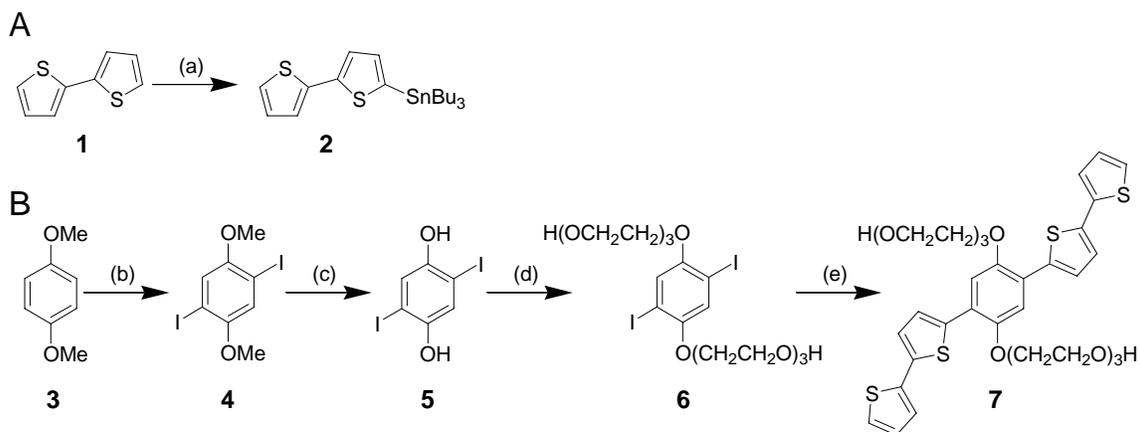
The dimer is subsequently free to be oxidized and couple again with another cation radical. The process continues as long as the radicals are stable and reactive. Termination may occur by chain transfer or radical coupling with oxygen or other radical scavenger present. As the coupling reactions continue, the rigidity of the molecule makes for poor solubility and often the polymer will precipitate at the oligomer stage. Thus, further reactions must occur in the solid phase or across the interface in a heterogeneous reaction. Electrochemical techniques are superior under these conditions as the oxidation is localized to the interface at the working electrode. Over the course of a reaction, the continued polymerization coats the surface with a layer of increasing thickness. It is the ability to grow films that enables a great deal of further testing and remains a critical step in the synthesis of conducting polymer actuators.

The remainder of this chapter will highlight the different methods for achieving oxidative polymerization of simple and complex monomers. With the variety of techniques employed, the parameter space is enormous. For a researcher faced with a limited quantity of monomer, only a few options may be tried before the monomer must be synthesized again. With that in mind, choice of the right method for synthesis of a conducting polymer is crucial.

## 2.1 Monomer Synthesis

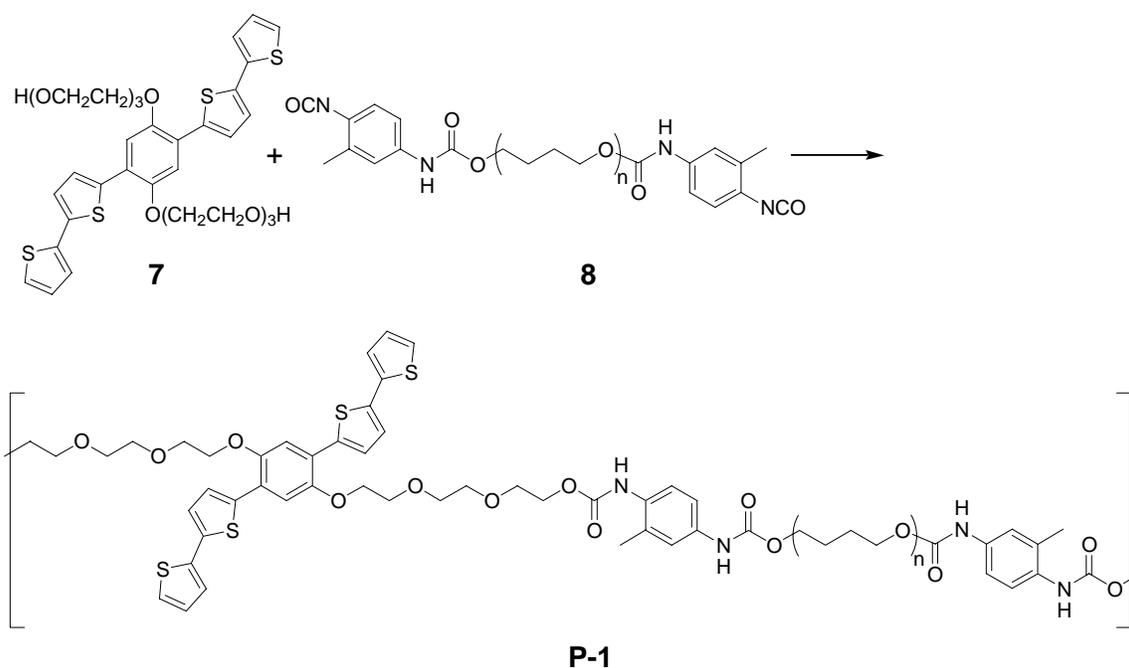
The topic of monomer synthesis is largely left to the synthetic organic specialist. Once a target functionality has been identified, i.e. one that will change its conformation upon oxidation and reduction, the choice of pendant groups and electroactive species employed is often specific to that monomer. Other variations in polymer structure may provide mechanical stability through cross-linking, as was the target of the monomer synthesis depicted in Scheme 2.2. It is also likely that a library of monomers will be

synthesized with minor variations to affect solubility, structure, or additional reactivity. For example, after a core to the monomer has been synthesized and prepared for coupling with a bithiophene via Stille coupling (Scheme 2.2 (e)), it is straightforward to make the EDOT and thiophene versions as well. Few of the novel monomers are synthesized directly for chemical polymerization due in part to the conflicting goals of film production and solubility requirements (discussed in the next section). The versatility of electrochemical techniques presents numerous opportunities for new monomer systems and will be discussed in Section 2.3.



**Scheme 2.2.** (A): (a) *n*-BuLi, SnBu<sub>3</sub>Cl, THF, -77 °C, 24%. (B): (b) I<sub>2</sub>, KIO<sub>3</sub>, H<sub>2</sub>SO<sub>4</sub>, AcOH, H<sub>2</sub>O, 74%; (c) BBr<sub>3</sub>, CH<sub>2</sub>Cl<sub>2</sub>, -78 °C, H<sub>2</sub>O quench, quantitative; (d) Cl(CH<sub>2</sub>CH<sub>2</sub>O)<sub>3</sub>H, K<sub>2</sub>CO<sub>3</sub>, DMF, 23%; (e) **2**, Pd(PPh<sub>3</sub>)<sub>2</sub>Cl<sub>2</sub>, DMF, 55%.

One target monomer, Compound **7**, was synthesized according to literature procedures<sup>2,3,4</sup> in order to demonstrate mechanical enhancement via covalent cross-linking. The reactive hydroxyl groups pendant to the main conjugated backbone of the phenylene-bis-bithiophene system could be connected via condensation with a linker. While the cross-linking strategy post electrochemical polymerization proved ineffective, the monomer could be combined with low molecular weight polymer (Scheme 2.3) to create an oligomeric monomer suitable for electrochemical polymerization. At high molecular weight, however, the polymer was insoluble and could not be electrochemically polymerized.



**Scheme 2.3.** Polymerization (Mn **8** = 900), Fe(acac)<sub>3</sub>, THF, 2 days (Mw = 6000).

Figure 2.1 compares the electrochemical polymerization of Compound **7** to that of the Compound **P-1** from the same electrochemical conditions. The resulting film coated electrodes shows a brittle and powdery film in the case of the small molecule monomer, **7**, and a thin but homogeneous film of the polymerized oligomer **P-1**.

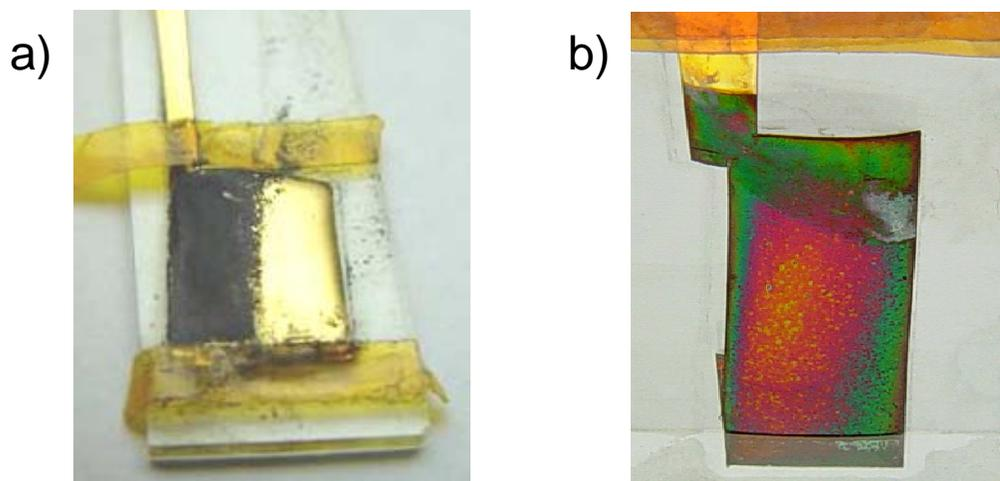


**Figure 2.1.** Electrochemical polymerization of Compound **7** (a), and Compound **P-1** (b) on a Au coated PET substrate. The oligomeric monomer coats the electrode more evenly.

## 2.2 Chemical Polymerizations

The principles of oxidative polymerization do not mandate the use of electrochemical techniques. For example, poly(3-hexylthiophene) is a well known and often studied conducting polymer that is almost universally synthesized chemically. Polypyrrole and poly(3,4-ethylenedioxythiophene) may also be synthesized chemically, though the electrochemically synthesized variants have generally superior conductivity and mechanical properties.

When designing for a chemical polymerization, the key structural requirement after conjugation is solubility. Successful polymerization to high molecular weight requires that oligomers and low molecular weight polymers be reactive and soluble enough to polymerize further. If an oligomer precipitates out of solution the polymerization must continue as a heterogeneous process, an increasingly unlikely prospect as the concentration of monomer and reactive polymer is decreasing. An unsuccessful chemical polymerization will terminate before the entanglement molecular weight is achieved, leaving a mechanically unstable coating on the reaction vessel walls.

Nonetheless, for a suitably soluble system, the chemical polymerization allows for the precise choice of oxidant to selectively generate cation radicals at the appropriate location on the monomer. There are several candidates for oxidant, though  $\text{FeCl}_3$  is a common choice. Once the polymerization is complete, the oxidant must be washed away and the polymer typically suspended in solution. In rare cases, as occurs with polypyrrole, the chemical oxidation directs polymer to any available interface and may be used for coating purposes.<sup>5</sup> The polypyrrole obtained this way is conductive, though not nearly as conductive as polypyrrole prepared electrochemically.

For applications utilizing soluble conducting polymers, the polymer is cast as a film and doped into an electrically conductive state. Poly(3-hexylthiophene) is readily doped with  $\text{I}_2$  vapor, to obtain films with conductivities as high as 1000 S/m (as measured by the van der Pauw technique described in the next chapter). The polymers may also be doped electrochemically, though this process is more difficult if the solution cast polymer

is initially in an insulating state, as is the case with poly(3-hexylthiophene). Even if the polymer is deposited onto an electrode, the ability to transport enough charge through an insulating layer can be limiting as the thickness of the polymer is increased. Once doped, however, the conductivity of the polymer increases dramatically, facilitating electrical and ionic transport.

## 2.3 Electrochemical Polymerization

Electrochemical polymerizations offer at once a wide variety of parameters and complexities to the conducting polymer community,<sup>6</sup> as demonstrated in the thorough text by Bard and Faulkner.<sup>7</sup> For this type of polymerization, the monomer, solvent, and an electrolyte are placed into a three electrode cell. The working electrode is the controlled electrode and forms the surface for polymerization. The reference electrode offers a stable potential by which to measure the voltage at the working electrode. The counter, or auxiliary, electrode balances the circuit and enables currents to flow through the electrolyte. The counter electrode is often ignored from a synthetic standpoint, but should not be forgotten. In particular, if the counter electrode is small, the electrical and ionic transport at the counter electrode may limit the overall transport in the system. A counter electrode should typically be a non-reactive surface with approximately ten times the surface area of the working electrode. In practice it can be difficult to obtain the surface area requirement while maintaining minimal solution volumes and additional care should be taken before strong conclusions are drawn in such systems.

The reference electrode may be one of the standard reference electrodes, for which a known voltage versus the Standard Hydrogen Electrode, or SHE, may be used. As most of the standard electrodes are aqueous, however, their use requires an additional interface between water and the solvent used for polymerization. This interface has a junction potential that may also depend on the applied potential. A useful way to avoid such complexities is to measure the oxidation and reduction of a known redox couple, such as the one electron ferrocene/ferrocenium couple, prior to the electrochemical testing and again after the test is concluded. This technique measures a stable reference electrode and allows for the use of nonaqueous reference electrodes or simple wire

pseudoreference electrodes. Sawyer et al.<sup>8</sup> also provide a good description of the use and preparation of common nonaqueous reference electrodes. For the active synthetic electrochemist, the measurement of all references with ferrocene enables good reproducible results.

In all electrochemical polymerizations, the use of a potentiostat is adequate for control of the electrochemistry. In simplified systems, such as a galvanostatic polymerization with two electrodes (no reference electrode), a current source can be used, though the lack of reference electrode will limit the understanding of the potential at the electrodes and its relation to the oxidation of the monomer. Potentiostats may also be constructed from simple circuit elements,<sup>7</sup> though stand-alone instruments are quite common. Further customization can be obtained with a computer controlled data acquisition card and an analog controlled potentiostat such as those manufactured by Amel srl (Milan, Italy).

Electrochemical polymerization techniques are divided into controlled current and controlled potential experiments. The simplest constant potential and constant current techniques will be described in Sections 2.3.1 and 2.3.2. Time varying potential and current waveforms are also used and will be described in Sections 2.3.3 and 2.3.4 respectively.

### ***2.3.1 Potentiostatic Polymerization***

The potentiostatic polymerization offers a logical progression from the chemical polymerization in which an oxidizing agent of fixed strength is used. In a potentiostatic polymerization, the potential is fixed versus time and the current is measured. A likely scenario would have the potential fixed just at the oxidation potential of the monomer, mimicking the role of an oxidizing agent. This would generate oxidized monomer species available for coupling at the working electrode surface. As the monomer species oxidizes and reacts, more monomer diffuses toward the electrode from the bulk solution. In an electrochemical system, transport occurs by convection, migration, and diffusion. For an unstirred bath, the effects of convection can be neglected, especially at short time



scales.<sup>7</sup> The addition of an electrolyte in solution, typically an alkyl ammonium salt of hexafluorophosphate or tetrafluoroborate, overwhelms the concentration of oxidized or reduced reactive species in solution and supports electrical current through the cell via migration. Diffusion is the key driving force affecting monomer concentrations near the interface during electrochemical oxidation.

At the working electrode surface monomers and dimers continue to oxidize and react, forming tetramers and octamers and so on. In general, the additional conjugation of the oligomers stabilizes the oxidized form and lowers the oxidation potential. Thus at a potential sufficient for monomer oxidation, the oligomers will also oxidize, though they may react at a different rate. Once the polymer has a high enough molecular weight to affect solubility, it precipitates on to the electrode surface. Long polymerization times, however, may lead to trails of polymer or wisps of oligomer in solution away from the electrode, which can discolor the solution. This demonstrates the balance of solubility and transport for oligomers of increasing molecular weight. It is unclear whether the polymer coating the electrode continues to react with monomer and oligomer species in solution or with other polymer species in the bulk of the film. Unlike the chemical polymerization, this heterogeneous reaction is not limited by concentration as the bulk solution continually refreshes the monomer concentration near the electrode, provided sufficient monomer is available in the bath. Careful construction of the bath and electrode sizes will maintain this condition, ensuring an even polymerization during the course of the experiment.

One additional feature of the electrochemical polymerization is the incorporation of anions into the film during polymerization. As the polymer is deposited on the electrode it maintains the potential of the electrode. This leads to the presence of positive charges along the backbone of the polymer and subsequent interaction with the counterion also attracted to the working electrode. This charge incorporation is the equivalent of electrochemical doping, causing the electrochemically deposited polymer to be synthesized in a conductive state. The advantage of synthesizing a material in the

conductive state is that further electrochemistry is straightforward and does not require reoxidation of the polymer.

The measurement of an electrochemical polymerization is based on the current that is passed during the experiment. Each monomer or oligomer oxidation requires the removal of one electron from the working electrode. Thus, each coupling reaction requires two electrons and the reaction rate is directly related to the current by Faraday's law which states the equivalency of charge and reaction consumed as 96485.4 C/mol, or Faraday's constant  $F$ . From this law, the rate equation

$$rate (mol s^{-1} m^{-2}) = \frac{i}{n F A}, \quad 1$$

may be obtained, in which  $i$  is the current in the cell,  $n$  is stoichiometric number of electrons consumed per reaction,  $A$  is the electrode area.<sup>7</sup> For the polymerization reaction, each monomer is oxidized twice, which sets  $n = 2$ .

In addition to the current consumed by the polymerization reaction, the current required to dope the polymer is also passed through the electrochemical cell. With a typical dopant concentration between 0.25 and 0.33 for the oxidized polymer, it is estimated that charge is accumulated on the backbone at nearly one positive charge per three or four monomer units, increasing  $n$  in Equation 1 to 2.25 or 2.33. Other currents in the electrochemical polymerization can be attributed to the initial charging of the electrode surface (which acts primarily as a capacitor) and to leakage currents that occur without reaction of monomer or polymer. Taking the charging current to be an initial and fast response (capacitances are on the order of 0.1 to 0.4 F/m<sup>2</sup>)<sup>7</sup> and the leakage current to be small relative to the polymerization current, the steady state current reached in a potentiostatic polymerization indicates the deposition rate of polymer at the electrode. Experimentally it has been observed that approximately 1 kC of charge passed per m<sup>2</sup> of electrode surface will produce a film of 1  $\mu$ m thickness for polypyrrole<sup>6</sup> and the same has been measured in poly(3,4-ethylenedioxythiophene).

Using 2.25 for the stoichiometric coefficient  $n$  and  $1.0 \text{ A/m}^2$  as a representative current density, Equation 1 gives a reaction rate of  $4.606 \times 10^{-6} \text{ mol s}^{-1} \text{ m}^{-2}$ . Assuming a polymer density of  $1000 \text{ kg/m}^3$ , the molar densities of pyrrole and (3,4-ethylenedioxythiophene) are  $14.93$  and  $7.03 \text{ kmol/m}^3$  respectively. Dividing the reaction rate by the molar volumes gives polymer growth rates at the interface of  $3.09$  and  $6.55 \times 10^{-10} \text{ m s}^{-1}$  per  $\text{m}^2$  of electrode area. Thus for a 1000 second deposition, consuming 1 kC of charge, the Faraday relation gives approximately  $0.3$  and  $0.7 \text{ }\mu\text{m}$  film thicknesses for polypyrrole and poly(3,4-ethylenedioxythiophene) respectively, corroborating the experimental evidence.

The potential chosen for polymerization should be sufficient for monomer oxidation but not significantly higher for fear of over-oxidation and degradation of the polymer or solvent. Experimentally, a cyclic voltammogram, measured by sweeping the potential in a triangle waveform, should be used to estimate the useful potential for oxidation, though more on the role of potential will be discussed in Section 2.3.3.

### **2.3.2 Galvanostatic Polymerization**

Galvanostatic polymerization requires the application of a constant current to the electrochemical system, forcing oxidation and polymerization at the working electrode. One distinct advantage of the galvanostatic polymerization is the direct relationship between time and thickness of polymer on the electrode. Again assuming negligible effects from initial charging of the interface and leakage currents in the cell, a constant current produces a linear increase in charge with time. A second advantage of the galvanostatic polymerization is the flexibility of potential versus time to accommodate changes in the solution concentration or passivation of the electrode surface. As polymer is deposited on the electrode, it is in the oxidized conductive state. The polymer possesses a finite conductivity, however, and at sufficient thicknesses the resistive drop through the thickness of the film may lower the potential at the surface sufficiently for the cessation of monomer oxidation. In a potentiostatic polymerization, this passivation leads to the end of the polymerization whereas in a galvanostatic system, the feedback required by current control causes the potential at the electrode surface to rise until the current density

is restored. This makes galvanostatic polymerization techniques superior to potentiostatic techniques for the growth of thicker films, especially with less conductive materials.

The increase in potential versus time as is often seen in galvanostatic polymerizations may also lead to degradation of the polymer or reaction with solvent or impurities as the galvanostatic technique does not offer the same selectivity. Once the monomer concentration is exhausted, the potential will increase to accommodate a different reaction. The potentiostatic polymerization will stop in the absence of monomer. This elucidates an often-overlooked relationship in the galvanostatic polymerization design between the surface area of the working electrode and the volume of solution. It is imperative that the solution contains sufficient monomer for complete polymerization on the electrode to a desired thickness. The effect of the polymerization on the bulk concentration should be negligible if the polymer is to be deposited uniformly. Taxing a system with a large working electrode and small volume will quickly exhaust the monomer supply and over-oxidize the polymer on the electrode, further inviting additional unwanted reactions.

### ***2.3.3 Potentiodynamic Polymerization***

Potentiodynamic conditions use a potential waveform that varies with time. Most often, this method employs a triangle wave in potential as is used in cyclic voltammetry. Cyclic voltammetry measures the oxidation and reduction of monomer, polymer, or a reference standard such as ferrocene. While small molecules often exhibit one or two oxidation and reduction peaks, polymers exhibit broad oxidation waves and reduction waves. During polymerization, the oxidation step is followed by a chemical coupling rather than a reduction, so each corresponding oxidation peak is not balanced by a reduction peak. Polymer that is deposited on the electrode however, can also be reversibly oxidized and reduced. Thus the complex polymerization voltammogram exhibits large oxidation peaks superposed over a broad polymer oxidation and a corresponding polymer reduction peak. During the course of a polymerization, polymer accumulates on the electrode and the current magnitude corresponding to oxidation and

reduction also increase. Therefore, an increase in current magnitude with each cycle is generally thought to be sufficient evidence for polymerization at the electrode. A sample polymerization voltammogram is presented in Figure 2.2, highlighting these observations.

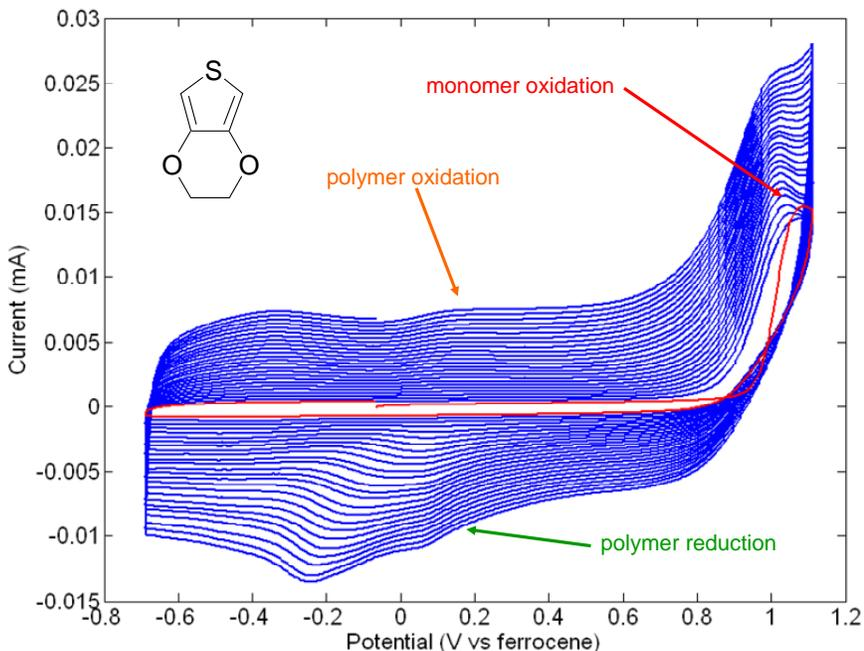


**Figure 2.2.** Potentiodynamic polymerization of EDOT monomer. The monomer concentration is 1.0 mM in a solution containing 0.1 tetrabutylammonium hexafluorophosphate (TBAPF<sub>6</sub>) in dichloromethane. The polymerization scan rate is 50 mV/s with a Pt button working electrode and the potential is measured versus a ferrocene standard. The first potential cycle is shown in red.

It has been observed that, after many scans, the magnitude of the current change with each cycle may eventually decrease. This makes the electrochemical deposition of thick films especially challenging because the cycled oxidation and reduction are eventually rendered useless. If the film is not sufficiently conductive, a voltage drop will develop through the thickness of the film and the potential at the interface will not be sufficient for oxidation and polymerization. In this situation, the current reaches a steady state corresponding to the reversible oxidation and reduction of polymer with no additional monomer oxidation and polymerization. In such systems, the polymerization and current increases can be revived by expanding the potential window during each cycle to allow for a greater oxidation potential, as demonstrated in Figure 2.3.

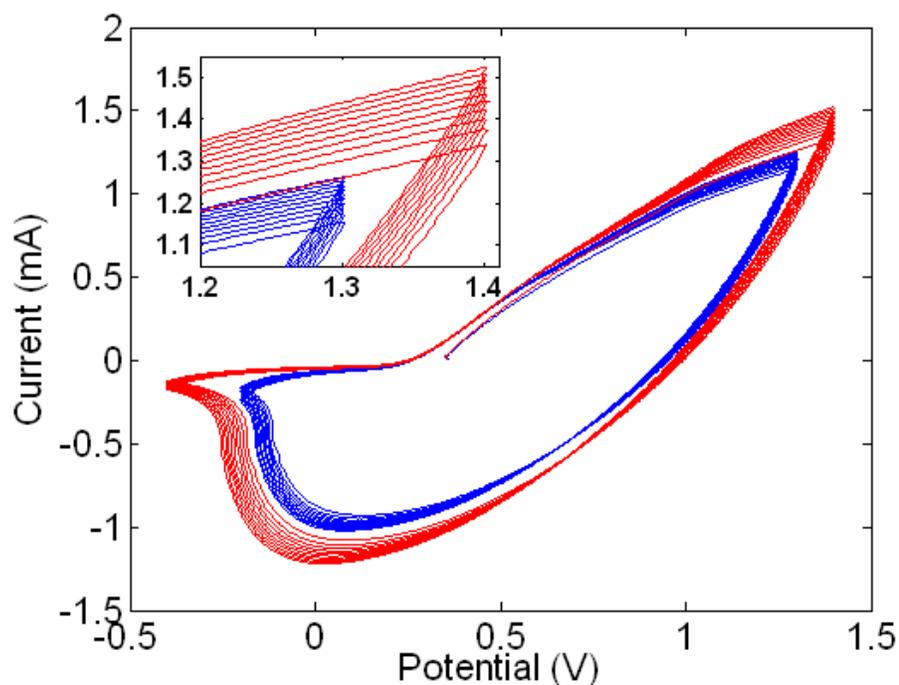


**Figure 2.3.** Potentiodynamic polymerization of oligomer **P-1** showing a decrease in current growth per cycle (blue curve) and subsequent improved growth upon application of greater potential limits (red curve). Inset magnifies the anodic limit.

The increase in potential at the interface allows the polymerization to resume, noting that initial cycles at such high potentials may have damaged the polymer or monomer. Applying this observation, the best polymerization waveform for thick films may be achieved with a steady increase in potential over time to maintain a constant polymerization rate. It will be shown below that the same can be accomplished with a carefully constructed current waveform.

The most significant difference between a potentiodynamic polymerization and the constant current and potential techniques is the periodic oxidation and reduction of the polymer. It is not known whether the reduction improves the polymerization, though by switching the potential, the final proton elimination step in the carbon-carbon bond formation could be assisted. Both potentiostatic and galvanostatic polymerization methods maintain a highly oxidative state at the surface of the electrode. It is not clear how the protons are eliminated in this state, though numerous ideas have been proposed. In the case of galvanostatic pyrrole polymerization, a small amount of water in solution

may aid this elimination.<sup>9</sup> Heinze and coworkers have also suggested that the lack of proton elimination is the key step in termination of the polymerization,<sup>10</sup> though it should be recalled that conjugated systems can stabilize charge at intervals of a few monomers.

If the film is over-reduced, however, it will become resistive and passivate the electrode. This condition may require an anodic potential to return to the polymer to a conductive state for further polymerization. All of these possibilities bring up the critical decisions that separate the potentiodynamic polymerization. Before beginning a polymerization, it must be decided at what scan rate and between which potentials will the polymerization be accomplished. If the electrode is used to measure the oxidation and reduction of the monomer, it is likely that a thin layer of polymer will form on the very first sweep. A fresh electrode is required for each diagnostic scan and polymerization if the desired polymer is to be synthesized from one reaction rather than layers of independent polymer films.

Figure 2.4 demonstrates the typical experimental progression for a potentiodynamic polymerization of a novel monomer. In the first scan, only the electrolyte and solvent are scanned with the electrodes. Typical conditions include a Pt button electrode, a Ag wire reference electrode, and a stainless steel sheet counter electrode in 0.1M TBAPF<sub>6</sub> in dichloromethane or similar solvent. A scan rate of 100 mV/s is appropriate for button electrodes while larger electrodes require slower scan rates. The oxidation and reduction limits are expanded with each test of one cycle to observe the limits for solvent breakdown as demonstrated in Figure 2.4a. In the figure, the flat region between -0.8 and 1.5V represent the available electrochemical window of the solvent. The lack of oxidation and reduction peaks in that region, combined with the small magnitude of the current response, indicates a clean electrode and solvent.

Following the solvent scan, a few milligrams of ferrocene would be dissolved in the solution and a scan would run with much narrower limits to observe the oxidation and reduction of the ferrocene. It is found that ferrocene is typically oxidized within a few hundred millivolts of the open circuit potential. A well polished electrode and clean

electrolyte will show a close spacing (58 mV in a perfect one electron system)<sup>7</sup> between the oxidation peak and reduction peak of the ferrocene. The  $E_{1/2}$  value, which is used to calibrate the reference electrode, is the arithmetic mean of the two potentials, or 0.488 V in Figure 2.4b.

Following the ferrocene scan, the solution is removed, the electrodes are rinsed, and a fresh solution containing solvent, electrolyte and typically 1.0 mM monomer is placed in the cell. Observation of the oxidation peak for the monomer is made by sequentially scanning further in the oxidative or anodic potentials until a peak is observed, as depicted in Figure 2.4c. The presence of a peak demonstrates the kinetic limitation of monomer diffusion to the electrode. Absent the limiting concentration of monomer, the current would increase with the potential beyond the oxidation potential of the monomer. Once the diffusion of monomer reaches a maximum, however, the monomer supply cannot be replenished in time for reaction and the concentration of neutral monomer at the electrode falls to zero. This point is critical in designing both the potentiostatic and galvanostatic polymerizations as it presents the point above which unwanted reactions will occur. In practice, a polymerization potential below the peak but sufficiently above the baseline is preferred.



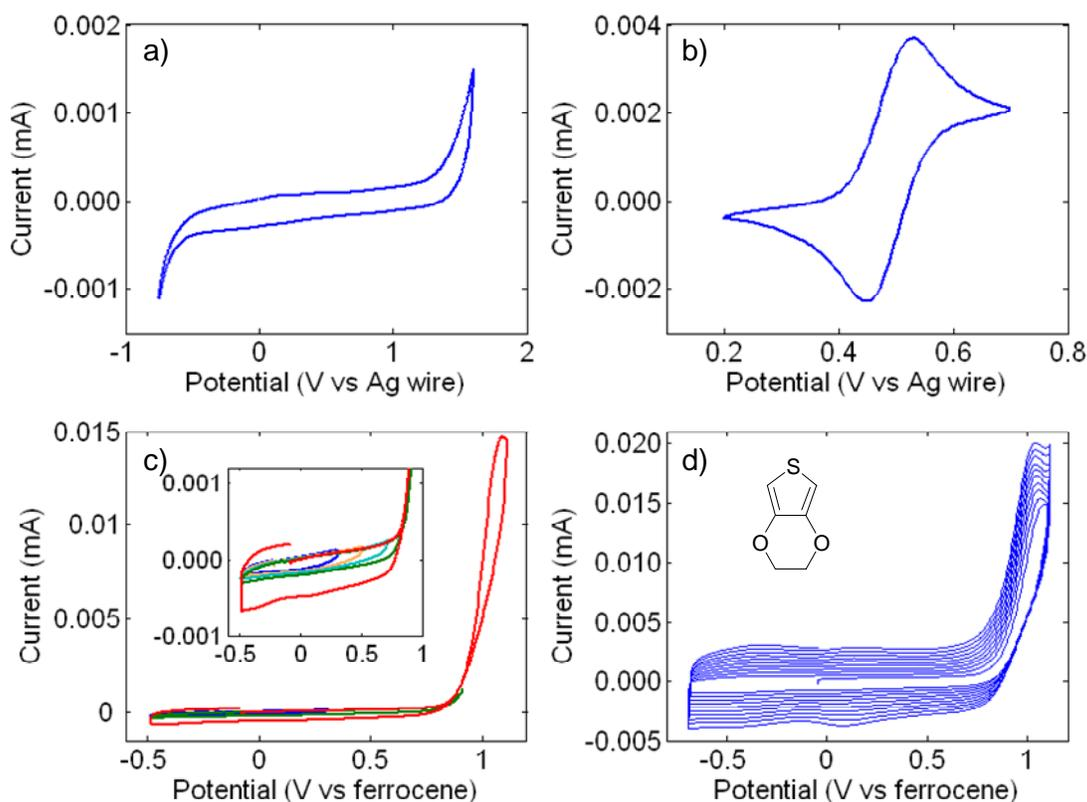


**Figure 2.4.** Potentiodynamic polymerization protocol for EDOT monomer in dichloromethane. Initial scan of solvent and electrolyte (a), followed by ferrocene scan (b), monomer oxidation search (c), and polymerization (d).

In Figure 2.4c, the oxidation of the monomer begins at 1.1 V versus ferrocene with the inset depicting the successive tests increasing in potential to observe the monomer oxidation.. As is shown in Figure 2.4d, the oxidation peak is not resolved until the potential is scanned to 0.6 V versus ferrocene. With each subsequent scan, the oxidation and reduction currents increase, indicating the addition of polymer to the electrode. Note that the broad oxidation and reduction of the polymer are not observed in the first peak and that the monomer oxidation is not coupled to a reduction. In the polymerization reaction, the coupling reaction forming polymer is faster than the reduction of the monomer, so the cyclic voltammogram indicates greater oxidation than reduction.

### **2.3.4 Galvanodynamic Polymerization**

The limitations of potentiodynamic methods are overcome with a time varying current waveform, termed galvanodynamic. In formulating a galvanodynamic waveform, it is desirable to retain all of the advantages of the techniques described above. Specifically, it is useful to obtain a polymerization that is steady in time and does not require periodic increasing of the potential window to correct for electrode passivation. The current controlled method allows the potential to rise to a suitable value for the reaction rate determined by the Faraday law and discussed in Section 2.3.2.

The second objective in improving the current controlled polymerization is the periodic reduction of the film that allows the improved proton elimination step in the polymerization. The current controlled analog of the potentiodynamic sweep is not sufficient to meet these conditions. Even if the current magnitudes were kept low enough not to exhaust the monomer concentration, eventually enough polymer would be on the electrode to simply charge and discharge with the cycled current. In order to sustain polymerization, there must be more oxidation than reduction over the course of the experiment to account for the oxidation of additional monomer.

Combining the two objectives, a brief mode of constant current coupled with the swept current ensures that charge and polymer are accumulated on the electrode over time. The shape of such a waveform is shown in Figure 2.5. The potential response to such a waveform, also shown in Figure 2.5, for a few cycles, is a combination of the galvanostatic response with a higher frequency oscillation superposed.

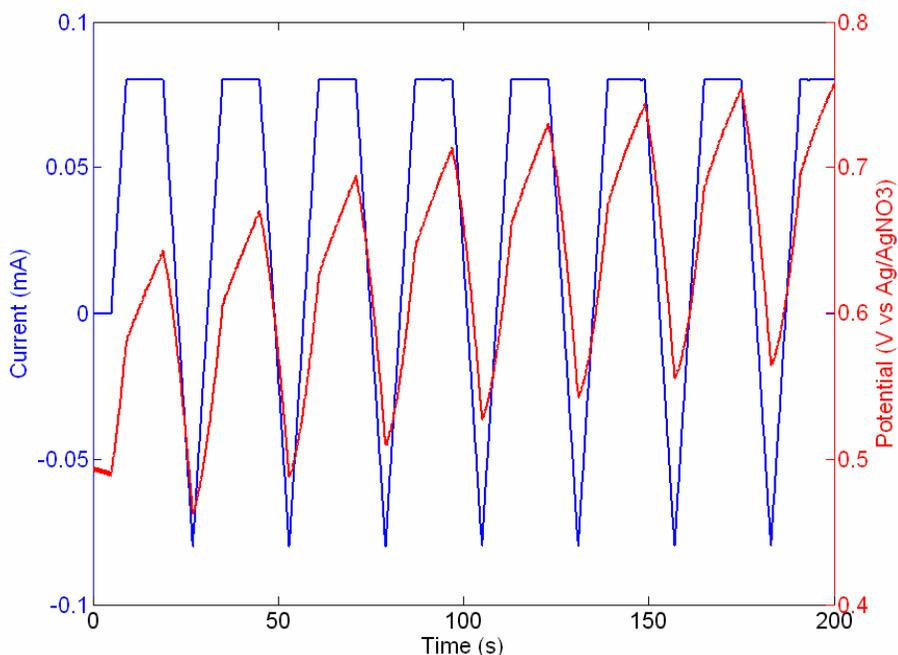


**Figure 2.5.** Galvanostatic deposition waveform and potential response for oligomer **P-1**.

The oscillation in current allows for reduction and oxidation of the polymer during a polymerization. Furthermore, this technique has been successfully used to grow films of novel monomers, such as the one depicted in Figure 2.5, when no other technique listed above would work. The development of this polymerization technique demonstrates the combination of two different electrochemical techniques used in polymerization. The combination of constant current and swept current represents a new way to approach polymerizations and one that highlights the availability of new techniques. The parameter space for electrochemical polymerization is already wide enough without changing the nature of the waveforms, though selective waveform generation may enable the successful synthesis of numerous novel conducting polymer systems.

## 2.4 Summary

Conducting polymers can be synthesized chemically and electrochemically, preserving the conjugated structure of the monomer and generating high molecular

weight polymer when successful. Chemical polymerizations require high polymer solubility for good conversions, while electrochemical polymerizations utilize the electrode interface for polymerization of insoluble polymers. As with other polymerizations, many different techniques are used in electrochemical polymerizations including constant and time varying potential and current experiments. Potential control is used to set the driving force and measure the potential at which a monomer will oxidize and react. Current control sets a rate of reaction allowing for any reaction to occur in order of lowest potential. Small scale tests such as cyclic voltammetry are used to observe the oxidation of monomer and oxidation and reduction of polymer. As desired thicknesses increase, however, the utility of cyclic voltammetry decreases. Conventional conducting polymers such as polypyrrole and poly(3,4-ethylenedioxythiophene) are readily polymerized at constant potential or current. Careful consideration of the current requirements has led to the development of an electrochemical technique that can be used to synthesize novel conducting polymers.

## 2.5 Experimental

**2: 5-(Tributylstannyl)-2-2'-bithiophene.**<sup>4</sup> 2-2' bithiophene ( 3.49 g, 0.0210 mol) was dissolved in THF (100 mL) and cooled to -78° C. n-Bu Li (1.15 eq, 0.0242 mol) was added dropwise to the solution, followed by SnBu<sub>3</sub>Cl (1.35 eq, 0.0284 mol). The solution was allowed to warm to room temperature and stirred for an additional 6 hours. Following solvent evaporation, the product was dissolved in hexanes and filtered. Further purification was performed in a Kugelrohr distillation apparatus. Product eluted at 240 °C to give 24% yield. <sup>1</sup>H NMR (CDCl<sub>3</sub>, ppm): 7.31 (d, 1H), 7.20 (2d, 2H), 7.08 (d, 1H), 7.03 (t, 1H), 1.60 (m, 6H), 1.35 (m, 6H), 1.14 (t, 6H), 0.96 (m, 9H).

**4: 1,4-diiodo-2,5-dimethoxybenzene.**<sup>2,3</sup> 1,4-dimethoxybenzene (16.06 g, 0.116 mol), I<sub>2</sub> (1.1 eq, 0.129 mol), and KIO<sub>3</sub> (0.4 eq, 0.0465 mol) was dissolved in a 50 mL solution of 1:10:10 H<sub>2</sub>SO<sub>4</sub>:H<sub>2</sub>O:AcOH. The solution was refluxed for 6 hours and quenched in 2.0 M KOH (500 mL) after cooling to room temperature. The precipitate was recrystallized in EtOH. 74% yield. <sup>1</sup>H NMR (CDCl<sub>3</sub>, ppm): 7.20 (s, 2H), 3.84 (s, 6H).

**5: 1,4-diiodo-2,5-hydroquinone.**<sup>3</sup> Compound **4** (10.37 g, 0.0266 mol) was dissolved in CH<sub>2</sub>Cl<sub>2</sub> (500 mL) and cooled to -78 °C. BBr<sub>3</sub> (2 eq, 0.0532 mol) dissolved in CH<sub>2</sub>Cl<sub>2</sub> (53.2 mL) was added dropwise through a condenser, which was replaced with a drying tube. The solution was allowed to warm to room temperature and stirred for 48 hours. The solution was quenched with ice-water mixture and precipitate was collected and used without further purification. quantitative yield. <sup>1</sup>H NMR (Acetone-d<sub>6</sub>, ppm): 7.30 (s, 2H), 8.73 (s, 2H).

**5: 1,4-diiodo-2,5-bis(2-(2-(2-hydroxyethoxy)ethoxy)ethoxy)benzene.** Compound **5** (4.00 g, 0.0111 mol) in DMF (50 mL) was slowly added to a solution of K<sub>2</sub>CO<sub>3</sub> (8 eq, 0.0888 mol) in DMF (50 mL) stirring at room temperature. The solution was stirred for an additional 30 min, followed by a slow addition of 2-(2-chloroethoxy)-ethoxy-ethanol (4 eq, 0.0444 mol) in DMF (50 mL). The solution was heated to 75 °C and stirred for 3 days. The crude product was dissolved in dichloromethane and washed with HCl (pH 2.0). Product further purified by column chromatography (EtOAc). 23 % yield. <sup>1</sup>H NMR (CDCl<sub>3</sub>, ppm): 7.26 (s, 2H), 4.14 (t, 4H), 3.92 (t, 4H), 3.81 (m, 4H), 3.74 (m, 8H), 3.65 (m, 4H).

**7: 1,4-bis(2-2'-bithiophene)-2,5-bis((2-(2-(2-hydroxyethoxy)ethoxy)ethoxy)benzene).**<sup>4</sup> Compound **6** (0.522 g, 0.833 mmol) was dissolved in DMF (70 mL). Pd(PPh<sub>3</sub>)<sub>2</sub>Cl<sub>2</sub> (0.05 eq, 0.0416 mmol) was added, followed by Compound **2** (4 eq, 3.33 mmol). The solution was stirred for 6 days at 100 °C. The crude product was washed with twice with KF and twice with NH<sub>4</sub>Cl. The product was recrystallized from a minimum of CH<sub>2</sub>Cl<sub>2</sub> in hexanes. 55 % yield. m.p. 142 °C. <sup>1</sup>H NMR (CDCl<sub>3</sub>, ppm): 7.51 (d, 2H), 7.30 (s, 2H), 7.25 (m, 4H), 7.20 (d, 2H), 7.06 (t, 2H), 4.32 (t, 4H), 4.00 (t, 4H), 3.80 (m, 4H), 3.73 (m, 8H), 3.62 (m, 4H).

**P-1: poly(1-4-bis(2-2'-bithiophene)phenylene-co-butanediol).** Compound **7** (0.112g, 1.58 mmol) and diisocyanate terminated poly(butanediol) Mn 900 (1eq, 1.58 mmol) was dissolved with Fe(acac)<sub>3</sub> (0.005 eq, 7.9 × 10<sup>-7</sup> mol) in THF (15 mL). The

solution was stirred at 85 °C for 48 hours and allowed to cool. The brown solid was characterized by GPC (Mw 6000, THF, polystyrene standard).

## 2.6 References

1. Moratti, S. C. The Chemistry and Uses of Polyphenylenevinylenes. In *Handbook of Conducting Polymers*. Skotheim, T.A; Elsenbaumer, R. L.; and Reynolds, J.R. Eds.; Marcel Dekker: New York, 1998; 2<sup>nd</sup> Ed.
2. Bailey, G. C.; Swager, T. M. Masked Michael Acceptors in Poly(phenyleneethynylene)s for Facile Conjugation. *Macromolecules* **2006**, *39*, 2815-2818.
3. Zhou, Q.; Swager, T. M. Fluorescent Chemosensors Based on Energy Migration in Conjugated Polymers: The Molecular Wire Approach to Increased Sensitivity. *J. Am. Chem. Soc.* **1995**, *117*, 12593-12602.
4. Yu, H.-H. Molecular Actuators: Design, Syntheses and Applications toward Actuation and Sensory Materials. Ph.D. Thesis, Massachusetts Institute of Technology, Cambridge, MA, 2003.
5. Ayad, M. M. Influence of HCl on polypyrrole films prepared chemically from ferri chloride. *J. Polym. Sci., Part A: Polym. Chem.* **1994**, *32*, 9-14.
6. Pickup, P. G. Electrochemistry of Electronically Conducting Polymer Films. In *Modern Aspects of Electrochemistry*; White, R. E.; Bockris, J. O'M.; Conway, B.E. Eds. No. 33; Kluwer Academic / Plenum Publishers, New York, 1999; 549-597.
7. Bard, A. J.; Faulkner, L. R. *Electrochemical Methods, Fundamentals and Applications*, 2<sup>nd</sup> ed.; Wiley & Sons, New York 2001.
8. Sawyer, D. T.; Sobkowiak, A.; Roberts J. L. Jr.; *Electrochemistry for Chemists*, 2<sup>nd</sup> ed.; Wiley & Sons, New York, 1995.
9. Zhou, M.; Heinze, J. Electropolymerization of pyrrole and electrochemical study of polypyrrole. 3. Nature of "water effect" in acetonitrile. *J. Phys. Chem. B* **1999**, *103*, 8451-8457.
10. Bof Bufon, C. C.; Vollmer, J.; Heinzl, T.; Espindola, P.; Hermann, J.; Heinze, J. Relationship between chain length, disorder, and resistivity in polypyrrole films. *J. Phys. Chem. B* **2005**, *109*, 19191-19199.

### **3. Characterization of Conducting Polymers**

The characterization of most conducting polymers is limited to the measurement of bulk properties of films and coatings. There is often difficulty in obtaining a freestanding film and a typical result was presented in Figure 2.1. As discussed in Chapter 2, once a polymer is deposited on an electrode it is typically insoluble. Whether the insoluble characteristics of the films are derived from chemical or physical cross-linking on the electrode, the material peeled off for actuation tests is not readily dissolved in any solvent. The insolubility limits the availability of molecular weight measurements, NMR analyses, and other solution-based characterization techniques. Various spectroscopy experiments such as x-ray and electron diffraction allow for detailed structure analysis at small scales. Thus, current research has not produced a clear picture of conducting polymer structures or structure-property relationships. For conducting polymer actuators, the actuation properties are the most widely studied.

While the limitations in characterization provide numerous hurdles for conducting polymer actuator research, there is not a shortage in alternative characterization techniques. Furthermore, the bulk properties that can be measured including the electrical conductivity and mechanical properties are utilized in understanding the actuation response in conducting polymers. Beginning with the electrical characterization, Section 3.1 outlines the various conductivity tests utilized in thin films. Section 3.2 outlines the passive mechanical characterization, leaving the active mechanical characterization for Chapter 4. Since conducting polymer actuators are stimulated electrochemically, multiple electrochemical characterization techniques are used and some have been developed to further examine the response of films to electrochemical stimuli. Electrochemical characterization comprises Section 3.3.

#### **3.1 Electrical Characterization**

Electrical conductivity in polymers is the focus of numerous books and reviews and was the topic of the research for which the Nobel Prize in Chemistry of 2000 was awarded. At its outset, the discovery of metal-like conductivity in poly(acetylene) led to



the development of the field.<sup>1</sup> Furthermore, when the conductivity of materials is compared on a per mass basis, conducting polymers are more favorable due to relatively low densities. Thus, for a given current carrying application, conducting polymers often offer a low cost and low weight solution.

Conductivity on the individual chain level is simple to imagine, yet complex in practice. The very nature of the conjugated backbone in conducting polymers suggests an electron mobility based on the sharing of  $\pi$  electrons as was discussed in Chapter 1. This topic is covered well by Roth, who demonstrates that the free electrons alone are not sufficient for good conductivity.<sup>2</sup> Due to the Peierls distortion, which localizes electron pairs, conducting polymers require defects or dopants to carry charge over long distances. Similar to the band structure of semi-conductors, it is the presence of dopants in conducting polymers that enable conductivity. Conducting polymers at high levels of doping are capable of supporting one ionic dopant molecule every three or four monomer units. This doping level can be obtained during electrochemical synthesis as discussed in Chapter 2. The dopant level can be controlled electrochemically, making the in-situ measurement of conductivity a relevant topic and one covered in this chapter. Chemical dopants such as  $I_2$  may also be used to enhance conductivity, though the relative concentrations and dedoping processes are difficult to control. Chemical dopants can be used to enhance conductivity in a polymer that will undergo further electrical or electrochemical treatment.

The interchain conductivity is more difficult to visualize than conductivity in the single chain case because no direct electrical contact exists between chains. This conductivity is necessary, however, since conducting polymers sustain electrical currents beyond the nanometer and single chain scale. Whether the mechanism is based on hopping or tunneling between individual chains or dependent on percolation between domains of highly organized chains, the evidence of good interchain communication lies in the bulk conductivity of the material. Virtually all distances probed by typical electrical measurement devices even to the micron scale test only the bulk conductivity. Other techniques such as high frequency (microwave) measurement techniques do test

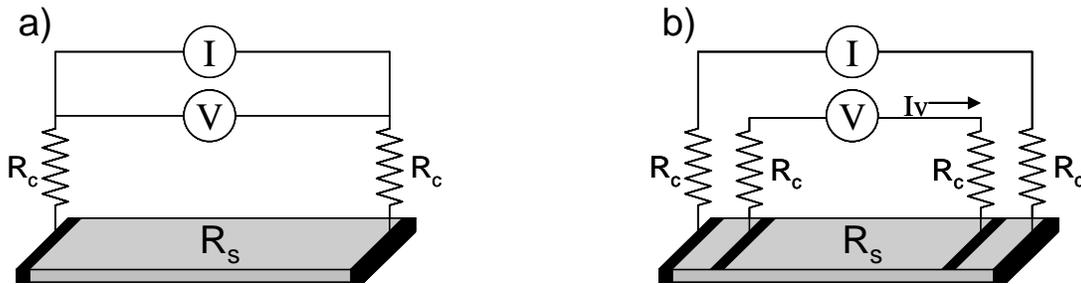
smaller length scales but with limited applicability to practical devices. The typical standard for “good” conductivity of conducting polymer is 100 S/cm, or  $1 \times 10^4$  S/m with the unit Siemens equivalent to  $\text{Ohms}^{-1}$ .

In principle, the measurement of electrical conductivity is very simple. Given a wire or bar of uniform cross sectional area  $A$  with constant current  $I$  passing through the cross section, the voltage  $V$  at a given length  $L$  determines the conductivity by

$$\rho = \frac{I L}{V A} = \frac{L}{R A}, \quad 1$$

where  $R$  in Ohms may be substituted for  $V/I$  in a DC resistance measurement.

A two-point measurement utilizes the same probes for current input and voltage measurement, as depicted in Figure 3.1a. The single contacts add error to the measurement by the contact resistance between the probes and sample. The contact resistance can be overcome by making a four-point connection with the input current. As depicted in Figure 3.1, the addition of the voltage probes in a four-point measurement significantly reduces the effect of the contact resistance since the voltage drop across the contact is proportional to the current through the contact. A voltage measurement requires very little current ( $I_v \ll I$ ), so the voltage drop across the contacts is negligible.



$$\frac{V}{I} = \frac{I(2R_c + R_s)}{I} = 2R_c + R_s$$

$$\frac{V}{I} = \frac{I_v(2R_c) + I R_s}{I} = R_s \text{ for } I_v \ll I$$

**Figure 3.1.** Comparison between two-wire (a) and four-wire (b) resistance measurement based on current  $I$ , voltage  $V$ , sample resistance  $R_s$  and contact resistance  $R_c$ . In the four wire resistance measurement, the current in the voltage measurement is smaller, which reduces the effect of the contact resistance.

Other conductivity schemes with appropriate equations for bulk conductivity are shown in Figure 3.2. Of the methods depicted, the four-wire contact method is the most straightforward because the current is assumed to be constant throughout the cross section of the material. This makes the direct application of Equation 1 possible.

More complicated geometries rely on assumed current paths between the probes. For the commonplace four-point method, the current density is assumed to be in concentric arcs, either in two dimensions for a thin film or in three dimensions for a thick film. It is important to record the method of conductivity measurement with the value for reference and to note of the assumptions in the measurement.

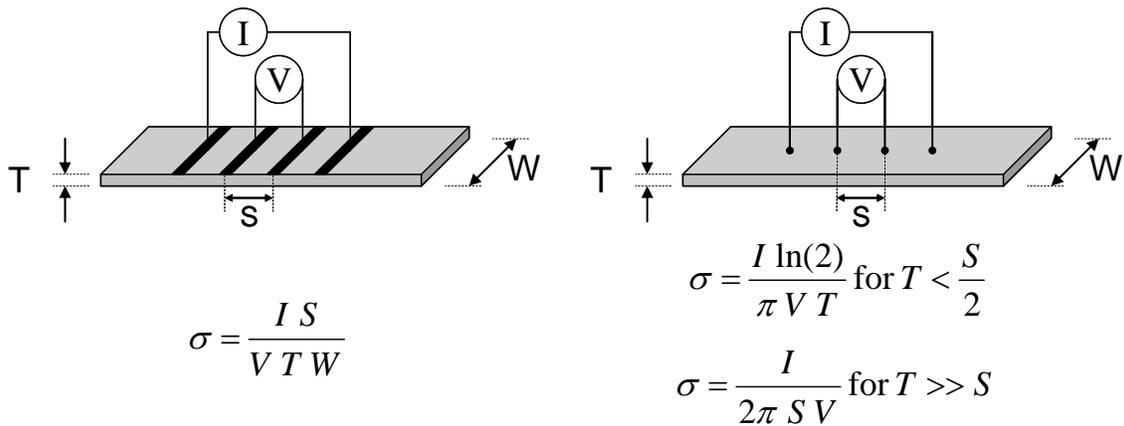


**Figure 3.2.** Conductivity ( $\sigma$ ) measurement configuration and equations for four-wire and four-point methods for a film of width  $W$ , thickness  $T$ , and electrode spacing  $S$ .

In 1958, van der Pauw developed a method for measuring the electrical conductivity of semiconductors without the need for precise geometrical measurements aside from the thickness.<sup>3</sup> In this measurement scheme depicted in Figure 3.3, contact is made on the corners of a sample and the current and voltage probes are applied in each of the 90 degree rotations. The conductivity is measured by solving the equation in the figure.

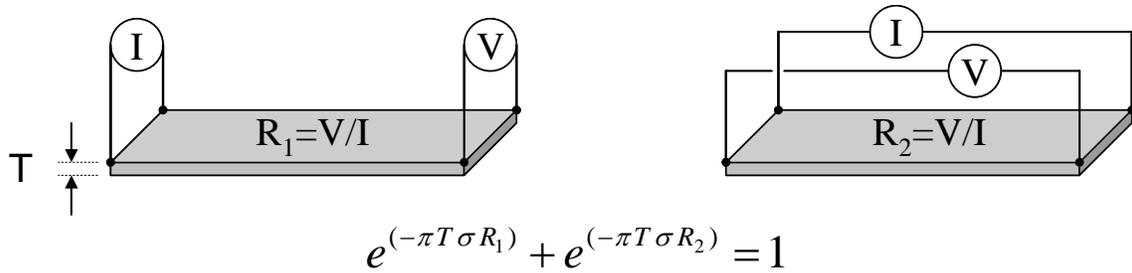


**Figure 3.3.** Schematic diagram and equation for van der Pauw conductivity measurement technique for a sample of thickness  $T$ .

Figure 3.4 depicts a measurement device manufactured for the van der Pauw technique. The spring loaded probes, at 3mm centers, should be placed at the corners of a 3 mm square film mounted on an insulating substrate (typically a piece of tape). Four independent four-wire resistance measurements are made with the redundant 180 degree rotations used to verify good connectivity in the sample. The equation is solved for the resistance and the thickness by Newton's method (see Appendix A for MATLAB code used), which gives the bulk conductivity. The use of this simple device in conjunction with a hand-held micrometer has improved the repeatability of conductivity measurements, though it cannot be used to measure anisotropies in the conductivity.

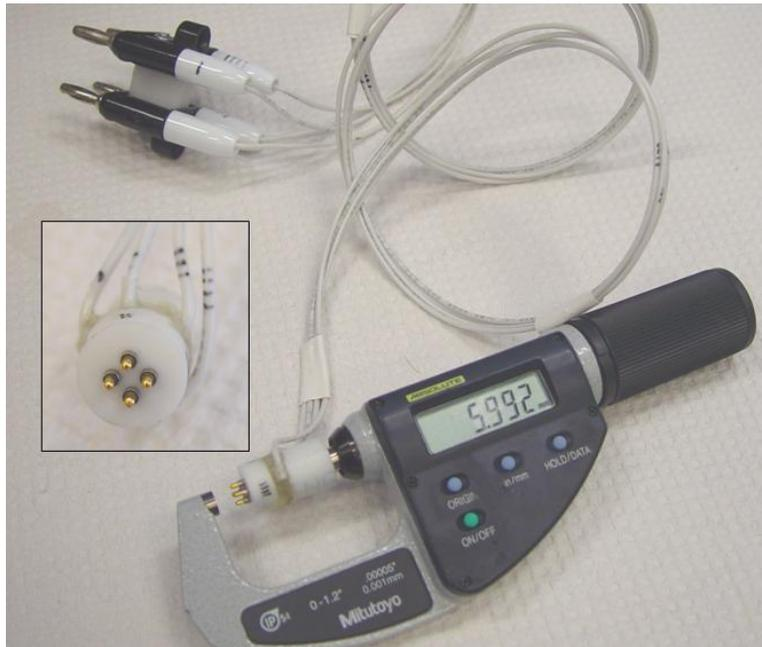


**Figure 3.4.** Van der Pauw conductivity probe fitted to hand-held micrometer.

## 3.2 Mechanical Characterization

The mechanical behavior of conducting polymers does not differ significantly from most polymers, though the apparent cross-linking that complicates traditional characterization methods also confounds the observation of mechanical properties. For example, the glass transition temperatures of well-known conducting polymers are not as deterministic as in their non-conductive cousins. The polymers can be modeled by traditional viscoelasticity with an array of time constants and glassy and rubbery moduli for simple step and linear experiments. Dry films peeled from an electrode typically exhibit moduli in the range of 100 to 1000 GPa with relaxation time constants of less than one second. The use of solvents and electrolytes in many tests, however, demonstrates the dependence of mechanical properties on the environment. With actuating polymers, it is known that individual ions and solvent molecules penetrate the polymer deeply. The effect of this swelling in electrolyte undoubtedly affects the interchain mechanical properties often demonstrated by a decrease in modulus by a factor of two and an increase in relaxation time constant to several seconds. Furthermore, the oxidation and reduction of the polymer also affects the modulus of the polymer greatly, as will be discussed in Chapter 4.

The effect of an applied potential on the material properties can also be seen during a mechanical test at constant force. Under typical test conditions, the polymer will be at constant length for a given force. Once the electrochemical waveform is applied, additional elongation, or creep, is observed. This plastic deformation between tests is an impediment to application of conducting polymer actuators if they are to operate under a stable set of mechanical conditions. It also confounds test results because a polymer that does not return to its original length could be considered to have a new rest length and possibly new rest thickness and width. The temptation to measure each sample between each test is nullified by the observation that each test invariably affects the polymer, suggesting that all tests should be performed with a fresh film. If testing continues to a point of reasonable repetition of performance, it is imperative that the test history of the sample be recorded.

### 3.3 Electrochemical Characterization

Electrochemical characterization of conducting polymers consists of a wide battery of tests applied to conducting polymers while in electrolyte solution. Excellent reviews on the subject have been written by Heinze<sup>4</sup> and Pickup.<sup>5</sup> Cyclic voltammetry is often used to assess the basic transport properties of a conducting polymer film or coating, though the simplicity of single electron transfers are not seen in polymers since polymers typically present an array of time constants to many processes including electrochemical behavior. While much of the community works exclusively with electrodes with polymer coatings less than one micrometer thick, the electrochemistry of freestanding films is complicated by finite conductivity and transport through the length of the film. For polymers that span a gap between electrodes, additional information can be gained about transport in the bulk film. One such typical test is the in-situ conductivity test in which each end of the polymer is modified independently and assumptions are made about the connectivity through the bulk. Cyclic voltammetry and in-situ techniques will be discussed in the Sections 3.3.1 and 3.3.2.

One popular technique that directly measures the ion ingress and egress in a thin polymer film utilizes an Electrochemical Quartz Crystal Microbalance, or EQCM. EQCMs measure the mass change of the electrode as a function of potential. Techniques using frequency modulation to measure transport phenomena as a function of frequency have also been applied to conducting polymers. The most popular technique in this area is Electrochemical Impedance Spectroscopy, in which a sinusoidal potential wave of varying frequency is applied to the electrochemical cell. Making use of an equivalent circuit, useful deductions about the properties of a given polymer are often made. The last electrochemical technique to be discussed is a hybrid technique combining EQCM and impedance spectroscopy in which the frequency dependence of mass change in the polymer can be detected. This technique is useful in demonstrating the bandwidth for electrochemical processes in conducting polymers.

### 3.3.1 Cyclic Voltammetry

The common synthesis technique described in Section 2.3.3 can also be used to characterize conducting polymers. With suitable conditions and reference, the oxidation and reduction of a polymer film can be observed, as can any redox couples located within the film. The additional material volume and finite conductivities broaden the relative electrochemical peaks. Furthermore, as polymer films are peeled from the electrode, the currents and potentials propagate through the length and thickness of the film. The size limitations can be accommodated by accounting for the larger capacitances in the interfaces and larger resistances through the length of the film. One example of the length effect of finite conductivity in conducting polymers was derived by Madden for polypyrrole<sup>6</sup> and holds for any conducting polymer on suitable length scales. Low conductivity in polymer actuator applications may lead to the improper conclusion that entire film is activated when only the section nearest electrical contact is responding to stimulus.

Beyond the relative locations of oxidations and reductions of the polymer film, a sense of its capacitance can be gained from the separation in the current between anodic and cathodic sweeps. Though this capacitance is dependent on potential, the voltammogram elucidates the range over which many of the assumptions regarding actuation can be made. From the potential sweep rate  $\nu$  and cell current  $I$ , the voltammetric capacitance is given by

$$C_{CV} = \frac{I}{\nu}, \quad 2$$

though the average of the anodic and cathodic currents at a given potential are usually used.<sup>7</sup> The capacitance is relevant because it measures the ability of the polymer film to take up ions, a factor that is relevant to ion swelling actuation. The polymer is only active in the region in which it demonstrates a capacitance. As an example, Figure 3.5 shows the capacitance of poly(3,4-ethylenedioxythiophene), or PEDOT, synthesized in dichloromethane. The polymer exhibits a broad capacitive region during a scan rate dependence test, with very sharp transitions from oxidation to reduction. These sharp transitions also indicate high conductivity and fast transport, all of which combine to make PEDOT a useful conducting polymer actuator (discussed in Chapter 5).

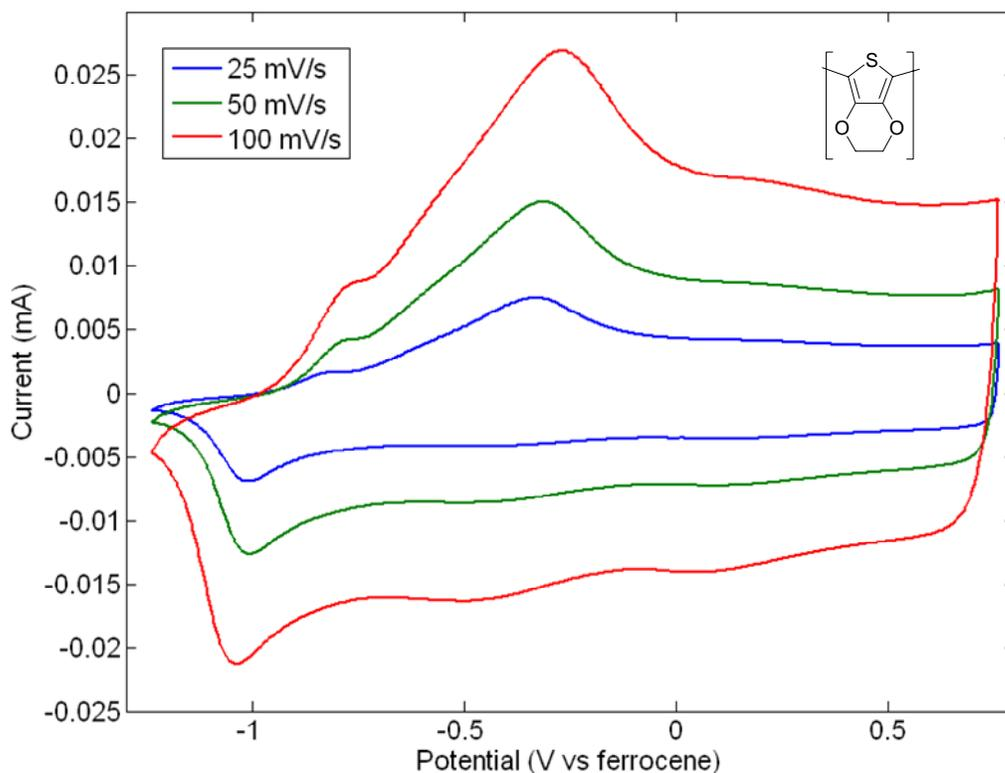


**Figure 3.5.** Cyclic voltammogram of PEDOT potentiodynamically synthesized from 1.0 mM monomer in 0.1 M TBAPF<sub>6</sub> in dichloromethane. Scan rate test also in 0.1 M TBAPF<sub>6</sub>/dichloromethane.

Further information regarding the ion transport in a conducting polymer film can be observed by examining the rate dependence of the current during a cyclic voltammogram. For a set of scan rates, a linear dependence of the current magnitude on the square root of the scan rate is indicative of diffusion limited transport.<sup>8</sup> Diffusion limitations are expected, though other kinetic limitations such as conductivity and passivation can slow the response of the polymer.

### 3.3.2 In-situ testing

In-situ testing is the measurement of a polymer property during an electrochemical test. One of the most relevant tests is the in-situ conductivity test, first developed by Kittlesen et al.<sup>9</sup> The principle of an in-situ conductivity test is depicted in the schematic shown in Figure 3.6.



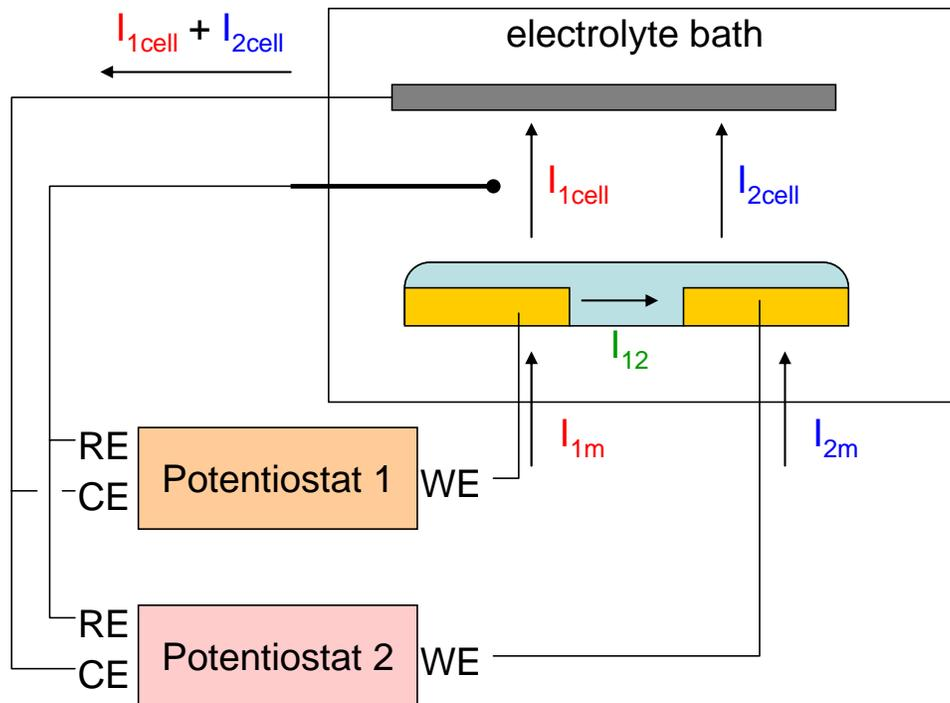


**Figure 3.6.** Schematic of in-situ conductivity test with two potentiostats serving as bipotentiostat for a polymer spanning a gap between two electrodes. RE, CE, and WE represent the reference electrode, counter electrode, and working electrode respectively.

In the figure above, the currents are represented by arrows and labeled according to the unknown currents in the electrochemical cell ( $I_{1cell}$  and  $I_{2cell}$ ) and measured currents ( $I_{1m}$  and  $I_{2m}$ ). For in-situ conductivity test, the potential is scanned relative to the reference electrode in a similar fashion to the cyclic voltammetry experiment, though often at a slower scan rate and with a constant potential offset (typically 10 to 20 mV) between the two working electrodes. The relevant parameters to the conductivity of the polymer spanning a gap between two electrodes, corresponding to Equation 1, is the potential across the gap and the drain current, depicted  $I_{12}$  in the figure. From Kirchoff's rule,

$$I_{1m} = I_{1cell} + I_{12}, \quad 3$$

and

$$I_{2m} = I_{2cell} - I_{12}. \quad 4$$

Assuming uniform coverage of the polymer on each electrode and a small potential offset between the two working electrodes,

$$I_{1cell} = I_{2cell}, \quad 5$$

and

$$I_{12} = (I_{1m} - I_{2m})/2, \quad 6$$

which gives the drain current as function of the measured currents and the potential offset. The critical assumption that the cell currents are equal must be tested independently by scanning each electrode without connecting to the other. Furthermore, the validity of the measurement can be checked by solving for  $I_{1cell}$  and  $I_{2cell}$  from Equations 3 or 4 once  $I_{12}$  has been calculated. This calculation gives the CV portion of the in-situ measurement, as shown in Figure 3.7, and corroborates the independent measurements made with each electrode.

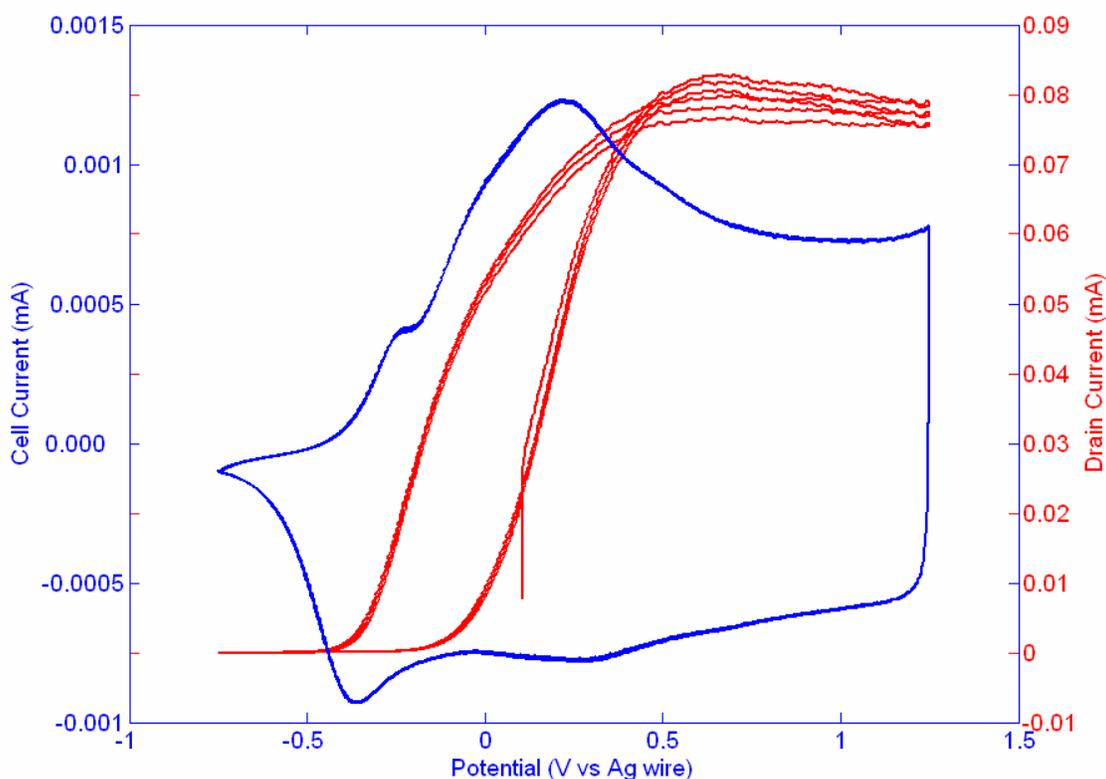


**Figure 3.7.** In-situ conductivity scan of PEDOT in 0.1 M TBAPF<sub>6</sub> in propylene carbonate at 10 mV/s.

In the figure, the CV is very repeatable while the drain current varies slightly between cycles. The drain current goes to zero when the polymer is reduced and increases and plateaus upon oxidation. The relative conductivity values depend on the precise geometries of the polymer coating, making quantitative measurement difficult,

especially with small scale electrodes. This test can also be carried out on a larger scale, though care must be taken to assure that the assumptions in the measurement hold.

### **3.3.3 Electrochemical Quartz Crystal Microbalance**

Thin polymer coatings can also be monitored for mass changes during an electrochemical experiment with an electrochemical quartz crystal microbalance, or EQCM. The principle of the EQCM measurement is based on the resonance of a quartz crystal coated with gold, which serves as the working electrode in an electrochemical cell. The crystal resonates at a frequency proportional to its mass allowing for a mass change of 5660 Hz  $\text{m}^2/\text{kg}$  in vacuum or 4200 Hz  $\text{m}^2/\text{kg}$  in aqueous solution measured with a 5 MHz crystal.<sup>8</sup> With a typical electrode area of 126.7  $\text{mm}^2$  (12.5 mm diameter), mass changes of 1  $\mu\text{g}$  produce a frequency change of 33 Hz and are readily measured.

This technique is popular for polymer coated electrodes, though the thickness of the polymer will affect the result as the polymer viscoelasticity and surface roughness interact with the viscous solution.<sup>10</sup> Thus, for films approaching thickness relevant to actuation, EQCM is not a valid technique. Despite the promise of ion intercalation prediction, results obtained from EQCM have not corroborated observed ion selectivity in poly(3,4-ethylenedioxythiophene).

### **3.3.4 Frequency modulation techniques**

As a great deal of the interest in characterizing conducting polymers is focused on the response speed to various stimuli, techniques employing frequency modulation are useful. In addition, the use of frequency modulation allows for a single experiment to verify information that might otherwise require a large number of experiments at different scan rates. Frequency modulation techniques range from the ubiquitous electrochemical impedance spectroscopy, or EIS, to novel characterization techniques utilizing the EIS instrumentation.

The topic of electrochemical impedance spectroscopy is very general and it is used experimentally in a wide range of materials and electrochemical systems. The text

edited by Macdonald is particularly helpful in understanding the fundamental techniques as well as the interpretation of results.<sup>11</sup> As with EQCM, the experiments are performed on polymer coated electrodes in order to obtain relevant information about ionic and electronic transport within the film.

The direct application of EIS to actuation is less straightforward once the films are grown sufficiently thick to be peeled from an electrode. In the case of EIS, a sinusoidal input (current or potential) with a varying frequency is applied and the complex impedance is measured. Most of the work with electrochemical systems is centered on the Randle's circuit, depicted in Figure 3.8 and utilized by Madden<sup>12</sup> in modeling the performance of polypyrrole.

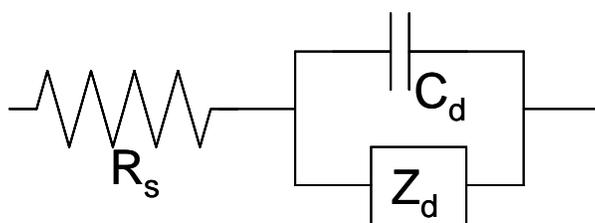


**Figure 3.8.** Randle's Circuit with solution resistance  $R_s$ , double layer capacitance  $C_d$  and polymer diffusion impedance  $Z_d$ .

The topic of equivalent circuits and the nature of the polymer impedance  $Z$  will be dealt with in Chapter 8. Here it suffices to introduce the concept of EIS to demonstrate its utility in generalizing the EQCM technique described above. Figure 3.9 depicts two experiments performed on poly(3,4-ethylenedioxythiophene) in 0.1 M TBAPF<sub>6</sub> in propylene carbonate. The experiment is a combination of EIS and EQCM in which the quartz crystal resonance is monitored while the frequency of the working electrode modulation is swept. The result indicates the frequency response range of the polymer film on the electrode. In Figure 3.9, frequencies above a few hundred mHz will not measure the potential dependence of the response. The bandwidth limitation is relevant for conducting polymers in general and actuators in particular as films are made increasingly thick.

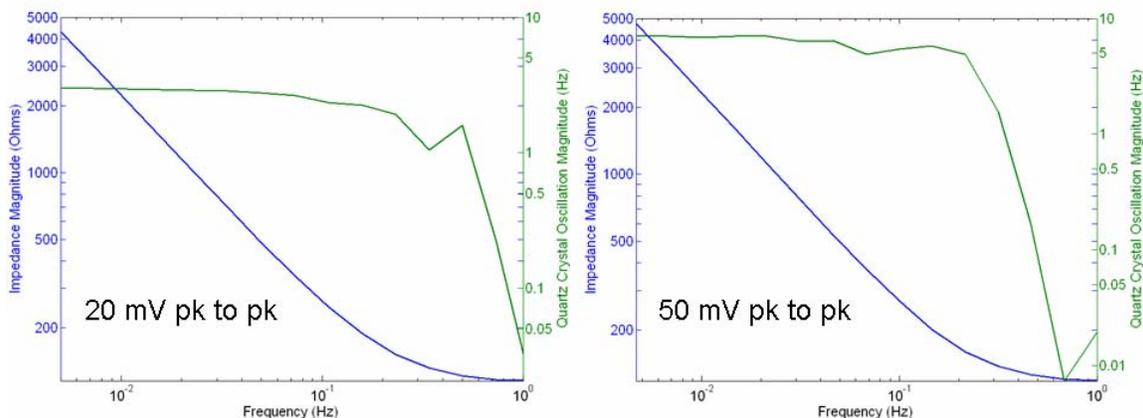


**Figure 3.9.** EQCM Impedance response of PEDOT in 0.1 M TBAPF<sub>6</sub> in propylene carbonate.

### 3.4 Summary

Once synthesized, conducting polymers are characterized by a wide array of tests despite the fact that many traditional polymer characterization techniques are not relevant. For conducting polymers to be used as actuators, a focus is placed on the bulk properties that will be relevant in application, particularly the electrical and mechanical properties. Electrochemical techniques provide a method for determining transport relations in the polymer as well as observing electrochemical doping and dedoping. Creative use of polymer coated electrodes enables numerous tests to be performed in-situ such as conductivity or mass change via EQCM. Adding the capabilities of frequency modulation has enabled new tests to be developed that probe the relevant time scales of traditional electrochemical experiments. While no test exists to accurately predict actuation behavior without testing actuation directly, a number of instrumental and experimental improvements have been shown to help with conducting polymer research. The topic of conducting polymer actuation characterization is covered in the next chapter.

### 3.5 References

1. Shirakawa, H.; Louis, E. J.; MacDiarmid, A. G.; Chiang, C. K.; Heeger, A. J. Synthesis of Electrically Conducting Organic Polymers - Halogen Derivatives of Polyacetylene, (CH)<sub>x</sub>. *J. Chem. Soc., Chem. Commun.* **1977**, 16, 578-580.
2. Roth, S. *One-Dimensional Metals*; VCH: New York, 1995.
3. Van der Pauw, L. J. A method of measuring the resistivity and hall coefficient on lamellae of arbitrary shape. *Phillips Technical Review* **1958/59**, 20, 220-224.
4. Heinze, J. Electrochemistry of Conducting Polymers. In *Organic Electrochemistry* M. Dekker, New York, 2001.
5. Pickup, P. G. Electrochemistry of Electronically Conducting Polymer Films. In *Modern Aspects of Electrochemistry*; White, R. E.; Bockris, J. O'M.; Conway, B.E. Eds. No. 33; Kluwer Academic / Plenum Publishers, New York, 1999; 549-597.
6. Madden, P. G. A. Development and Modeling of Conducting Polymer Actuators and the Fabrication of a Conducting Polymer Based Feedback Loop. Ph.D. Thesis, Massachusetts Institute of Technology, Cambridge, MA, 2003.
7. Bobacka, J.; Lewenstam, A.; Ivaska, A. Electrochemical impedance spectroscopy of oxidized poly(3,4-ethylenedioxythiophene) film electrodes in aqueous solutions. *J. Electroanal. Chem.* **2000**, 489, 17-27.
8. Bard, A. J.; Faulkner, L. R. *Electrochemical Methods, Fundamentals and Applications*, 2<sup>nd</sup> ed.; Wiley & Sons, New York 2001.
9. Kittlesen, G. P.; White, H. S.; Wrighton, M. S. Chemical Derivatization of Microelectrode Arrays by Oxidation of Pyrrole and N-Methylpyrrole: Fabrication of Molecule-Based Electronic Devices. *J. Am. Chem. Soc.* **1984**, 106, 7289-7396.
10. Inzelt, G.; Kertesz, V.; Nyback, A. S. Electrochemical quartz crystal microbalance study of ion transport accompanying charging-discharging of poly(pyrrole) films. *J. Solid State Electrochem.* **1999**, 3, 251-257.
11. *Impedance Spectroscopy. Emphasizing Solid Materials and Systems*. Macdonald, J. R. Ed.; Wiley & Sons, New York, 1987.
12. Madden, J. D. W. Conducting Polymer Actuators. Ph.D. Thesis, Massachusetts Institute of Technology, Cambridge, MA, 2000.

## 4. Characterization of Conducting Polymer Actuators

Linear actuators are characterized by active stress, active strain, strain rate, and work capacity. Measurement of the input energy also allows for characterization by efficiency, though the choice of input energy can make efficiency comparisons difficult. For example, skeletal muscle is highly efficient, with a chemical input energy that is locally stored in the form of ATP. For engineered materials, the input energy is typically electrical, and that electrical energy may be used to generate heat or a magnetic field. In the case of conducting polymer actuators, an electrical input energy drives an electrochemical system in which not all of the energy is used in the actuation mechanism. Thus, higher efficiencies can be attained if the remaining energy is harnessed (as it could be in the volumetric capacitance of the conducting polymer).

Typically, actuators are compared on the basis of achieved strain at a given stress. In this scheme, conducting polymers and skeletal muscle are considered large stroke soft actuators because they achieve more than 1% strain at stresses on the order of 1 MPa. In order to measure the actuation, the sample to be clamped into an apparatus capable of measuring and controlling both stress and strain. In practice this is often achieved with a stiff single-axis stage and load cell at either end of the sample. A versatile instrument focused on those two quantities can perform a battery of mechanical tests relating stress and strain, break strength, or frequency dependence. While numerous commercial instruments exist that focus on these material properties, few are well-suited to combine simultaneous input energy, especially in the form of electrochemical potential or current. As such, numerous electrochemical dynamic mechanical analyzers have been developed in the pursuit of conducting polymer actuator testing, with the most recent version depicted in Figure 4.1.

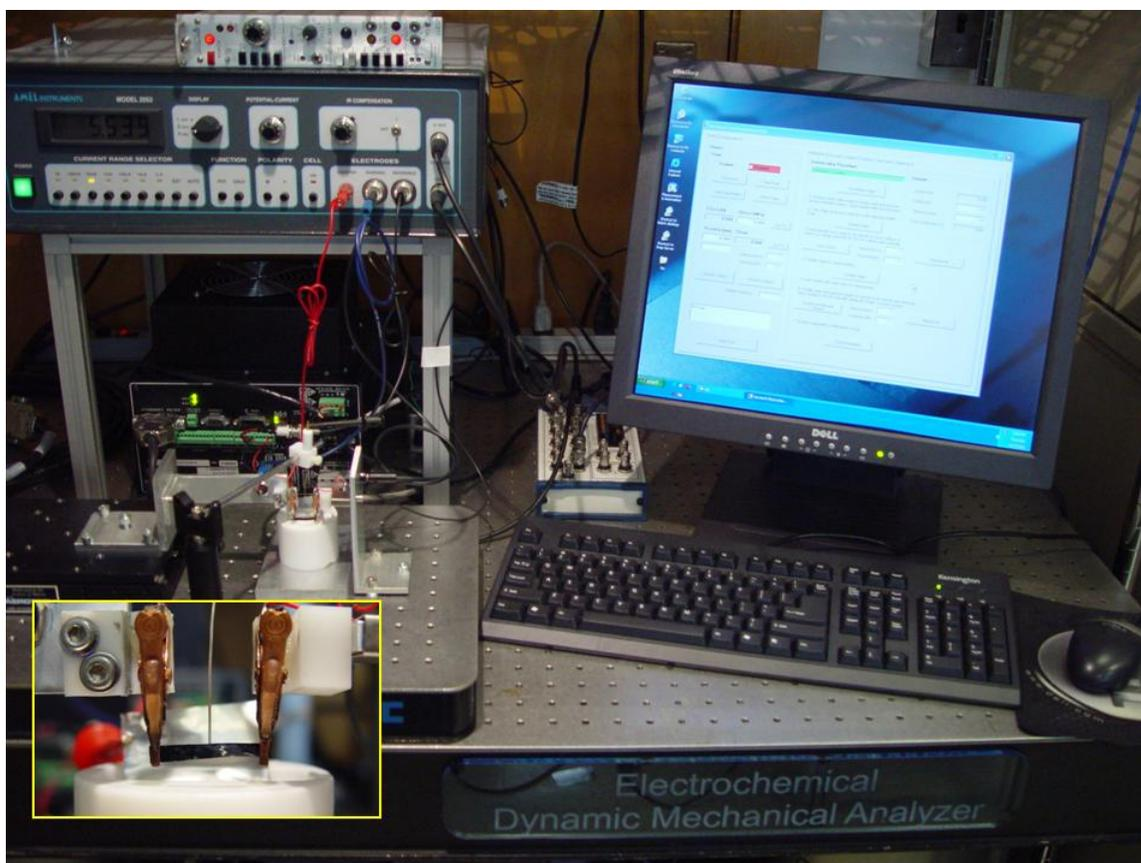


**Figure 4.1.** Electrochemical Dynamic Mechanical Analyzer used for testing conducting polymer actuators. Inset shows clamped sample suspended above the electrochemical bath.

## 4.1 Systematic View

In the case of the conducting polymer actuator active test, the inputs are exclusively electrochemical and are controlled via a potentiostat, with the polymer as working electrode, a suitable reference electrode, and large counter electrode. If potential is controlled, then current is measured and vice versa. Similarly one of the mechanical outputs is chosen for measurement with the other chosen as the control. This results in a two-input and two-output system. Measurements made at constant length are termed isometric and used to observe the generation of active stress. Measurements made and constant force are termed isotonic and used to observe the generation of active strain. In principle, constant force and length are not the only possibilities for testing, and much information could be gained from a more complicated investigation of actuation during dynamic mechanical loading.



There are two objectives addressed in the actuation test of a sample. First, it is desired to measure the ultimate actuation performance (strain and stress generation) that can be achieved with a given material. Second, it is desired to know the nature of the relationship between input and output. In the case of polypyrrole and poly(3,4-ethylenedioxythiophene), the proper input signal to examine is the charge, or the charge per unit volume in the electrochemical cell. The relation

$$\varepsilon = \alpha\rho, \tag{1}$$

in which the strain  $\varepsilon$  is proportional to a constant ratio  $\alpha$  and the charge per unit volume  $\rho$  has been observed.<sup>1</sup> Thus, in typical measurements, the potential, the current and the charge are plotted with the mechanical data. As will be shown below, plotting the mechanical measurand versus the charge will lead to a straight line indicating the magnitude of the strain to charge ratio  $\alpha$ . This parameter is derived from the ion swelling mechanism, relating a small strain in the sample for each ion that is inserted. Other actuation mechanisms, such as those discussed in Chapter 1, will not show the same dependence, which may prove useful in detecting their presence.

As in the case of electrochemical testing, control of potential at the working electrode is equivalent to controlling the driving force for actuation. At sufficient time scales and sufficiently small potential changes, the response of the polymer will be linear in response to voltage.<sup>2</sup> This observation will not hold, however, at extremes in potential. High potentials will lead to polymer degradation and reaction with solvent, electrolyte, or impurities. Low potentials will reduce the polymer and cause it to become insulating, thereby limiting electrical transport and actuation. Controlling the current in electrochemical systems is the equivalent of controlling the rate of response. The potential will rise to meet the rate requirement of the given current, often approaching the limits of potential in the system if care is not taken.

The relation between potential and current is affected by a number of factors present in the electrochemical system. The electrolyte bath acts as a resistance between the working and counter electrodes. The interface between polymer and solution behaves

as a capacitor thereby suggesting the common Randle's circuit equivalent for the electrochemical behavior of conducting polymer actuation as depicted in Figure 4.2.

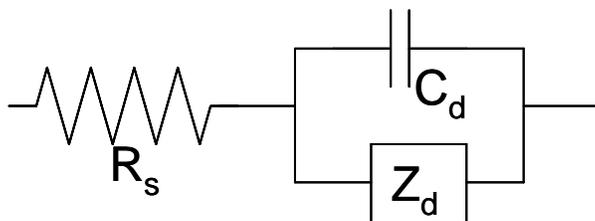


**Figure 4.2.** Randle's equivalent circuit used in conducting polymer actuator modeling.

In the figure above,  $R_s$  is the solution resistance and  $C_d$  is the double layer capacitance. The impedance of the polymer is given by  $Z_d$  and the nature of  $Z_d$  has been extensively discussed, particularly by John Madden in his Ph.D. thesis.<sup>2</sup> Leaving the discussion of suitable models relating  $Z_d$  to actuation for Chapters 8, the Randle's circuit is sufficient to demonstrate the basic response of a conducting polymer actuator to a relevant potential or current input waveform. For a given experiment, the potential measured by the potentiostat is the sum of the potential in the electrolyte and the potential across the double layer that drives actuation. The applied potential is low-pass filtered by an RC time constant in the circuit that slows the actuation response. The current measured by the potentiostat is the sum of the current passing through the double layer capacitance and the current into the polymer. The rate of the polymer response is related to the latter current. At high frequencies, the double layer capacitor short circuits and the all of the current is applied to the polymer. Thus a faster response can always be obtained by controlling current instead of potential. With current control, however, the potential on the polymer may increase quickly to a value that may degrade or reduce the polymer.

A useful potential control method was developed by John Madden to improve the speed of potential control without risking the degradation of current control.<sup>2,3</sup> In this resistance compensation method, the potential is increased by an amount equivalent to the potential across the solution. Assuming the solution resistance is constant and can be measured independently, the potential is equal to the current in the cell multiplied by the

solution resistance. The potential on the polymer can then be feedback-controlled. The solution resistance may also be used once the test is complete to calculate the actual potential that is applied to the polymer. This technique was used in the case of polypyrrole actuation at elevated temperatures discussed in Chapter 8.

## 4.2 Isometric Testing

As stated above, isometric tests occur at constant length, or strain. These tests are straightforward to implement because the instrument is used to apply and maintain an initial mechanical state while the electrochemical waveform is applied. As such, the test does not require any feedback or control on the part of the instrument, allowing higher sampling frequencies. Since most applications for actuators involve motion, however, it can be difficult to make connections between isometric test results. For instance, in the case of actuation by ion intercalation, ion swelling mechanism yields the relationship between charge and strain described by eq 1. In an isometric test, the strain is held constant, yielding the relation

$$\sigma = E\varepsilon - E\alpha\rho \quad 2$$

in which the stress  $\sigma$  is effected by the initial loading  $\varepsilon$  and the product of the modulus  $E$  and  $\alpha$ . Thus, the same strain to charge ratio can be measured in an isometric test if the modulus is known. Equation 2 in the absence of the active mechanical component is the stress relaxation, used in measuring the viscoelastic properties of polymers.

In potential controlled experiments, the application of square waves of different amplitude demonstrates the use of voltage as a driving force. If the frequency of the square wave is sufficiently low, the magnitude of stress response will scale with the amplitude of the potential waveform. Figure 4.3 depicts a typical response of polypyrrole to a square wave in the ionic liquid 1-butyl-3-methyl-imidazolium hexafluorophosphate, or BMIMPF<sub>6</sub>. As the magnitude of the square wave is increased the response also increases as expected though in all three tests the stress is still increasing after 5 seconds.

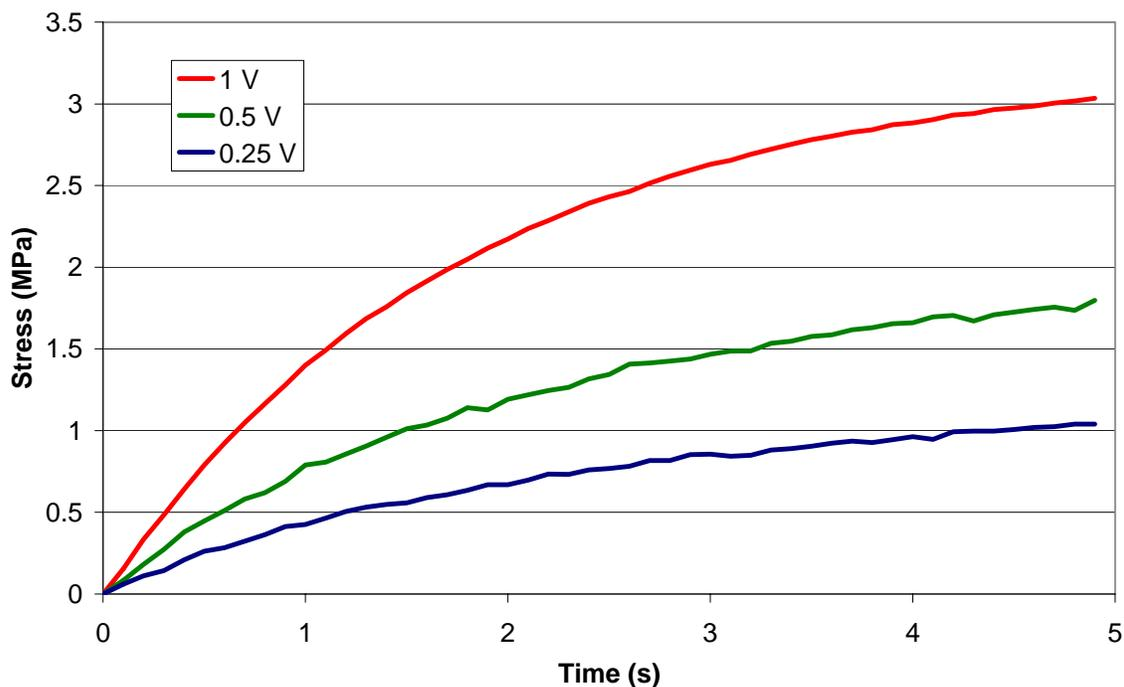


**Figure 4.3.** Average 0.1 Hz isometric response of polypyrrole in BMIMPF<sub>6</sub> as function of peak to peak amplitude.

Current control in isometric testing can be used to observe the response of the polymer at high frequencies, providing a measure of the fastest response times. Increasing the magnitude of the current square wave will cause the polymer to respond faster since the current magnitude indicates the rate of charging. This type of test was used with poly(3,4-ethylenedioxythiophene) to demonstrate an actuation response at 25 Hz as depicted in Figure 4.4, though the stress magnitude in that test was not large.

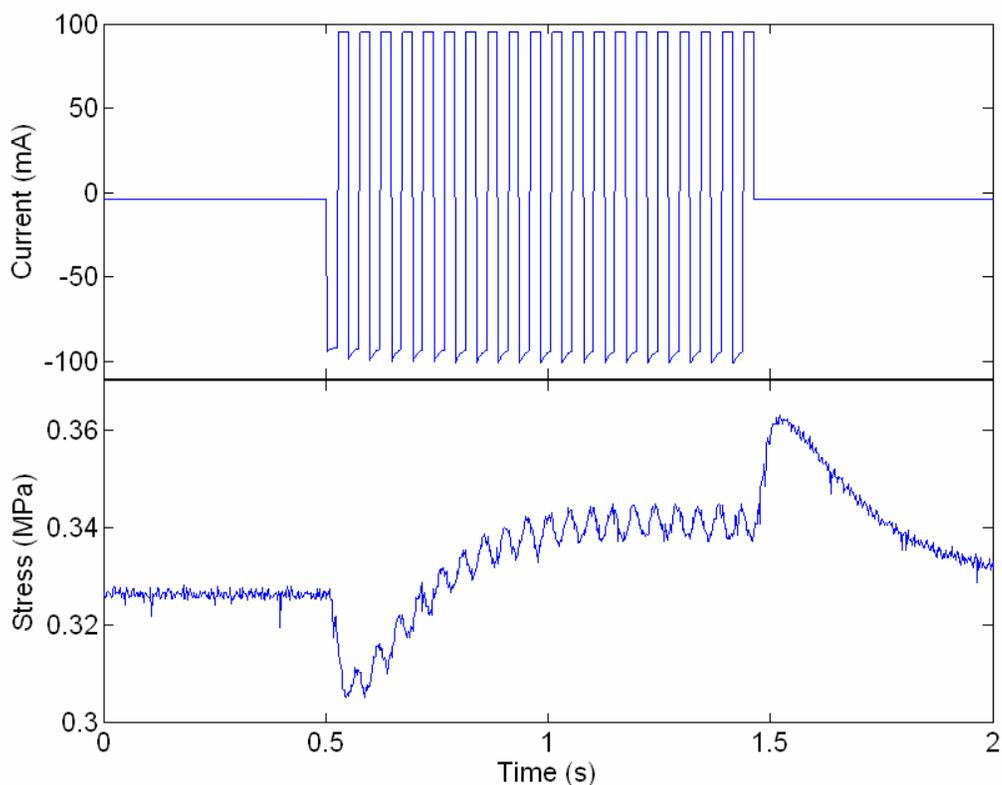


**Figure 4.4.** Isometric response of PEDOT in 0.05 M TBAPF<sub>6</sub> in propylene carbonate at 25 Hz.

Triangle potential waveforms, as in cyclic voltammetry, may also be used in isometric tests to detect the onset of activation at a particular potential. This procedure was used in testing poly(3-hexylthiophene), the topic of Chapter 7. The use of triangle potential waves also enables the variation from insulating to conducting material and the observation of the effects of the conductivity on actuation.

### 4.3 Isotonic Testing

Isotonic tests are measured at constant force, or stress, utilizing the mechanical components of the stage to allow the sample to expand and contract while maintaining a constant force. This test is the equivalent of lifting a known load off the ground against the force of gravity, though the force is controlled with the stage. This requires the use of feedback control through a data acquisition system which may limit the bandwidth of

measurement. The benefit of isotonic testing is that strain and strain rate are measured directly according to the relation

$$\varepsilon = \frac{\sigma}{E} + \alpha\rho, \quad 3$$

which shows the passive and active response analogs of Equation 2. Equation 3 without the active response is the familiar creep test of viscoelasticity.

Potential or current control can be used with the same advantages mentioned above in the case of isometric testing. The difficulty in characterizing the response is that strain and strain rate are rarely optimized in the same test or sequence of tests. The largest strains are observed by pushing the potential limits of the system as far as possible while also allowing the longest time for the polymer to respond. The fastest strain rates are typically obtained by applying potentials beyond the degradation limit or high currents for short times.

Figure 4.5 demonstrates a typical isotonic response of PEDOT to a slow potential triangle wave in the ionic liquid BMIMPF<sub>6</sub>. In the figure, both strain and charge are plotted to highlight the relationship in Equation 3. The determination of the strain to charge ratio  $\alpha$ , and the ion that is swelling the polymer can be elucidated by evaluating the result. Some care must be taken, however, to properly assign which ion is swelling the film, since numerous sign conventions are used in the measurement. In the tests presented throughout this work, a positive strain signifies elongation. The electrochemical convention used defines positive potentials and currents for oxidation. The charge is the integral of the current, with a positive slope for positive currents and negative slope for negative currents. Stray currents in the system may lead to underestimation of the strain to charge ratio.

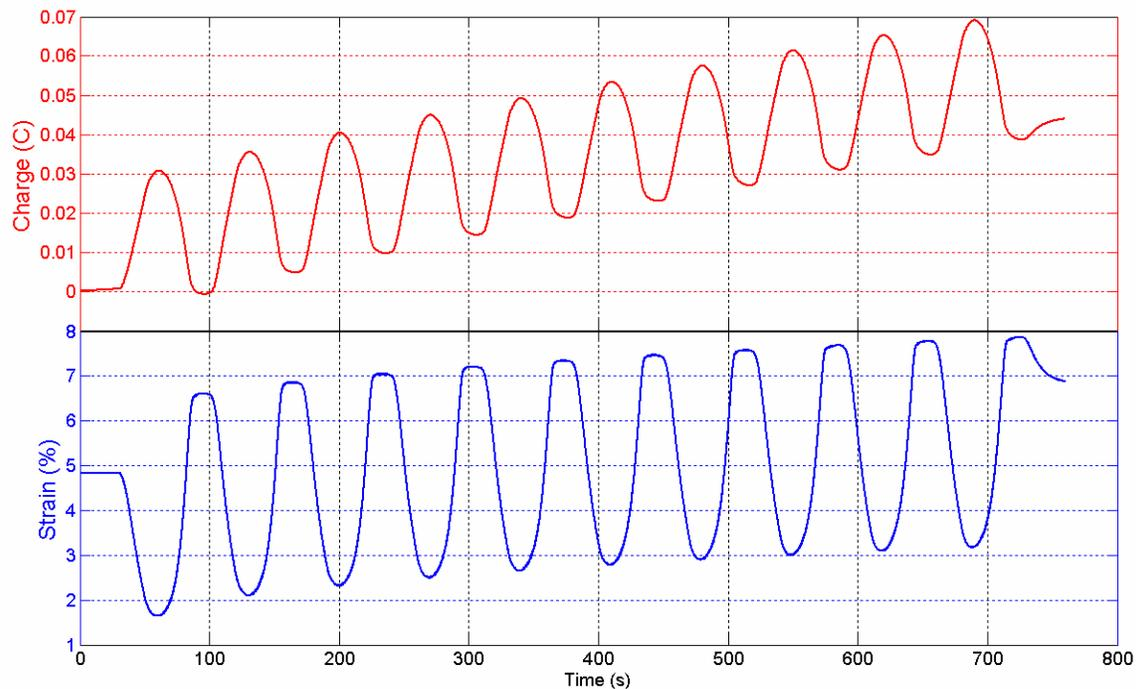


**Figure 4.5.** Isotonic response of PEDOT in BMIMPF<sub>6</sub>. Potential triangle wave input between -1.5 and 2.0 V versus Ag wire at 100 mV/s.

The strain in the figure shows a negative slope when the charge shows a positive slope. This indicates a contraction caused by the egress of the imidazolium cation. The ionic selectivity is important and will be discussed in the next chapter.

#### 4.4 Other Electrochemical Mechanical Tests

Beyond isometric and isotonic testing, a well-designed instrument is capable of providing dynamic strain or stress during an electrochemical experiment. One such experiment is the measurement of modulus as a function of oxidation state. In that test a sinusoidal stress input is implemented while the polymer film is slowly oxidized and reduced. The modulus is taken as the magnitude of the stress over the magnitude of the strain and the frequency is kept low enough to prohibit viscoelastic transitions. The result is depicted in Figure 4.6 for PEDOT in BMIMPF<sub>6</sub>. In the case shown, the polymer stiffened with oxidation. In the case of reduction, however, the results are less clear as the modulus decreased at -0.5 V but increased at -1.0 and -1.5 V.

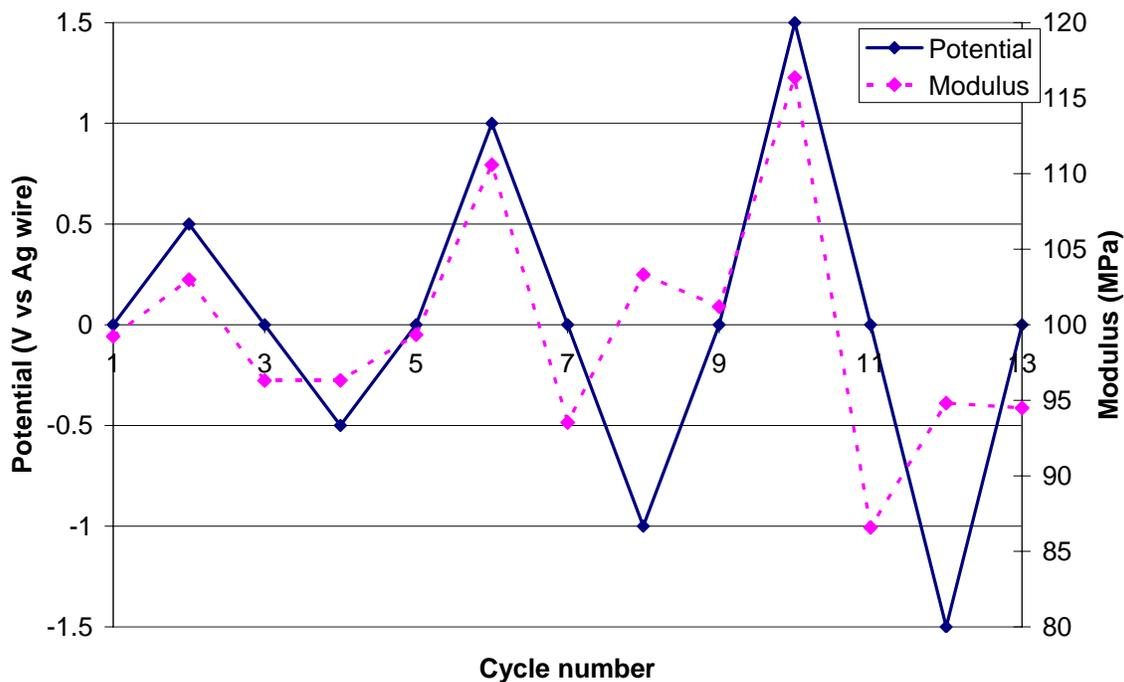


**Figure 4.6.** Potential and modulus test of PEDOT in BMIMPF<sub>6</sub>.

More complicated electrochemical techniques can also be combined with mechanical testing. For example, the combination of electrochemical impedance spectroscopy and an isometric test allows for the bandwidth of actuation to be tested under given conditions or for a specific sample.<sup>4</sup> Such a test was used to measure polypyrrole actuation at different temperatures, discussed in Chapter 8. The continued progress of instrumental development suggests new techniques that may be useful to understand the relationship between mechanical and electrical energy for a conducting polymer actuator.

## 4.5 Summary

Characterization of actuators requires a combined electrochemical and mechanical measurement that is not readily achieved from commercial instruments. Once a custom instrument is developed, numerous tests are used in understanding the relationship between the electrochemical and mechanical states. Isometric and isotonic tests measure



the fundamental properties of actuators including stress, strain, and strain rate. Other tests can be used to measure the changes in passive mechanical properties as a function of potential or measure the response as a function of frequency.

## 4.6 References

1. Della Santa, A; De Rossi, D.; Mazzoldi, A. Characterization and modeling of a conducting polymer muscle-like linear actuator. *Smart. Mater. Struct.* **1997**, *6*, 23.
2. Madden, J. D. W. Conducting Polymer Actuators. Ph.D. Thesis, Massachusetts Institute of Technology, Cambridge, MA, 2000.
3. Madden, J. D.; Cush, R. A.; Kanigan, T. S.; Hunter, I. W. Fast contracting polypyrrole actuators. *Synth. Met.* **2000**, *113*, 185-192.
4. Madden, J. D. W.; Madden, P. G. A.; Hunter, I. W. Polypyrrole actuators: modeling and performance. *Proc. SPIE Int Soc. Opt. Eng.* **2001**, *4329*, 72-83.

## 5. Poly(3,4-ethylenedioxythiophene) Actuation

Poly(3,4-ethylenedioxythiophene), or PEDOT, is a well-known and widely-studied intrinsically conductive polymer. It has been successfully used for numerous applications, including antistatic and transparent conducting coatings and it is commercially available.<sup>1</sup> PEDOT has also shown the ability to support ionic intercalation, one of the actuation mechanisms in conducting polymers,<sup>2</sup> highlighted in Chapter 4. In 1996, Chen et al. showed the bending of PEDOT-coated Au substrates in a range of solvents and electrolytes.<sup>3</sup> While similar work spawned the use of polypyrrole and polyaniline in actuators, PEDOT was not widely regarded for actuation. In this chapter, the development of actuation with PEDOT will be discussed from synthesis to electrolyte effects. In addition, the special role of ionic liquids will be investigated. Despite the improved performance of many actuating conducting polymers in ionic liquids,<sup>4</sup> the reason for the unusual preference of polypyrrole and PEDOT toward the cation in such systems has not yet been proposed.

### 5.1 Synthesis

PEDOT can be synthesized in a number of ways, including direct chemical oxidation, electrochemical oxidation, and transition metal catalyzed couplings. The monomer, 3,4-ethylenedioxythiophene, or EDOT, is a particularly suitable for polymerization because it is blocked at both  $\beta$  sites (3 and 4 carbon positions), which are known to cause structural and electronic defects in polythiophenes and polypyrroles. With this characteristic, the resulting polymer should be more regular and have improved molecular weights and conjugation lengths, leading to better mechanical and electrical properties. As with many of the other conducting polymers, insolubility problems plague the complete characterization of PEDOT, but its low bandgap and good material properties are often indicative of low defect density and successful polymerization.<sup>1</sup>

Freestanding films of PEDOT were prepared from a solution containing 0.06 M EDOT, 0.06 M tetrabutylammonium hexafluorophosphate (TBAPF<sub>6</sub>) and 0.6 M water in propylene carbonate (PC).<sup>5,6</sup> The EDOT was supplied by Bayer AG and was freshly

distilled before use, while all other reagents were used as received. The polymerization occurred in an electrochemical cell containing a glassy carbon working electrode and copper or stainless steel counter electrode. No effort was made to directly exclude oxygen during deposition. Deposition occurred at constant currents of 1.0 to 4.0 A/m<sup>2</sup> at -20 °C. The resulting films are glossy black, varying in thickness from 20 to 70 μm and with conductivities between 1 × 10<sup>4</sup> and 3 × 10<sup>4</sup> S/m and typical moduli of 200 to 500 MPa. The PEDOT films were readily peeled from the working electrode and were stored and tested in the electrochemical solution without monomer.

## **5.2 Active Characterization**

Following the electrochemical polymerization in propylene carbonate, the initial characterization of PEDOT was performed in 0.05 M TBAPF<sub>6</sub> in propylene carbonate. The initial tests were focused on understanding the role of the electrochemical input as well as the mechanical state of the polymer. As will be shown, the polymer showed no ionic selectivity, allowing both ions to diffuse in and out of the polymer. This was unexpected because polypyrrole generally excludes the ammonium cation in the same electrolyte.<sup>7</sup> Following the initial characterization, a study of PEDOT actuation in varying solvents and electrolytes demonstrated that ionic liquids produced the largest actuation response. The reason for this response was not known, so an additional study was completed in which the ionic liquid BMIMPF<sub>6</sub> was diluted with propylene carbonate.

### ***5.2.1 Actuation in Propylene Carbonate***

A number of waveforms were applied in an attempt to measure the precise relationship between strain and charge in PEDOT. The purpose was to demonstrate linear actuation in PEDOT, which was previously unpublished and compare it to the well-characterized polypyrrole. Figure 5.1 demonstrates the response of a PEDOT film to square waves of 5 mA. Under these conditions the sample expanded and contracted 0.5 % at a rate of 0.025 % per second against a load of 1.0 MPa.

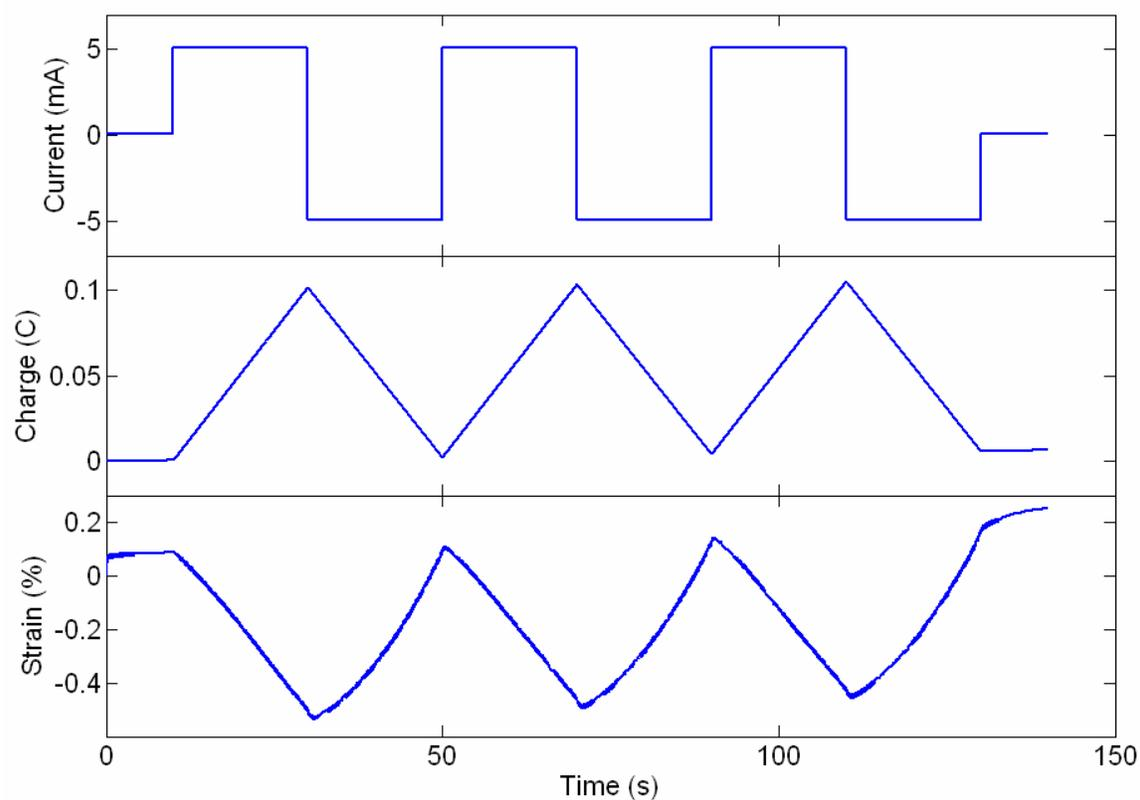


**Figure 5.1.** Isotonic response of PEDOT to current square wave in 0.1 M TBAPF<sub>6</sub> in propylene carbonate. Film held at 1.0 MPa.

The film could be characterized further by the relationship between strain and charge density, highlighted in Section 4.3. Dividing the charge by the volume of the film, the resulting linear relationship is demonstrated in Figure 5.2. The slope of the line gives the strain to charge ratio of  $-6.4 \times 10^{-11} \text{ m}^3/\text{C}$ , slightly less than the value of  $1 \times 10^{-10} \text{ m}^3/\text{C}$  calculated for polypyrrole in the same electrolyte system.<sup>7</sup>

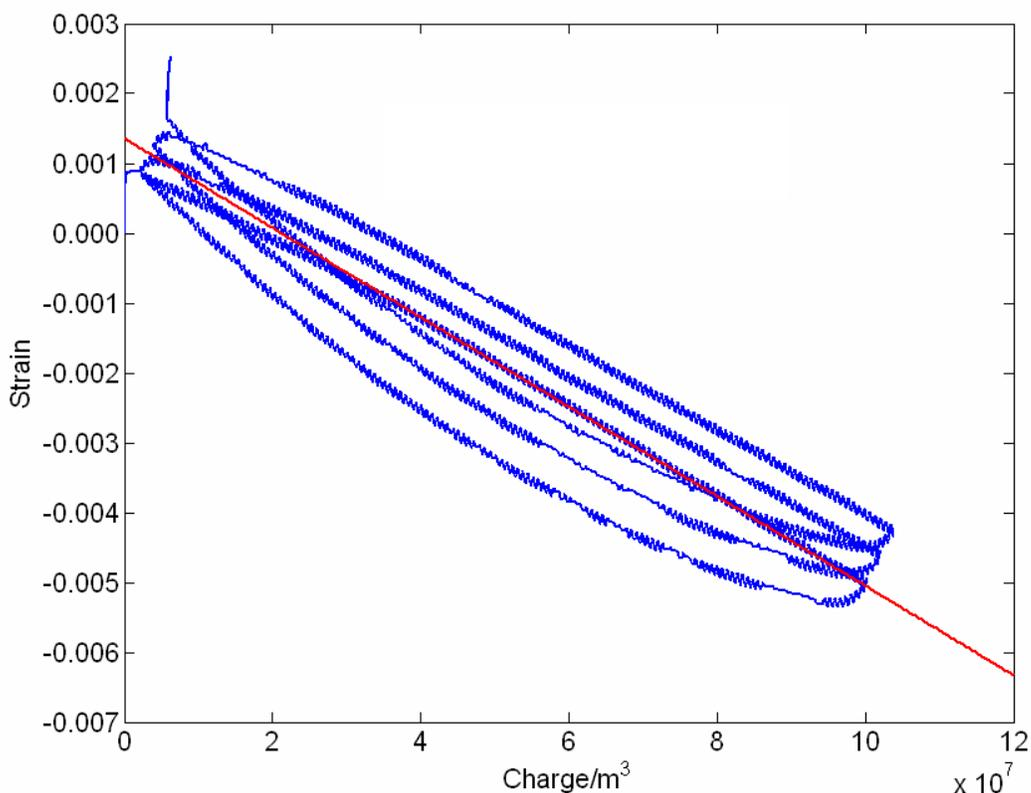


**Figure 5.2.** Calculation of strain to charge density ratio,  $\alpha$  from previous test. Value of  $-6.4 \times 10^{-11} \text{ m}^3/\text{C}$  given by linear regression.

Unfortunately, as testing continued in this electrolyte system, the PEDOT films began showing erratic behavior. Figure 5.3 provides a clear example of both ions swelling the polymer under similar conditions. Each current half cycle contributes to two distinct strain responses in opposing directions. When either a positive or negative current is applied, the sample first contracts and then elongates. In this case, the relevance of a relationship between strain and charge is diminished as the  $\alpha$  parameter has both a negative and positive value. Furthermore, the lack of ionic selectivity would be detrimental in an application for which a known output would be required from a input.

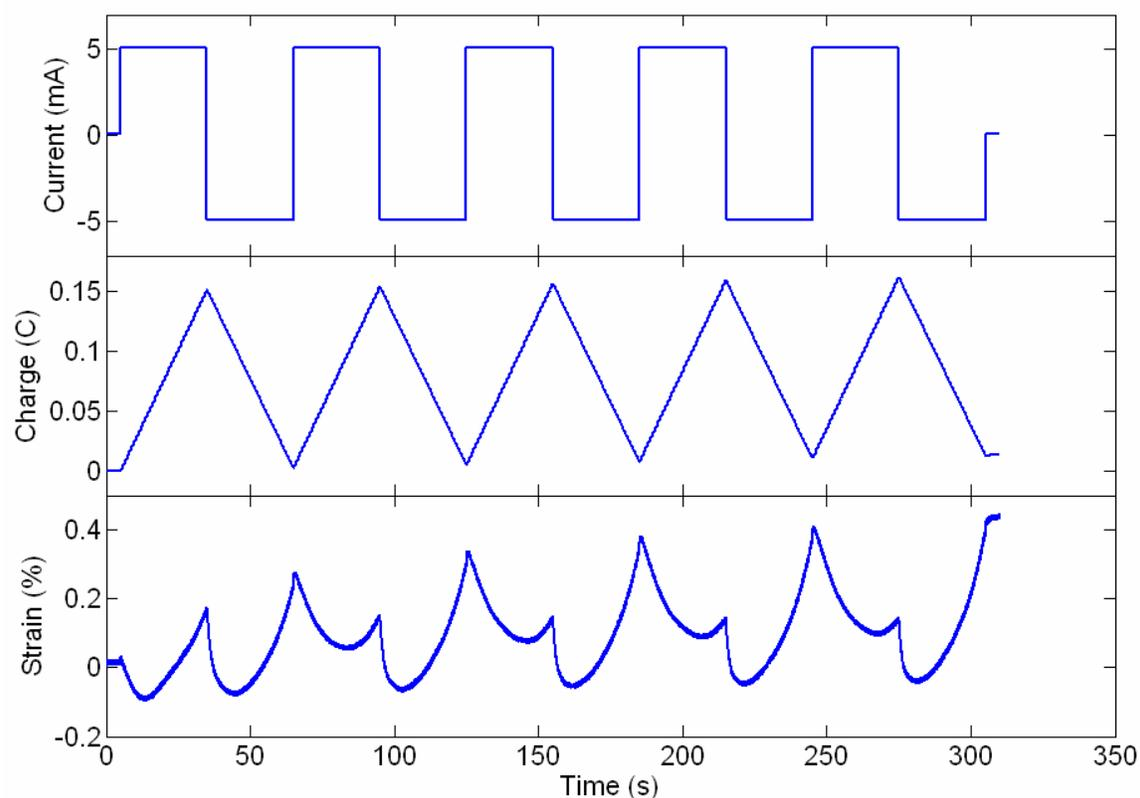


**Figure 5.3.** Isotonic response of PEDOT to current square wave in 0.1 M TBAPF<sub>6</sub> in propylene carbonate. Film held at 1.0 MPa, demonstrating strong dual ion movement.

The lack of selectivity in TBAPF<sub>6</sub> in propylene carbonate suggested that changing the electrolyte would lead to different responses and perhaps one more favorable for controllable actuation.<sup>8</sup> The results of the electrolyte study are presented in the next section.

### 5.2.2 Electrolyte Effects

The electrolyte test for PEDOT used a swept potential waveform rather than the constant current employed in the propylene carbonate case described above. The results are given in Table 5.1 below. Only the ionic liquids BMIMPF<sub>6</sub> and BMIMBF<sub>4</sub> showed ion selectivity and a single relation between charge and strain. In both cases it was the imidazolium cation rather than the anion that swelled the polymer. This observation was not expected, since the PF<sub>6</sub> anion readily penetrates the polymer in a propylene carbonate solution as shown in Figure 5.3. These ionic liquids also produce the most strain and

strain rate for the comparison, thereby demonstrating their utility as solvents for electrochemical actuation of conducting polymers.<sup>4</sup>

	<b>0.1 M TBAPF<sub>6</sub> in PC</b>	<b>0.1 M LiClO<sub>4</sub> in PC</b>	<b>0.1 M Na p-OTs in water</b>	<b>BMIMBF<sub>4</sub></b>	<b>BMIMPF<sub>6</sub></b>
<b>Contractile strain observed (%)</b>	<b>0.79 ± 0.08</b>	<b>0.95 ± 0.008</b>	<b>0.92 ± 0.007</b>	<b>3.7 ± 0.2</b>	<b>4.3 ± 0.4</b>
<b>Maximum strain rate observed (%/s)</b>	<b>0.07</b>	<b>0.07</b>	<b>0.07</b>	<b>0.2</b>	<b>0.2</b>
<b>Charge to strain polarity</b>	<b>-/+</b>	<b>-/+</b>	<b>-/+</b>	<b>-</b>	<b>-</b>

**Table 5.1.** Strains observed for PEDOT in various electrolytes against a load of 1.0 MPa. All tests were performed at 100 mV/s swept potential.

### 5.3 Ionic Liquids as Salt and Solvent

Following the observation that ionic liquids produced superior results for PEDOT actuation, it was thought that this might be due to the relative concentration of ions within the ionic liquid. Unlike the dissolved electrolyte systems, ionic liquids do not require a solvent, thereby greatly increasing the ionic strength of the solution. Typical electrochemical systems use an electrolyte concentration of 0.1 M while the ionic liquids BMIMPF<sub>6</sub> and TBAPF<sub>6</sub> have electrolyte concentrations of 4.2 and 5.1 M respectively. With diffusion a critical element to actuation,<sup>7</sup> an increased concentration would improve the transport of ions into the film and improve the strain response as well.<sup>9</sup> Figure 5.4 shows the relationship between strain and charge for varying concentrations of BMIMPF<sub>6</sub> in propylene carbonate.



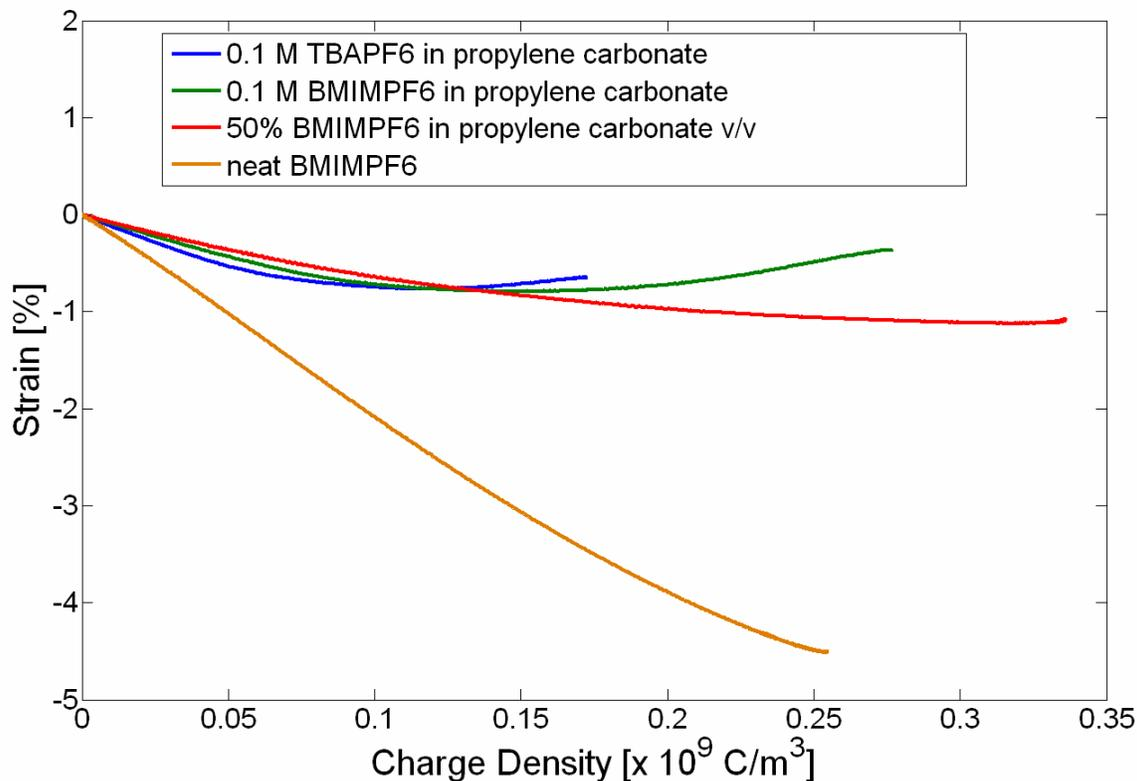


**Figure 5.4.** Strain to charge density relationship for PEDOT in dilute and concentrated BMIMPF<sub>6</sub> showing variation of strain to charge density as well as dual ion motion.

As discussed in Chapter 4, for conducting polymer actuators that rely on ion ingress and egress, the relationship between strain and charge is indicative of performance.<sup>7,10,11</sup> In Figure 5.4, the result of PEDOT actuation in 0.1 M TBAPF<sub>6</sub> in propylene carbonate is also plotted for comparison to the tests in ionic liquids. Actuation in dilute ionic liquids appears qualitatively similar to actuation in TBAPF<sub>6</sub> and propylene carbonate rather than the neat ionic liquid. Of all four electrolyte systems, actuation in neat BMIMPF<sub>6</sub> demonstrates the largest strain to charge ratio, demonstrated by the largest magnitude of slope in the figure. This dependence on concentration supports the argument that actuation is improved in ionic liquids because of the greater ionic strength.

Furthermore, in neat BMIMPF<sub>6</sub> the relationship remained linear throughout the charging and discharging, indicating the action of a single ion. The figure shows a progression from a two ion to one ion mechanism as the concentration of ionic liquid is increased. In 0.1 M BMIMPF<sub>6</sub> in propylene carbonate, the figure shows two linear

regions, from 0 to  $0.075 \times 10^9 \text{ C/m}^3$  and from 0.2 to  $0.275 \times 10^9 \text{ C/m}^3$ . The slope of the line in these two regions demonstrates strain to charge ratios of  $-8.74 \times 10^{-11} \text{ m}^3/\text{C}$  and  $5.04 \times 10^{-11} \text{ m}^3/\text{C}$  respectively. In neat BMIMPF<sub>6</sub>, the figure shows PEDOT to have a strain to charge ratio of  $-2.08 \times 10^{-10} \text{ m}^3/\text{C}$ . While increased ionic strength may lead to improved actuation performance, the correlation to selectivity cannot depend on concentration since the concentration of each ion is the same.

The films in neat BMIMPF<sub>6</sub> contract during charge injection, or with positive currents at positive potentials. For each potential, charge equilibration may be reached by ingress of one ionic species or egress of the counter ion. In this case, actuation is dominated by the imidazolium ion, a result that has been shown in polypyrrole with similar ionic liquids.<sup>12</sup> Initial actuation studies with different electrolytes suggested that the size of the ions determined the selectivity during actuation. This argument was extended to the use of polyelectrolyte counterions that would be unable to contribute to the actuation mechanism.<sup>9</sup> A size exclusion mechanism cannot, however, explain why the PF<sub>6</sub> ions readily insert in PEDOT during deposition and actuation in propylene carbonate, but not during actuation in ionic liquids. It is possible that both ions play a role at all times in ionically-driven actuation mechanisms as was suggested by Pei and Inganäs.<sup>13</sup> The enormous variation imposed by the addition of a solvent, however suggests that the nature of the solventless ionic liquid itself is a contributing factor to this result.

One possibility, supported by recent studies on ionic liquids at vapor interfaces, is that the interface between film and electrolyte is dominated by the imidazolium ion in the absence of solvent.<sup>14,15</sup> Of the two ions present in the ionic liquid, the imidazolium ion has a structure much closer to that of a surfactant. The addition of propylene carbonate to such a solution may insert a solvent layer at the interface which changes the nature of ion ingress as well as the polymer-ion interaction. The dipole of the solvent may also play a role in mitigating the effectiveness of or selectivity toward one particular ion. The porous nature of the film increases the role of this interaction as the internal surface area of the polymer is considered. Madden proposed that the surface and volumetric capacitance can be related by one thermodynamic relation between the solution and the

polymer.<sup>7</sup> The numerous possible driving forces for ion and solvent motion in conducting polymers complicates the predictability of actuation performance based solely on ion size or concentration. This observation of solvent dependent actuation in ionic liquids suggests that further study of conducting electrochemistry in ionic liquids is necessary, giving particular attention to the double layer and interfacial properties.

## 5.4 Summary

It is observed that PEDOT is a useful actuating conducting polymer, demonstrating a ratio between active strain and charge density of  $-2.08 \times 10^{-10} \text{ m}^3$  per C charge injected in the ionic liquid BMIMPF<sub>6</sub>. The performance of PEDOT in ionic liquids is similar to that of polypyrrole, suggesting that improvements that have been made with polypyrrole actuation may be applicable to PEDOT. The linear strain observed is also commensurate with current state-of-the-art conducting polymer actuators.

In studying conducting polymer actuators, it is critical that the role of solvents, ions, and ion concentrations be examined, as shown by the transition of performance and selectivity from dilute to neat BMIMPF<sub>6</sub>. While the increase of the ionic strength of the solution plays a role in the performance of the polymer, the complex nature of ion ingress and egress and the role of the interface is not completely understood. The relationship between kinetic limitations (principally diffusion) and thermodynamic interactions between the polymer and the electrolyte hinder the full characterization of any conducting polymer actuation based on ionic ingress and egress.

## 5.5 References

1. Groenendaal, L.; Jonas, F.; Freitag, D.; Pielartzik, H.; Reynolds, J. R. Poly(3,4-ethylenedioxythiophene) and Its Derivatives: Past, Present, and Future. *Adv. Mater.* **2000**, *12*, 481-494.
2. Baughman, R.H. Conducting polymer artificial muscles, *Synth. Met.* **1996**, *76*, 339-353.
3. Chen, X.; Xing, K.-Z.; Inganäs, O. Electrochemically Induced Volume Changes in Poly(3,4-ethylenedioxythiophene), *Chem. Mater.* **1996**, *8*, 2439-2443.
4. Lu, W.; Fadeev, A. G.; Qi, B.; Smela, E.; Mattes, B. R.; Ding, J.; Spinks, G. M.; Mazurkiewicz, J.; Zhou, D.; Wallace, G. G.; MacFarlane, D. R.; Forsyth, S. A.; Forsyth, M. Use of ionic liquids for pi-conjugated polymer electrochemical devices. *Science* **2002**, *297*, 983-987.
5. Aleshin, A.; Kiebooms, R.; Menon, R.; Heeger, A. J. Electronic transport in doped poly(3,4-ethylenedioxythiophene) near the metal-insulator transition. *Synth. Met.* **1997**, *90*, 61-68.
6. Giurgiu, I.; Zong, K.; Reynolds, J. R.; Lee, W.-P.; Brenneeman, K. R.; Saprigin, A. V.; Epstein, A. J.; Hwang, J.; Tanner, D. B. Dioxypyrrole and dioxothiophene based conducting polymers: properties and applications. *Synth. Met.* **2001**, *119*, 405-406.
7. Madden, J. D. W. Conducting Polymer Actuators. Ph.D. Thesis, Massachusetts Institute of Technology, Cambridge, MA, 2000.
8. Careem, M. A.; Vidanapathirana, K. P.; Skaarup, S.; West, K. Dependence of force produced by polypyrrole-based artificial muscles on ionic species involved. *Solid State Ionics* **2004**, *175*, 725-728.
9. Maw, S.; Smela, E.; Yoshida, K.; Stein R. B. Effects of monomer and electrolyte concentrations on actuation of PPy(DBS) bilayers. *Synth. Met.* **2005**, *155*, 18-26.
10. Della Santa, A.; De Rossi, D.; Mazzoldi, A. Characterization and modelling of a conducting polymer muscle-like linear actuator. *Smart. Mater. Struct.* **1997**, *6*, 23-34.
11. Madden, P. G. A.; Madden, J. D. W.; Anquetil, P. A.; Vandesteeg, N. A.; Hunter, I. W. The Relation of Conducting Polymer Actuator Material Properties to Performance. *IEEE J. Oceanic Eng.*, **2004**, *29*, 696-705.
12. Ding, J.; Zhou, D.; Spinks, G.; Wallace, G.; Forsyth, S.; Forsyth, M.; MacFarlane, D. Use of ionic liquids as electrolytes in electromechanical actuator systems based on inherently conducting polymers *Chem. Mater.* **2003**, *15*, 2392-2398.

13. Pei, Q.; Inganäs, O. Electrochemical applications of the bending beam method. 1. Mass-transport and volume changes in polypyrrole during redox. *J. Phys. Chem.*, **1992**, *96*, 10507-10514.
14. Rivera-Rubero, S.; Baldelli, S. Surface spectroscopy of room-temperature ionic liquids on a platinum electrode: A sum frequency generation study. *J. Phys. Chem B* **2004**, *108*, 15133-15140.
15. Halka, V.; Tsekov, R.; Freyland, W. Peculiarity of the liquid/vapour interface of an ionic liquid: study of surface tension and viscoelasticity of liquid BMImPF(6) at various temperatures. *Phys. Chem. Chem. Phys.*, **2005**, *7*, 2038-2043.

## **6. Poly(3,4-ethylenedioxythiophene) and carbon nanotube composites**

Development in novel conducting polymers is hampered by the synthetic difficulties already highlighted in Chapter 2. As noted therein, chief concerns include the conductivity and mechanical robustness of films synthesized. This has become especially evident in novel monomers. One approach to improving these problematic properties involves more careful control during electrochemical polymerization as in the case of the galvanodynamic polymerization discussed in Chapter 2. Another approach to improving mechanical and electrical properties involves blending the polymers with a filler capable of enhancing these properties. In commercial polymers, carbon black can be used for conductivity enhancement and carbon fibers can be used to improve the mechanical strength. The use of carbon nanotubes (CNTs) has provided an all-in-one filler, conductive and strong, to enhance both the mechanical and electrical properties.

While the choice of CNTs is logical, there is difficulty when the complexity of the material is increased. The effects of the CNTs must be separated from the actuation of the underlying polymer. CNTs are also known to actuate electrochemically.<sup>1</sup> Therefore, a control experiment containing a known actuating polymer and CNTs would demonstrate the enhancement caused by the CNTs. For this purpose, PEDOT was chosen due to the familiarity with its actuation properties as detailed in Chapter 5. Furthermore, owing to the different electrochemical synthetic techniques, an additional control experiment was performed involving a new synthesis of PEDOT without the CNTs.

### **6.1 Synthesis**

The blending of conducting polymers and carbon nanotubes is complicated by the insolubility of both components. While typical blending would involve mixing of two homogeneous phases, few conducting polymers beyond the alkylthiophenes accommodate such a scheme and CNTs are generally stabilized in solution at low concentrations only. One method that has been successfully implemented is a layer-by-layer approach. Utilizing short duration electrochemical polymerizations, thin layers of

PEDOT were deposited on an electrode, which was then removed from solution. Then, owing to the highly stable mixture of CNTs and poly(3-hexylthiophene) in chloroform,<sup>2</sup> a solution of CNTs was drop cast onto the polymer surface. Subsequent washing of the surface with excess chloroform removed the polymer while the CNTs remained on the surface. A new layer of polymer was electrodeposited on the CNTs and the steps were repeated. Following this sequence, as depicted in Figure 6.1, a layered composite of PEDOT and CNTs was grown onto an electrode. Once sufficient thickness had been achieved in the composite, the polymer was peeled from the electrode and characterized.

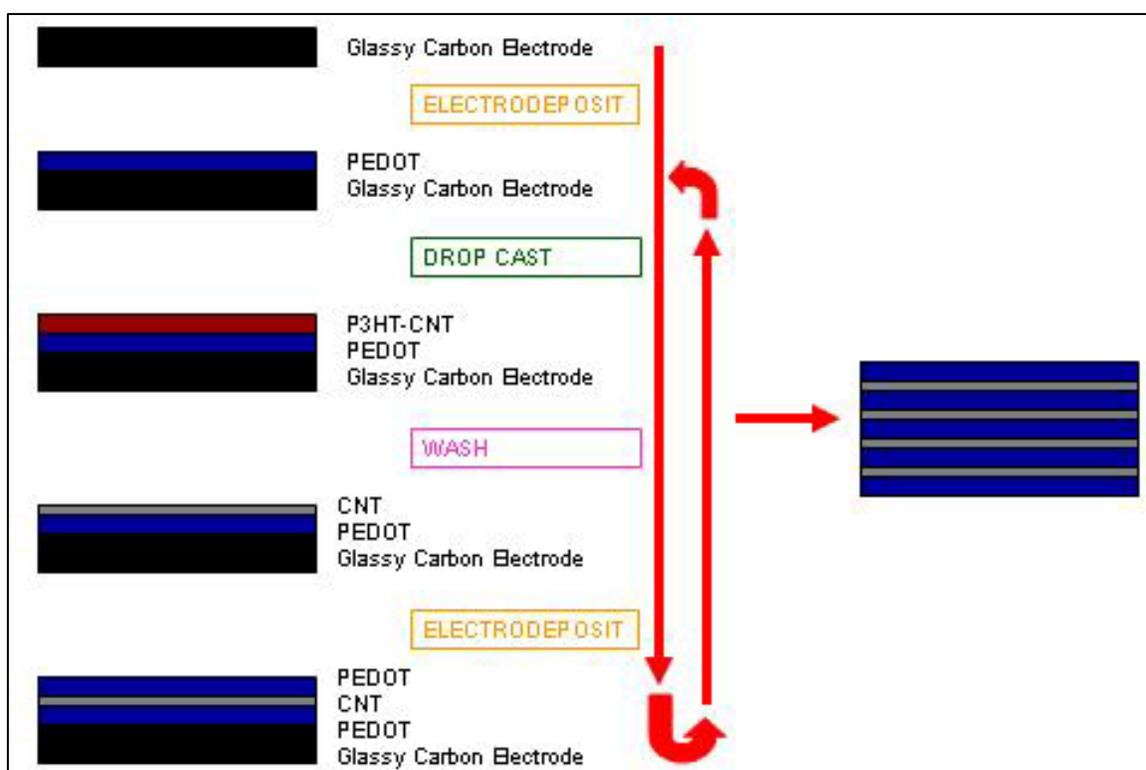


**Figure 6.1.** Schematic description of nine layer composite formation. Control films prepared without the drop cast or wash steps, maintaining 5 separate electrodepositions.

Nine-layer films were synthesized in this manner by Dr. Ali Shaikh, in which a 100 s potentiostatic deposition of PEDOT was combined with the CNT drop cast technique. The deposition solution contained 0.1 M EDOT monomer, 0.06 M water, and 0.1 M TBAPF<sub>6</sub> in propylene carbonate. A glassy carbon plate was used as the working electrode with a stainless steel counter electrode and a reference electrode of 0.001 M AgNO<sub>3</sub> in 0.1M TBAPF<sub>6</sub> in propylene carbonate. All depositions were performed in air

at room temperature. In addition, control samples were prepared with five independent electrodepositions, omitting the CNT drop casting step.

## 6.2 Passive Characterization

The films were tested for modulus and conductivity to demonstrate the improvement caused by the CNT incorporation. As hypothesized, the layered CNT structure demonstrated improvement in both properties as shown in Table 6.1. The conductivities were measured via four-point van der Pauw method, described in Chapter 3, and the modulus was taken prior to immersion into solvent at 0.5 Hz.

<b>Film properties</b>	<b>Thickness</b>	<b>Conductivity</b>	<b>Modulus</b>
	$\mu\text{m}$	$10^4 \text{ S/m}$	<b>MPa</b>
<b>Composites</b>			
<b>average</b>	18 - 20	2.5	198
<b>Controls</b>			
<b>average</b>	18 - 21	1.2	97

**Table 6.1.** Thickness conductivity and modulus for composite and control PEDOT/CNT films.

The conductivity enhancement achieved with CNT incorporation is caused by the percolation of conductive bodies within a matrix. For carbon black, high volume loading of carbon, typically on the order of 10 to 20 % (the percolation threshold) is required to achieve conductivity in a nonconductive material.<sup>3</sup> This volume fraction requirement is lower with CNTs, because of the high anisotropy in CNT structure, allowing similar conductivity enhancements at volume fractions of 0.1 %.<sup>3</sup> Unfortunately, in a layered structure synthesized by this method, it is unclear whether the CNTs will provide conductivity enhancement throughout the bulk of the sample or only in the two axes addressed in the drop cast step. If the structure remains stratified, the conductivity along the length of the film will be high in the layers of CNTs. While it is possible that CNTs possess a sufficient mobility in a polymer matrix to disperse in the solid phase, this is not required for inclusion in a conducting polymer that already demonstrates a reasonable conductivity. The mechanical enhancement provided by the CNTs is in the desired plane even without dispersion.



In the case of conductivity enhancement, further improvement of actuation in conducting polymers that utilize ion ingress, such as polypyrrole and PEDOT, would be demonstrated by expanding the electrochemical window of high conductivity. If a sample of PEDOT were as conductive in the reduced state, the ability to transport charge and accommodate ion diffusion would allow for actuation at all potentials. As in the case of carbon black noted above, at sufficient loadings, the CNTs would provide all of the electrical transport and enable reduced films to conduct. To test this possibility, an in-situ test, as described in Section 3.3.2, was performed on the control and composite structure. The results, depicted in Figure 6.2, show that both the composite and control samples demonstrated lower conductivity in the reduced state. This could be due to the lack of three dimensional percolation of the CNTs or insufficient volumetric loading.

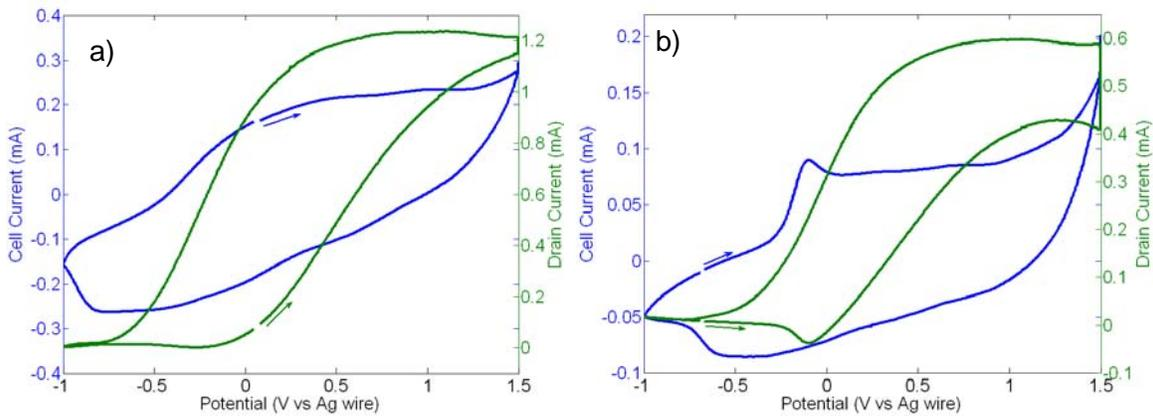


**Figure 6.2.** In-situ conductivity of PEDOT control film (a) and PEDOT/CNT composite film(b).

One distinction between the two samples tested, however, is the additional oxidation peak observed in the composite sample at -0.2 V. This oxidation peak is observed in the cell current signal and also occurs in the drain current when it apparently becomes less than zero. The observation of a negative drain current was independent of scan rates. A closer look at the individual current signals from the test indicated that at the point of this oxidation, both current signals were positive and demonstrated an oxidation peak. This oxidation may be caused by the nanotubes, occurring in the region of both electrode contacts. Since the drain current is low at this point, there is virtually no connection between the clamped ends of the sample. Thus the additional oxidation is

a faradaic current in a domain accessible to the electrodes in the reduced polymer state. Without the CNTs, the oxidation wave expands from the point of contact with the conductivity increase.<sup>4</sup> With the CNTs, the oxidation jumps through highly conductive domains.

### **6.3 Actuation**

Actuation tests were designed to provide meaningful comparison between control and composite samples. Each film was initially cycled between -0.5 and 1.0 V versus Ag wire to initiate the ionic incorporation and equilibrate the sample to the BMIMBF<sub>4</sub> ionic liquid environment. The actuation tests were performed in isotonic mode at a load of 0.5 MPa. The first test employed the identical waveform to the initial cyclic voltammogram with the strain recorded versus time. Following this test, two additional tests were performed with a voltage sweep between -1.0 and 1.5 V vs Ag wire, again at 50 mV/s and for 5 cycles in each test.

In order to demonstrate the additional response speed of the actuation caused by the CNT conductivity enhancement, potential square wave tests were performed between 0 and 0.5 V vs Ag wire at 0.05 Hz in an isometric and isotonic configuration. In these tests the average response was taken over a five cycle test. Discussion of the results in each test protocol follows in the next two sections.

#### **6.3.1 Potential Triangle Wave response**

Figure 6.3 depicts the strain observed in the composite and control samples in the third of three triangle wave tests. The shape and magnitude of the response is similar for each of the two materials, though the control sample exhibits a larger creep over the course of the test. Other control samples failed mechanically during this test, further indicating a relative lack of mechanical stability compared to the composite films. The creep effect observed is undesirable for applications because the gradual elongation over time would require the film to be tightened periodically. Furthermore, this creep appears to occur as a result of the electrochemical stimulation and is not a response to the waveform. Thus, since creep during actuation would be difficult to control in an application, its diminution would be desirable. The larger modulus of the composite

sample improves the passive response of the polymer without adversely affecting the active response.

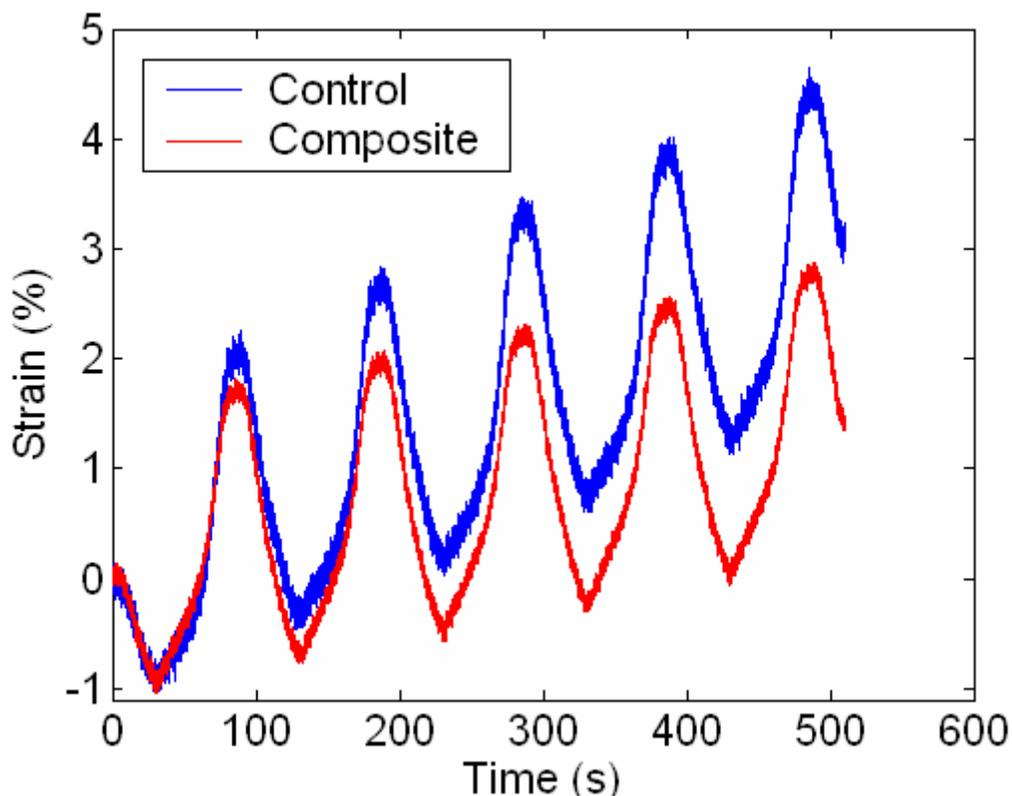


**Figure 6.3.** Strain response of control and composite films to 50 mV/s potential triangle wave between -1.0 and 1.5 V vs Ag wire.

The cyclic voltammograms obtained from the triangle potential waveforms during these tests are plotted in Figure 6.4. As in the case of the actuation responses, the voltammograms are similar for both the control and composite samples. The oxidation of the composite sample also shows an initial increase at -0.2 V, much like the in-situ conductivity test. This oxidation could also be the initial oxidation of reduced polymer in the vicinity of the CNTs. During a potential sweep, the oxidized polymer exhibits the characteristic relationship between strain and charge discussed in Chapter 4. The reduce polymer does not sustain high current magnitudes, however, and both the charging and actuation responses are diminished. The polymer films do not respond to the continued potential sweep until the oxidation and onset of conductivity is started. Thus, the additional conductivity provided by the CNTs could enhance the response further.

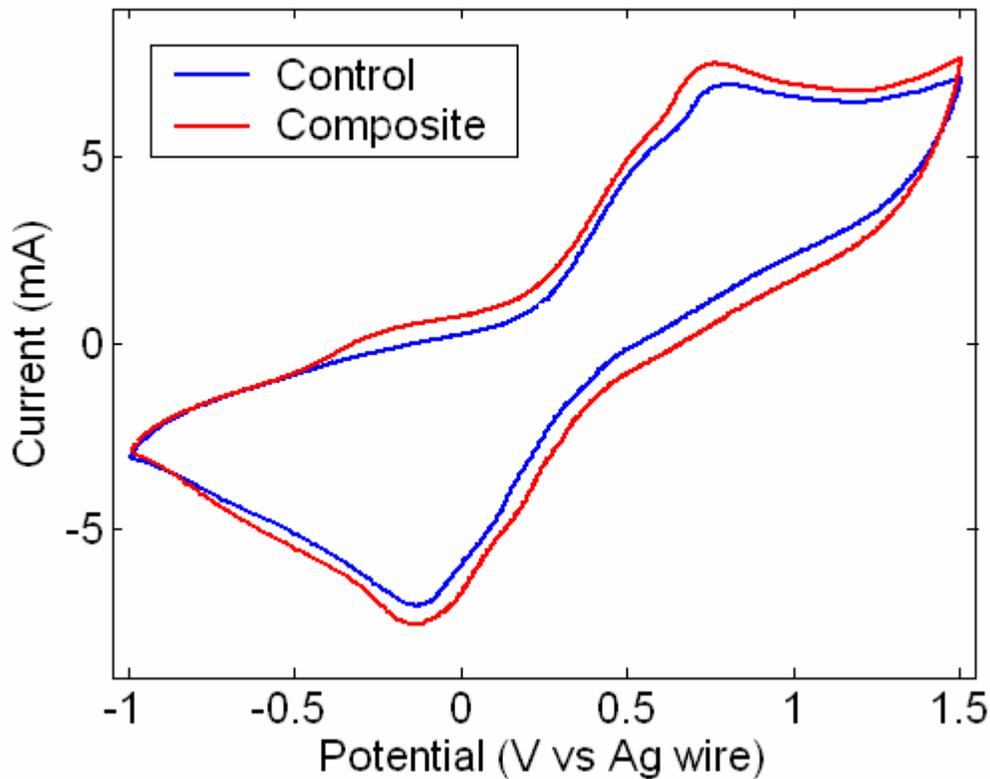


**Figure 6.4.** Cyclic voltammograms of control and composite films during isotonic test depicted in Figure 6.3.

### **6.3.2 Potential Square Wave response**

To demonstrate the relative response speed of the samples, a potential square wave was applied under isometric conditions. This test simplifies and speeds data acquisition by decoupling the response from a force feedback control algorithm in the electrochemical dynamic mechanical analyzer. It also enables the measurement of active stress generation and is an excellent compliment to the isotonic potential sweep technique used in the tests of the previous section. Figure 6.5 depicts the average active stress response of the control and composite samples to a potential square wave between 0 and 0.5 V versus Ag wire, applied at 0.05 Hz.

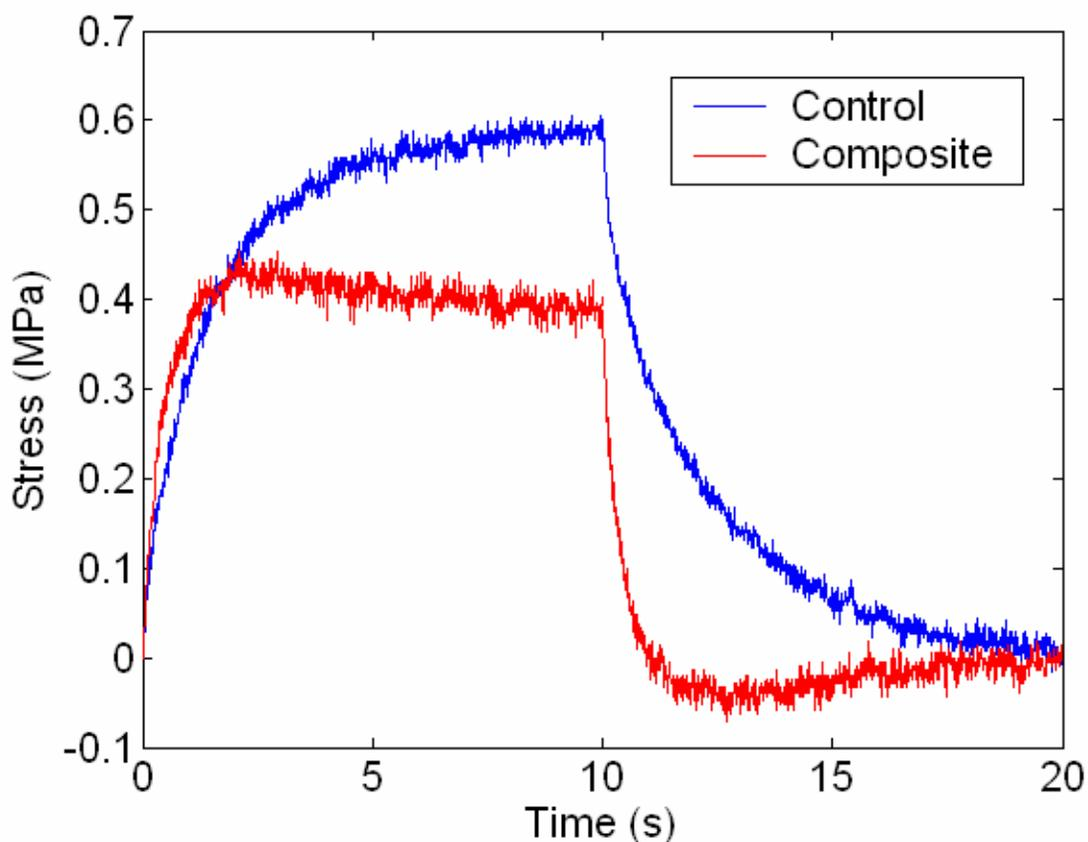


**Figure 6.5.** Average isometric response of PEDOT and composite film to 0.5 V peak to peak potential square wave at 0.05 Hz.

Both the control and composite films show an initially high stress rate that diminishes with time. The composite film maintains a higher stress rate for a longer time and the response also saturates to a final value more quickly. This increased response speed is attributed to the additional conductivity from the CNTs.

The overall magnitude of the stress response in the control sample, however, is larger than that observed in the composite sample. Since the modulus in the control sample is lower than that in the composite sample, it is unclear why more stress can be generated from the same waveform. The isotonic data in Figure 6.6, however, shows a similar total strain response in both films with the composite sample again exhibiting a faster response.

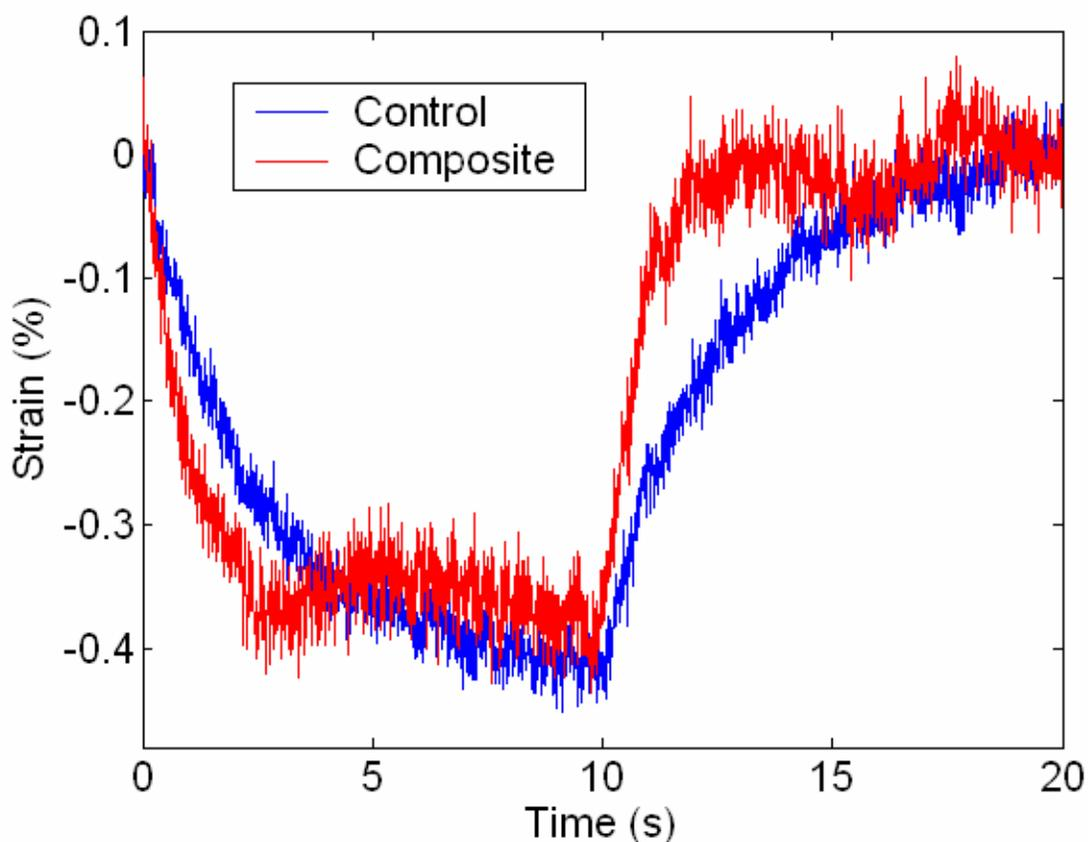


**Figure 6.6.** Average isotonic response of PEDOT and composite film to 0.5 V peak to peak potential square wave at 0.05 Hz.

## 6.4 Summary

PEDOT was successfully synthesized in a layered composite structure with carbon nanotubes. This structure exhibited improved conductivity and modulus over the control sample in each case by a factor of two. In actuation testing, the composite sample exhibited less creep during the course of a slow potential sweep experiment and faster responses to potential square waves. The addition of the carbon nanotubes did not significantly alter the magnitude of the response of the polymer. The cyclic voltammetry and in-situ conductivity tests demonstrated that the carbon nanotubes allowed better connectivity near the electrode contacts. The carbon nanotube loading was insufficient to render the polymer conductive at all potentials. The observed improvements over the control sample could lead to dramatic improvements in PEDOT that is synthesized

according to the procedure outlined in Chapter 5, shows a greater actuation response than the PEDOT synthesized in the control experiment.

## 6.5 References

1. a) Baughman, R. H.; Cui, C.; Zakhidov, A. A.; Iqbal, Z.; Barisci, J. N.; Spinks, G. M.; Wallace, G. G.; Mazzoldi, A.; De Rossi, D.; Rinzler, A.; Jaschinski O.; Roth, S.; Kertesz, M. Carbon nanotube actuators. *Science* **1999**, *284*, 1340-1344. b) Madden, J. D. W.; Barisci, J. N.; Anquetil, P. A.; Spinks, G. M.; Wallace, G. G.; Baughman, R. H.; Hunter, I. W. Fast Carbon Nanotube Charging and Actuation. *Adv. Mater.* **2006**, *18*, 870-873.
2. Gu, H. Massachusetts Institute of Technology. Unpublished work, 2006.
3. Sandler, J.; Shaffer, M. S. P.; Prasse, T.; Bauhofer, W.; Schulte, K.; Windle, A. H. Development of a dispersion process for carbon nanotubes in an epoxy matrix and the resulting electrical properties. *Polymer* **1999**, *40*, 5967-5971.
4. Warren, M. R.; Madden, J. D. Electrochemical switching of conducting polymers: A variable resistance transmission line model. *J. Electroanal. Chem.* **2006**, *590*, 76-81.



## 7. Poly(3-hexylthiophene) actuation

One of the most intriguing conducting polymers is poly(3-hexylthiophene), or P3HT, because it is fully-soluble in chloroform, even at high molecular weight. Indeed, other alkylthiophenes are soluble in their polymer form and the effect of alkyl chain length has been studied.<sup>1</sup> Chemically synthesized in its neutral form, it is readily drop cast onto a surface and doped with I<sub>2</sub> vapor, improving the conductivity by five orders of magnitude or more. The use of P3HT in actuation, much like PEDOT discussed in Chapter 5, is almost completely unknown, though initial work with poly(3-octylthiophene) demonstrated actuation in that system.<sup>2</sup> One of the reasons for this is undoubtedly the need for a chemical dopant, which complicates the use of P3HT electrochemically. A neutral film can readily be cast onto an electrode and peeled off with the mechanical properties necessary for an actuation test. Once clamped in an actuation test, however, the low conductivity of the sample limits the area of control to that immediately adjacent to the clamps. The voltage drop across the length of the sample would be too large to affect the electrochemical state of the middle of the sample. Only thin coatings of electrochemically doped or neutral P3HT are successful (as in field effect transistors) while actuation of freestanding films is limited.

In 2001, Fuchiwaki et al.<sup>3</sup> tested the electrochemical actuation in a number of materials including regioregular and regiorandom P3HT. To overcome the initially low conductivity of P3HT, the films were coated with a thin sputtered layer of Au to enhance conductivity without significantly interfering with the mechanical properties. The films were tested in an isotonic configuration in a solution of 0.2 M TBABF<sub>4</sub> in acetonitrile. The applied load was 0.2 MPa and the input was a slow potential triangle wave with a rate of 5 mV/s. Both regioregular and regiorandom P3HT demonstrated actuation behavior, though the elongation at each cycle was considerably larger than the subsequent contraction. The overall contractions (performing work against the load) were on the order of 1 %.

The ability to obtain freestanding films of blended P3HT and carbon nanotubes (CNTs)<sup>4</sup> suggested that actuation of this material would be useful, especially since its solubility provided an opportunity for further study and processing. As such, a series of actuation tests were performed on films of P3HT and blended P3HT blended with CNTs, doped and undoped with I<sub>2</sub>. It had been discovered that P3HT enhances the stability of CNTs in chloroform,<sup>4</sup> allowing freestanding films of high volume fraction CNTs in P3HT to be drop cast. Furthermore, as in the Au sputtering technique used by Fuchiwaki et al.,<sup>3</sup> the CNTs provide a conductivity enhancement in the undoped P3HT.

## 7.1 Synthesis

P3HT can be chemically synthesized in solution with FeCl<sub>3</sub>. Most of the initial work in the Swager group was pioneered by Dr. Ivory Hills, with additional contributions and development toward blending with CNTs performed by Dr. Hongwei Gu. The basic principle of the synthesis follows the oxidative coupling scheme described in Chapter 2 (noting that the solubility of P3HT in chloroform enables the entire polymerization to occur homogeneously and to high completion). The resulting polymer can have molecular weights of 100 kDa and, when cast onto a substrate, is mechanically stable enough to be peeled for further testing.

Solutions of P3HT can be combined with solutions of CNTs and dispersed in chloroform. Unlike the case of PEDOT and CNTs discussed in Chapter 6, the blend of P3HT and CNTs is homogeneous. Following a series of wash steps and centrifugation, the P3HT is believed to wrap around individual nanotubes, acting as surfactant and stabilizing the CNT dispersion.<sup>4</sup> Films cast from these solutions exhibit conductivities several orders of magnitude higher than pure P3HT and can undergo further conductivity enhancement upon exposure to I<sub>2</sub> vapor. The I<sub>2</sub> doping procedure involves exposure of the film to I<sub>2</sub> crystals in a sealed container. The speed of doping can be improved by evacuating the container to allow for greater vapor pressure of I<sub>2</sub> and this technique was used exclusively. Exposure times of 1 hour or more are sufficient to improve the conductivity of P3HT, which remains conductive for long times even after the I<sub>2</sub> vapor pressure is lowered.

## 7.2 Passive Characterization

Table 7.1 depicts the conductivities of doped and undoped P3HT films, with and without CNTs, measured via the four-point van der Pauw technique described in Chapter 3. The fraction of CNTs in the blend is characterized by weight ratio in the initial blending phase, though the final CNT loading is not independently characterized. The table shows that I<sub>2</sub> doping has a dramatic effect on P3HT conductivity and that the addition of CNTs also improves the conductivity, particularly in the undoped state. The data also suggest that additional loading of CNTs improves the conductivity, though the precise relation is not well elucidated as a function of the initial weight fraction.

	Conductivity (S/m)	
	Undoped	I <sub>2</sub> doped
P3HT	1.00 x 10 <sup>-2</sup>	8.50 x 10 <sup>2</sup>
P3HT:CNT 3:1 (wt)	1.77 x 10 <sup>2</sup>	5.00 x 10 <sup>3</sup>
P3HT:CNT 1:1 (wt)	1.13 x 10 <sup>3</sup>	1.60 x 10 <sup>4</sup>

**Table 7.1.** Conductivities of P3HT and P3HT/CNT blends as determined by van der Pauw conductivity measurement.

The passive mechanical characterization of P3HT with and without nanotubes at 0.5 Hz also demonstrates stiffness enhancement via the CNTs from an average modulus of 50 MPa unloaded to a range of 0.5 to 1.0 GPa with CNTs. The variation in these measurements may reflect the variation in CNT loading fraction. All blended samples exhibit higher moduli than pure P3HT.

P3HT shows unusual electrochemical behavior, with unbalanced oxidation and reduction currents in cyclic voltammetry experiments. Figure 7.1 shows a typical cyclic voltammogram for I<sub>2</sub>-doped P3HT in a solution containing 0.1 M TBAPF<sub>6</sub> in propylene carbonate. As the figure shows, the polymer exhibits very low capacitance in the oxidized region with the cathodic scan nearly overlaid on the anodic scan. In addition, the current magnitudes observed are highly asymmetric with considerably more current passing during oxidation than reduction.

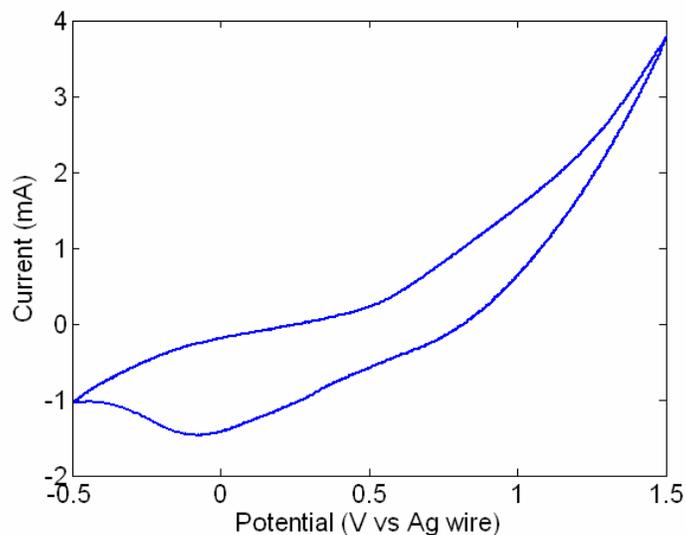


**Figure 7.1.** Cyclic voltammogram of freestanding P3HT doped with  $I_2$ . Film is immersed in 0.1 M TBAPF<sub>6</sub> in propylene carbonate.

### 7.3 Isotonic Characterization

P3HT samples were cycled between varying limits in several solvents to observe changes in strain corresponding to the electrochemistry. Tests in the ionic liquid BMIMBF<sub>4</sub> produced no actuation while tests in BMIMPF<sub>6</sub> gave an active contraction of 0.1%. The strain magnitude did not corroborate the actuation observed in the literature.<sup>3</sup> In acetonitrile, a 3:1 blend of P3HT and CNT actuated during an electrochemical cycle between -0.3 and 1.5 V versus Ag wire as depicted in Figure 7.2. This result resembles the actuation observed by Fuchiwaki et al.,<sup>3</sup> with the CNTs presumably playing the same conductivity enhancing role as the Au sputtered coating. In the first cycle, the sample elongates by 3 %, and then contracts by 1 %. The two subsequent cycles show a similar response, though the magnitudes of the elongation and contraction are reduced. The results were further corroborated by tests in propylene carbonate.

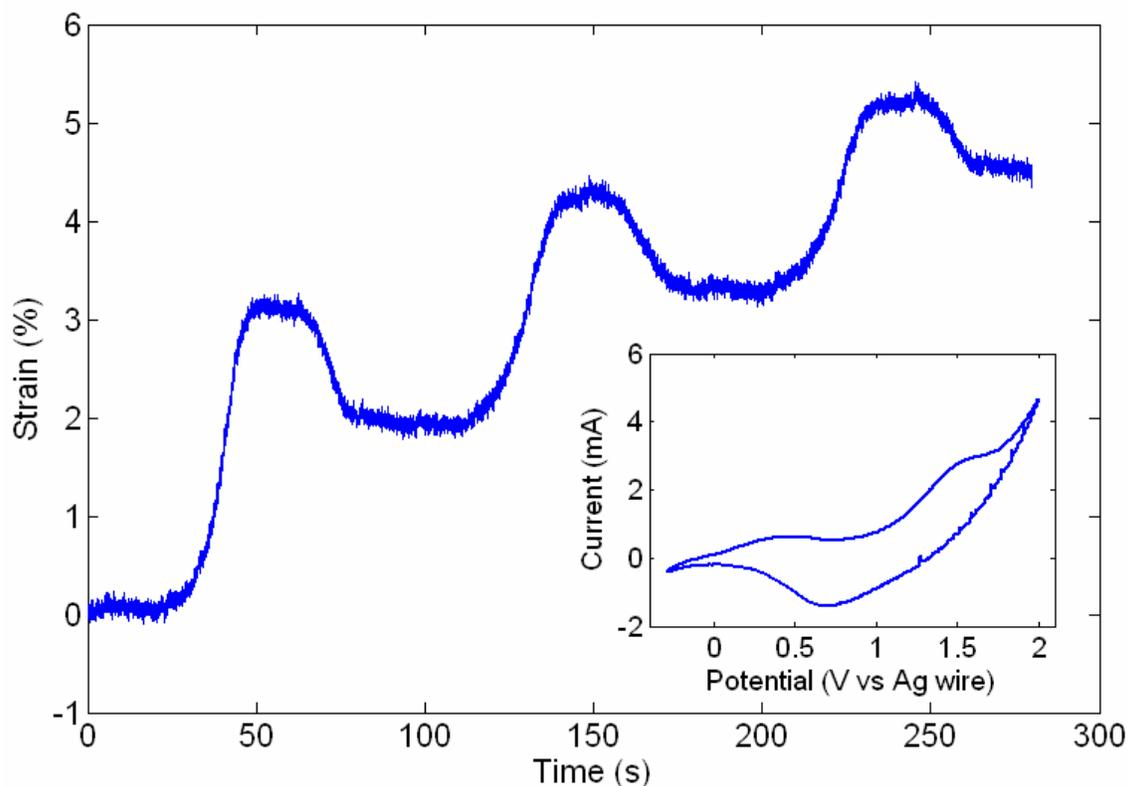


**Figure 7.2.** Isotonic response and cyclic voltammogram of undoped P3HT/CNT blend in 0.2 M TBABF<sub>4</sub> in acetonitrile at 50 mV/s against a load of 0.55 MPa.

In an isotonic test in propylene carbonate, P3HT films were also observed to behave asymmetrically in response to triangle potential waveforms. A further unusual property was observed. The elongation and contraction depended on the potential scan limits. Unlike the cases of polypyrrole and PEDOT, in which the passage of charge leads to actuation under isotonic conditions, the P3HT films demonstrated a threshold-like behavior, in which strain was not observed unless a sufficient potential was reached. Figure 7.3 demonstrates three successive test of 1:1 blend of P3HT and CNTs doped with I<sub>2</sub> in which the electrochemical window was shifted from the initial limits of 0 and 1 V to the limits of 0.5 and 1.5 V versus Ag wire. At the lowest potential window, little strain occurs. Increasing the anodic limit to 1.25 V demonstrates a slight elongation and contraction. Further increasing the limit to 1.5 V duplicates the response observed in acetonitrile.

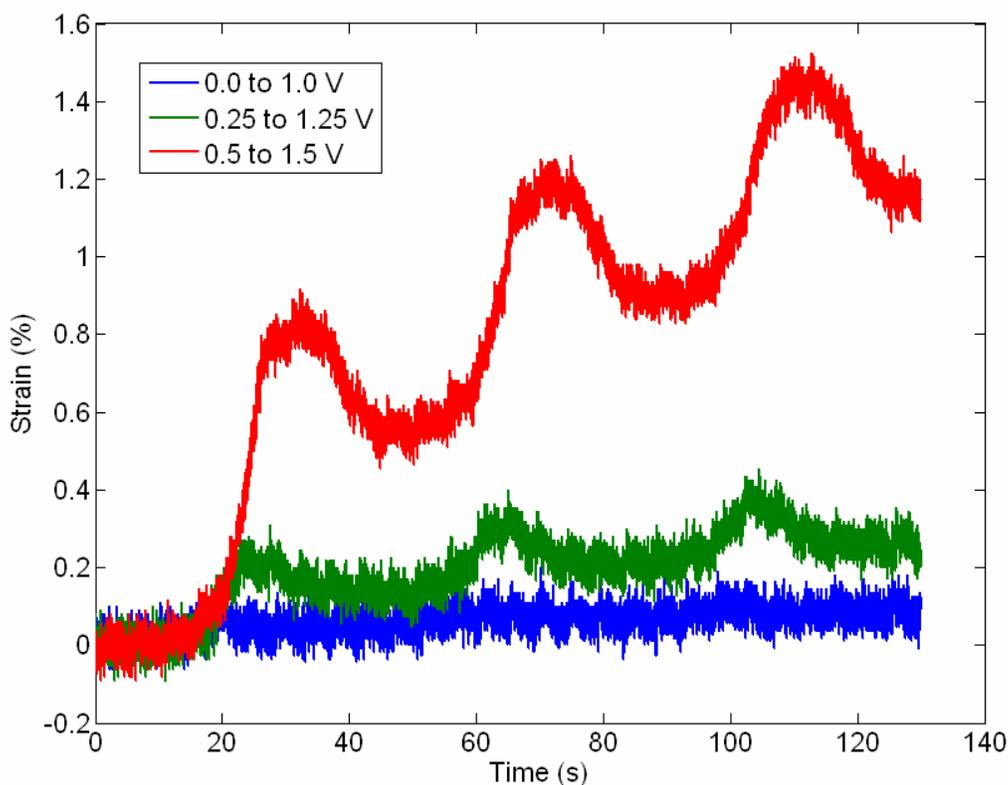


**Figure 7.3.** Strain response of P3HT/CNT blend to different electrochemical windows at 50 mV/s against a load of 0.5 MPa.

The behavior originally observed in P3HT sputter-coated with a Au layer<sup>3</sup> was only repeated at sufficiently high potentials. Furthermore, this potential region produces the asymmetric current response in propylene carbonate with greater elongation than contraction in each cycle. The nature of the actuation mechanism was not clarified until the isometric test was attempted.

## 7.4 Isometric Characterization

Since the isotonic tests showed an unusual dependence on the potential limits applied, isometric tests were tried under similar electrochemical conditions. The first full response observed is shown in Figure 7.4, in which potential, current, charge, and stress are plotted in a raw data format. In this test, an I<sub>2</sub> doped sample of 3:1 blended P3HT/CNT was cycled between 0.25 and 1.25 V versus Ag wire at 10 mV/s. The sample was prestressed to 0.5 MPa.

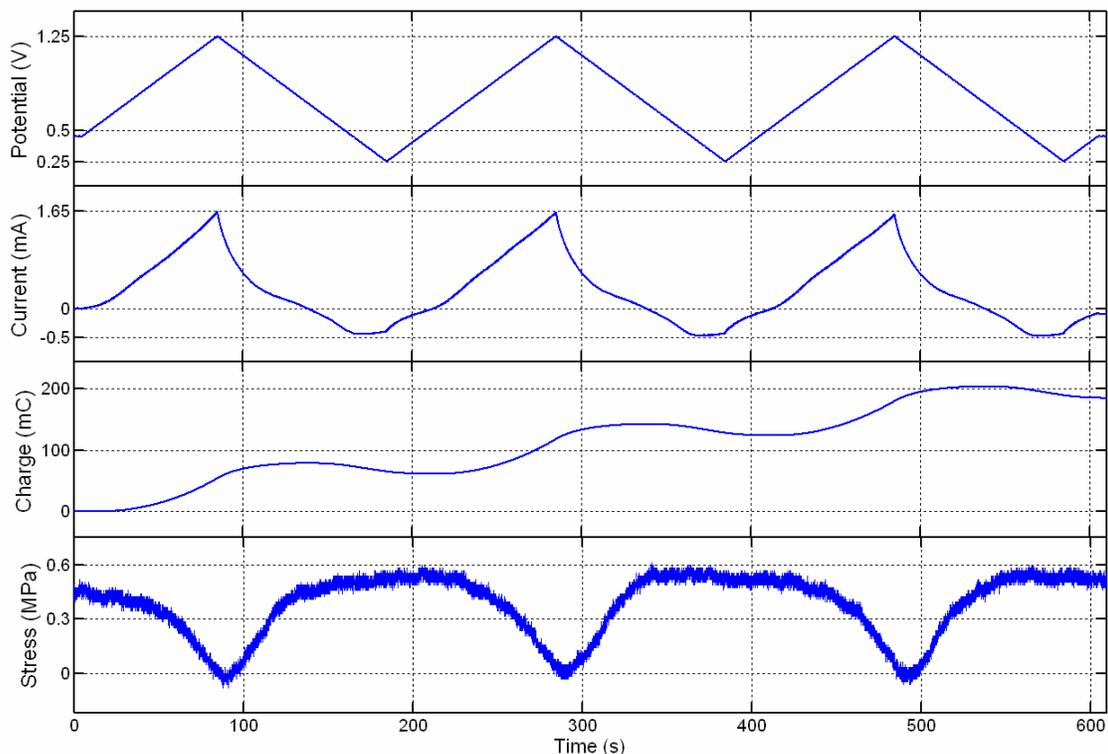


**Figure 7.4.** Isometric response of 3:1 P3HT/CNT blend in 0.1 M TBAPF<sub>6</sub> in propylene carbonate demonstrating the dependence of stress on potential rather than charge.

Unlike the isotonic response, the sample in Figure 7.4 returns to its initial state in each cycle of the isometric test, showing a less asymmetric response. The current is asymmetric, however, as reflected by the significant increase in charge over time. Unlike tests with polypyrrole and PEDOT, the mechanical response no longer has the shape of the charge response. Closer inspection of the isotonic response depicted in Figure 7.3 revealed that that charge and strain were also not directly related. This lack of this relationship, however, is much clearer in the isometric case since the stress response is symmetric.

More profound is the relationship between the shape of the potential waveform and the stress response. The peaks in stress correspond to the peaks observed in the potential and current waveforms rather than those observed in the charge signal. Furthermore, the stress appears to change direction while the current is still positive, indicating that the polymer continues to increase in charge while the mechanical response is reversing. At long time scales the actuation in PEDOT and polypyrrole becomes

potential dependent,<sup>5</sup> though the charge also depends on the potential at these time scales since the behavior is capacitive. In the case shown for P3HT the mechanical response is dependent on potential and independent of charge. The current response also demonstrates the same triangular shape with peaks corresponding to the peaks in the stress response. The data in Figure 7.3 refute the idea of a current dependence, however, since current is present in all three isotonic tests, though the mechanical response only occurs at sufficiently high potentials.

In the test depicted in Figure 7.4, the film relaxes completely, reaching a stress of 0 MPa during the potential sweep to 1.25 V. Since a thin film typically buckles before it exerts a compressive force, it is not clear from Figure 7.4 if the stress has a minimum state. It is also unclear whether the observed dependence of stress on potential is relative or absolute. If the response were absolute, the application of a potential would correspond to a single stress value, whereas if the response were relative, the stress at a given potential would also depend on the previous stress. Following the test depicted in Figure 7.4, the film was tested isometrically from a higher initial stress. In addition, the potential scan rate was decreased to observe if the relationship between stress and potential also depended on the rate of the potential change. The result of the second isometric test is shown in Figure 7.5. In the figure, the relative stress (stress change from the initial imposed value) is plotted versus the potential of the film. The results obtained in the previous test and depicted in Figure 7.4 are also plotted on the same axes.



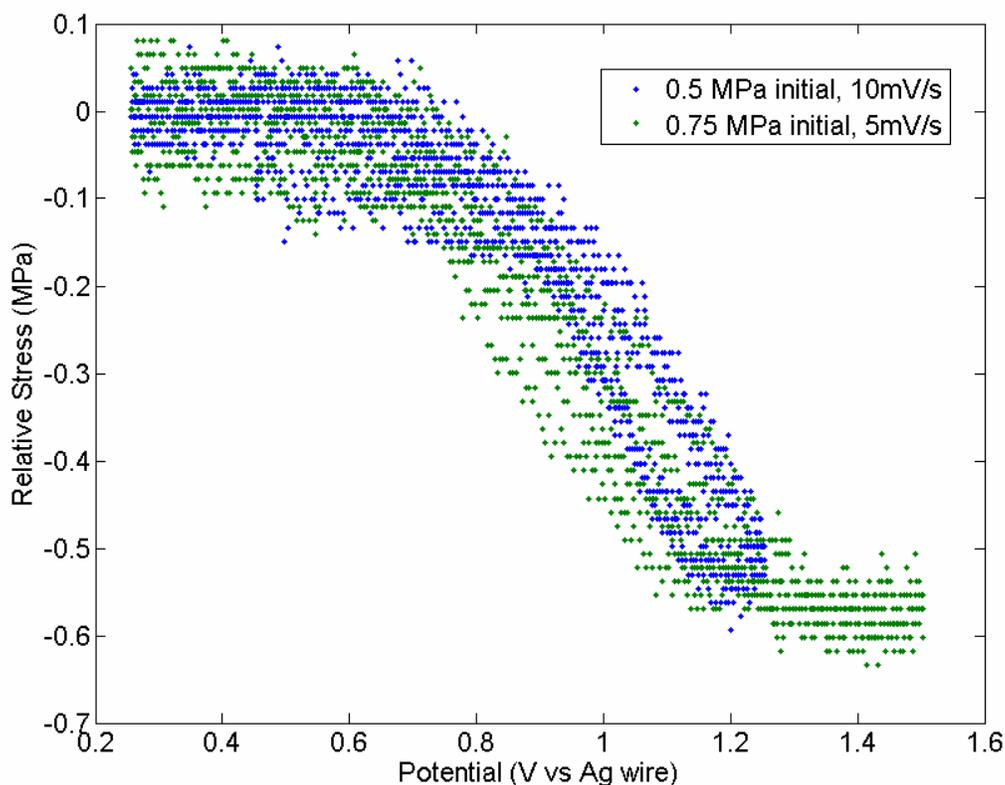


**Figure 7.5.** Relative stress versus potential for isometric test of P3HT/CNT blend.

From the results shown in Figure 7.5, a number of observations regarding the actuation mechanism in this system can be made. First, as the potential sweep is reversed, the stress in the film remains a function of potential with little hysteresis. At these scan rates, therefore, the film shows equilibrium behavior since the change in stress depends only on the potential. Next, in the test starting at 0.75 MPa, the lowest stress observed is greater than zero, suggesting that there is a lower limit to the stress change in this system. Lastly, the superposition of the two tests demonstrates that the mechanism is rate independent at these scan rates and that it is a relative stress not an absolute stress that is determined by the potential of the film. The next question addressed was the differences in the response in isotonic and isometric modes.

## 7.5 Potential Dependent Modulus

Relating the isometric and isotonic results observed in P3HT is critical to the understanding of the underlying actuation mechanism because it appears to be different than that observed in conventional conducting polymer actuators. If the different isotonic and isometric results are produced by the same mechanism, then the different mechanical responses must be reconciled. The stress response observed in the isometric tests could be caused by a change in the modulus of the P3HT as a function of potential. Since the sample does not change its length, merely changing the stiffness in the material would change the internal stress, which could be recovered. In the isotonic case, however, the lower modulus would lead to further elongation since the instrument maintains the stress in the sample. If the modulus then increased, caused by the cathodic potential sweep, the response of the polymer could have two possibilities. In the first, the film would stiffen at its new length but would not recover any of the plastic deformation that occurred as a result of the decrease in modulus. In the second possibility, the film would recover all of the elastic deformation and return to its initial state. The asymmetric response observed in the isometric test appears to be a combination of these two possibilities.

This hypothesis was tested on the doped P3HT/CNT sample utilized in the tests depicted in Figures 7.4 and 7.5. The film was held at constant potentials, each for 3 minutes, starting with 0.75 V versus Ag wire. At intervals of 0.25 V, the potential was increased to 1.5 V. At each potential, the film modulus was tested at 0.5 Hz. Following the oxidation, the film was reduced in 0.25 V increments maintaining the cycle of mechanical tests. The results, depicted in Figure 7.6, show the modulus of the film decreasing by a factor of three, from 525 MPa to 175 MPa, between 0.75 and 1.5 V versus Ag wire. The modulus increases during the subsequent reduction, though not to the initial values measured during the anodic sweep.

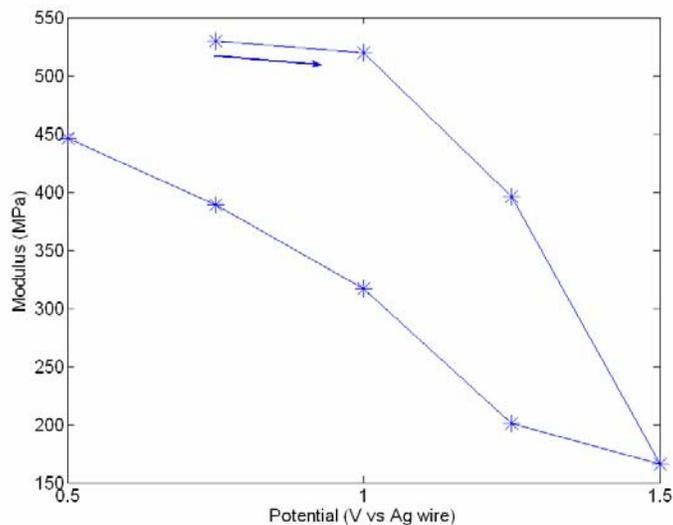


**Figure 7.6.** Modulus versus applied potential for P3HT/CNT blend.

While this observation corroborates the difference between the isometric and isotonic response, it is not sufficient to explain the results completely. The stresses used in the isotonic and isometric tests were on the order of 0.5 MPa. For a sample with a modulus of 500 MPa, this corresponds to a strain of 0.1 %. When the modulus is lowered to 175 MPa, the strain would increase to 0.29 %, an increase of only 0.19 %. In the isotonic test depicted in Figure 7.3, the observed elongation is 0.8 %. In the isometric test, a modulus change from 500 to 175 MPa would lead to a stress change of 0.33 MPa in an elastic body held initially at 0.5 MPa. The hysteresis observed in the modulus test depicted in Figure 7.6 also suggests that the modulus may have changed during the course of the tests and could be tested further.

## 7.6 Unblended P3HT

One additional question regarding the mechanism of the actuation in P3HT is the role of the CNTs included in the film. CNTs are known to actuate electrochemically,<sup>6</sup> so more than one effect could have occurred in the preceding tests. The potential dependent behavior presented above was independent of the I<sub>2</sub> doping, however, since the actuation was observed in doped and undoped samples. To test the effect of the CNTs, the isotonic tests were repeated with a sample of I<sub>2</sub> doped P3HT without CNTs. As noted earlier, P3HT in its neutral state without the CNTs incorporated has a conductivity that is too low

to use in actuation tests on mm length samples. The  $I_2$  doped samples, however, are sufficiently conductive as noted in Table 7.1. Figure 7.7 shows the isotonic response of and  $I_2$  doped sample to a slow potential triangle wave in propylene carbonate. The test conditions were identical to those presented in Figure 7.3 with the exception that the stress in the sample was held at 0.1 MPa rather than 0.5 MPa. This change was made to reflect the lower modulus in the samples without CNTs and after it was observed that the creep during actuation in the unblended samples was considerably larger than in the blended samples at the same loading.

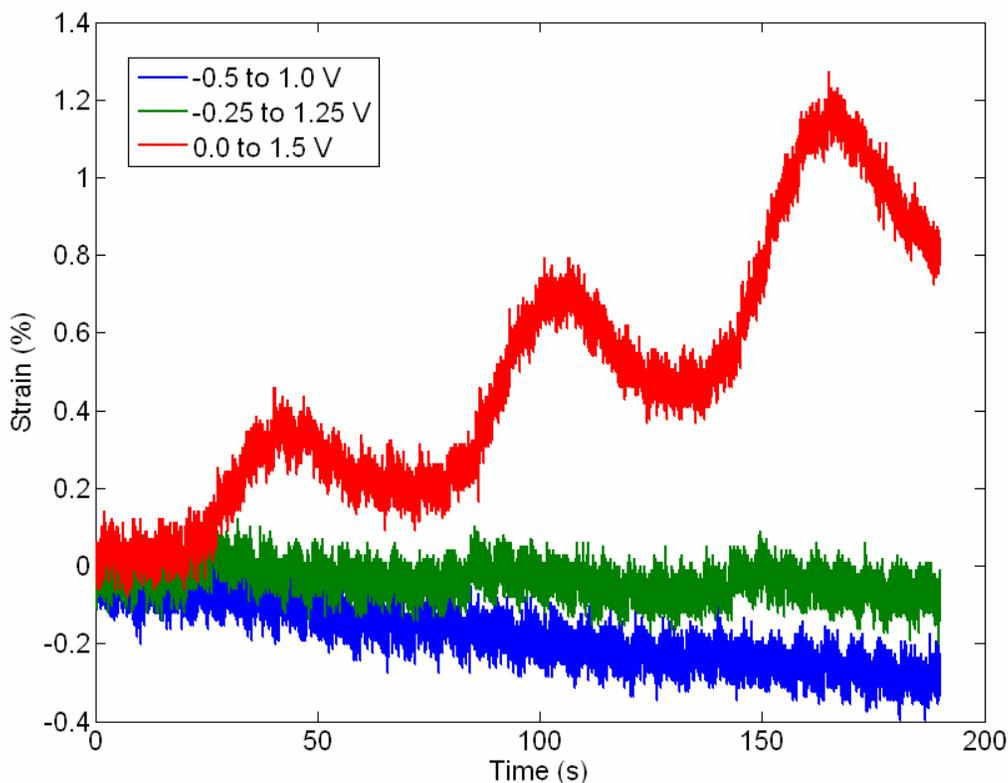


**Figure 7.7.** Isometric response of  $I_2$  doped P3HT to potential waveform over varying ranges in 0.1 M TBAPF<sub>6</sub> in propylene carbonate. All tests performed at 50 mV/s at 0.1 MPa.

As in the case of the CNT blended samples, the isotonic response of the P3HT shows the asymmetric elongation and contraction response. The response also shows the threshold behavior demonstrated in Figure 7.3 in which the polymer shows no elongation at 1.0 or 1.25 V. At sweeps to 1.5 V, the polymer elongates by nearly 0.5 % and contracts by 0.2% each cycle.

## 7.7 Summary

The data regarding P3HT presented in this chapter are unique to the field of conducting polymer actuators, to the author's knowledge. Furthermore, they demonstrate a significant deviation from the relationship between charge and mechanical response observed during ion ingress and egress. While actuation in polypyrrole and PEDOT can be dependent on potential alone at long times, this behavior is not independent of the charge waveform as demonstrated in the case of P3HT. Thus, in this system, the actuation mechanism must rely on changes that depend on potential rather than ion movements. While the modulus of the P3HT does change as a function of potential, this change alone is not sufficient for the actuation response observed. It also appears that the neither the CNTs nor  $I_2$  doping are required for the response, suggesting that the actuation mechanism is a property of P3HT. This result is also corroborated by the data obtained by Fuchiwaki et al.<sup>3</sup> as the system they used consisted of P3HT and Au with neither CNTs or  $I_2$  present.

One possible potential-dependent mechanism is the twisted to planar conformational change along the backbone of the conducting polymer as the bonds between monomers alternate between single and double character.<sup>7</sup> This transformation may also contribute to a change in interchain interactions, causing a change in the passive mechanical properties, such as the modulus. The observation of potential-dependent actuation may also represent a new interchain interaction similar to the quarterthiophene mechanism proposed in Chapter 1. While more evidence is needed to elucidate the nature of this actuation mechanism, the observation of strains greater than 1 % and independent of charge in a solution processable material represents a new direction for conducting polymer actuators.

## 7.8 References

1. Oztemiz, S.; Beaucage, G.; Ceylon, O.; Mark H. B. Synthesis, characterization and molecular weight studies of certain soluble poly(3-alkylthiophene) conducting polymers. *J. Solid State Electrochem.* **2004**, *8*, 928-931.
2. a) Pei, Q.; Inganas, O. Electroelastomers: Conjugated Poly(3-octylthiophene) Gels with Controlled Crosslinking. *Synth. Met.* **1993**, *55-57*, 3724-3729. b) Chen, X.; Inganas, O. Doping-induced volume changes in poly(3-octylthiophene) solids and gels. *Synth. Met.* **1995**, *74*, 159-164.
3. Fuchiwaki, M.; Takashima, W.; Kaneto, K. Comparative study of electrochemomechanical deformations of poly(3-alkylthiophene)s, polyanilines and polypyrrole films. *Jap. J. Appl. Phys.* **2001**, *40*, 7110-7116.
4. Gu, H. Massachusetts Institute of Technology. Unpublished results, 2006.
5. Madden, J. D. W. Conducting Polymer Actuators. Ph.D. Thesis, Massachusetts Institute of Technology, Cambridge, MA, 2000.
6. a) Baughman, R. H.; Cui, C.; Zakhidov, A. A.; Iqbal, Z.; Barisci, J. N.; Spinks, G. M.; Wallace, G. G.; Mazzoldi, A.; De Rossi, D.; Rinzler, A.; Jaschinski O.; Roth, S.; Kertesz, M. Carbon nanotube actuators. *Science* **1999**, *284*, 1340-1344. b) Madden, J. D. W.; Barisci, J. N.; Anquetil, P. A.; Spinks, G. M.; Wallace, G. G.; Baughman, R. H.; Hunter, I. W. Fast Carbon Nanotube Charging and Actuation. *Adv. Mater.* **2006**, *18*, 870-873.
7. Otero, T. F.; Grande, H.-J.; Rodríguez, J. Reinterpretation of Polypyrrole Electrochemistry after Consideration of Conformational Relaxation Processes. *J. Phys. Chem. B* **1997**, *101*, 3688-3697.

## 8. Polypyrrole actuation at elevated temperatures

Polypyrrole is a well characterized conducting polymer capable of actuating in both linear and bending modes and subject to considerable study. Recently it was observed that polypyrrole bimorph actuators were heating during actuation and that the increased temperature improved the response speed of the bimorphs.<sup>1</sup> This result suggested further characterization of linear actuation with temperature control to quantify the rate improvement and determine its origin, specifically with regard to the model developed by Madden.<sup>2</sup> The model highlights two time constants critical to actuator performance limited by capacitive charging and diffusion.<sup>3</sup> The charging time constant

$$\tau_{RC} = R C_v, \quad 1$$

is an electrical time constant defined by the solution resistance  $R$  and the volumetric capacitance  $C_v$  of the polymer. The diffusion time constant

$$\tau_D = \frac{a^2}{4D}, \quad 2$$

represents the time required for ions with diffusion coefficient  $D$  to intercalate into a polymer film of thickness  $a$ . Solution resistance and diffusion coefficients are both known to depend on temperature, suggesting a decrease in both time constants as the temperatures is increased. As such, the observation of improved actuation speed allows for the testing of the model and the relevance of the time constants.

For the purpose of testing linear actuation above room temperature an electrochemical dynamical analyzer was constructed for use within an environmental test chamber. Isometric tests were used exclusively as the determination of response speed was encumbered by the slow response of the instrument in isotonic mode. Several electrochemical waveforms were applied including potential square waves and sinusoidal signals of varying frequency. The application of potential square waves was modeled with an equivalent circuit and discrete time simulation based on the assumptions included in the original model proposed by Madden.<sup>2</sup> The work was performed with Michael Del

Zio who also reported a portion of the results.<sup>4</sup> The emphasis here will be on the underlying mechanisms and the relevance and effectiveness of the analysis.

## 8.1 Experimental Techniques

Freestanding polypyrrole films were obtained electrochemically by galvanostatic polymerization from a two-electrode cell consisting of a glassy carbon working electrode and copper counter electrode. The deposition solution consisted of 0.06 M pyrrole (Aldrich, freshly distilled before use), 0.05 M tetraethylammonium hexafluorophosphate (Aldrich, used without purification), and 0.6 M water in propylene carbonate (Aldrich, used without further purification). Polypyrrole was deposited on the working electrode at  $1.0 \text{ A/m}^2$  at  $-40 \text{ }^\circ\text{C}$  for approximately 8 hours, obtaining a free-standing film approximately  $20 \text{ }\mu\text{m}$  thick with a conductivity of  $1 \times 10^4 \text{ S/m}$ .

The mechanical tests were performed in the ionic liquid 1-butyl-3-methylimidazolium hexafluorophosphate, or BMIMPF<sub>6</sub> (Solvent Innovations GmbH, used without further purification). In BMIMPF<sub>6</sub>, polypyrrole is actively swelled by the imidazolium cation as is PEDOT, discussed in Chapter 5. All tests were performed in isometric mode to observe active stress generation versus time for a given electrochemical waveform. The testing apparatus was designed for use in an environmental chamber (Cincinnati Sub Zero), capable of maintaining temperature with  $1 \text{ }^\circ\text{C}$  resolution. The film samples were clamped between two alligator clips, which were fixed to a load cell and rigid stage on one side and a single axis stepper motor on the other (Parker Hannifin). The stepper motor was used to adjust preload in the sample before each test and the load cell was used to measure the force generated versus time and recorded to a PC via a National Instruments DAQ card.

For electrochemical modulation, the polymer was immersed in a bath of the ionic liquid with a silver wire pseudoreference electrode and stainless steel counter electrode. The electrochemical stimulus was controlled by a single channel of a VMP2 multichannel potentiostat (Princeton Applied Research) which recorded the potential and current in the cell and was externally synchronized by the digital output in the DAQ card. The entire



configuration was designed to fit entirely in the environmental chamber and the temperature in the bath was monitored independently with a thermocouple.

Each sample was initially equilibrated by electrochemical cycling between -1.0 and 1.0 V versus the Ag wire reference electrode at 50 mV/s until a steady cyclic voltammogram was obtained, typically within ten cycles. The mechanical tests at temperatures of 25, 50, 75, and 100 °C were performed by mounting the sample into the warmed bath and pre-stressing the film to 2.0 MPa before testing. Subjecting the polymer to the slow heating cycles between temperatures led to degraded performance, so the sample was remounted before each test. Individual films were tested at each temperature both in heating (25 to 100 °C) and cooling (100 to 25 °C) scans with similar result. At each temperature, a square wave between 0.0 V and 1.0 V versus Ag wire was applied for measurement of the response speed. The potential limits were chosen to maintain the conductive, oxidized form, without reducing the polymer to its insulating form. Initial tests were carried out at 0.1 Hz, though tests at 0.033 Hz enabled better resolution of the full polymer response.

In addition to the fixed frequency square wave response, simultaneous stress and impedance measurements were taken to obtain the frequency response of polymer films at 25 and 75 °C. The films tested in this manner followed the same equilibration and prestress protocol, but were subjected to a 500 mV peak to peak sinusoidal potential waveform centered at 0.5 V versus Ag wire. The frequency sweep was accessed through the impedance capability of the potentiostat which was controlled with software supplied with the instrument as noted above.

## 8.2 Observations

Figure 8.1 depicts the stress generation in polypyrrole, responding to the oxidative (0 to 1.0 V versus Ag wire) half cycle of a 0.033 Hz square wave at 25, 50, 75 and 100 °C. As the temperature is increased, both the initial rate of stress increase and the final stress also increase, though the final stress is similar at 25 and 50 °C. The curves presented in the figure represent the average normalized response from the 2<sup>nd</sup> to 10<sup>th</sup>

cycles. The potential step in the first cycle begins at the open circuit potential and consequently the stress generated from the open circuit potential to 1.0 V did not give the same result as subsequent cycles. In each case, the stress increased upon the rise in potential to 1.0 V, indicative of the egress of the imidazolium ion.

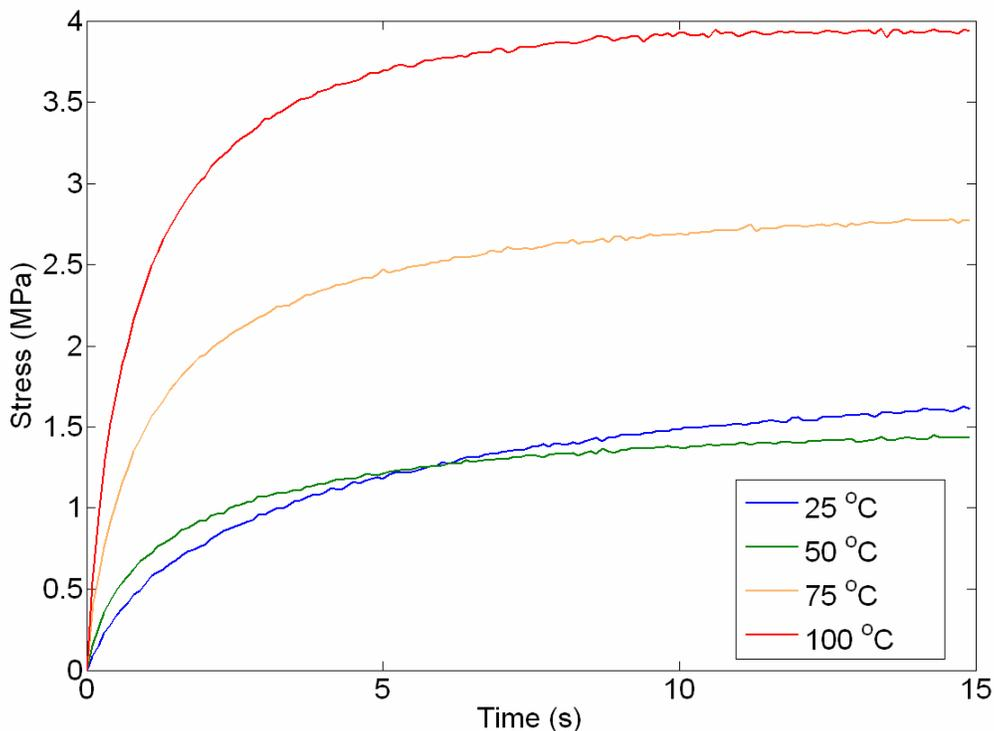


**Figure 8.1.** Isometric stress generation of PPy in BMIMPF<sub>6</sub> at 25, 50 75, and 100 °C during 1.0 V peak to peak square wave input at 0.033 Hz. Data averaged over 9 cycles neglecting first cycle from open circuit potential.

Over the span of many cycles, the amount of stress generated by a film in each cycle decreases, indicating the practical lifetime of an actuator performing in that particular configuration. Figure 8.2 shows the magnitude of the stress change observed per cycle at 25, 50, and 75 °C. In these tests, the input square wave used the same potential magnitude. The frequency was increased to 0.25 Hz to shorten the duration of a full experiment, though the actuation response is not fully developed in the half cycle. Polypyrrole has exhibited high lifetimes in ionic liquids,<sup>5</sup> though the samples tested above 25°C showed much lower lifetimes than the literature or the room temperature case.

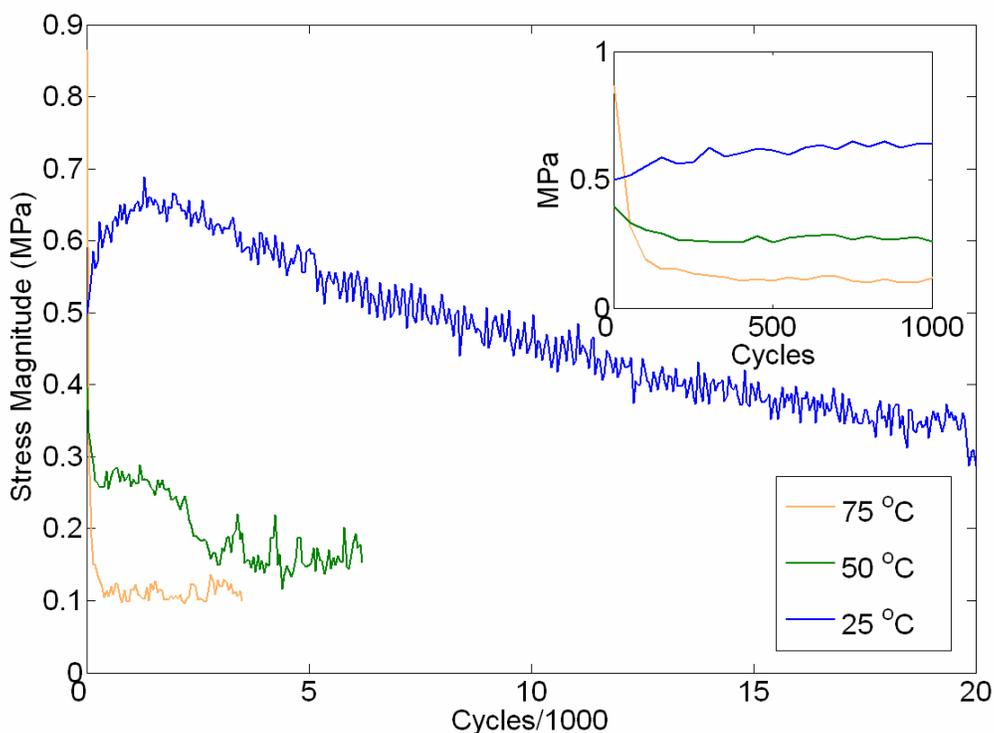


**Figure 8.2.** Active stress in polypyrrole at 25, 50 and 75 °C versus number of cycles for 1.0 V peak to peak square wave activation at 0.25 Hz. Inset shows initial 1000 cycles.

The short lifetime at 75 °C precluded further testing to 100 °C, though it should be noted that even at 75 °C the electrochemical activity did not diminish to the same extent as the mechanical response depicted here. This suggests that the ultimate failure was mechanical rather than electrochemical and Wallace et al. have demonstrated that the response may be recovered after a period of some rest.<sup>5</sup> The data in Figure 8.2 also corroborates the findings presented in Figure 8.1, in which the magnitude of stress response was similar at 25 and 50 °C and larger at 75 °C. The effect of cycle number on the response speed was not measured during the lifetime test.

With so many tests at different frequencies it can become difficult to compare between different test conditions. Madden et al.<sup>3</sup> demonstrated that this difficulty could be overcome by sampling the mechanical performance in a range of frequencies rather than one. Making use of the impedance spectroscopy capability of the potentiostat, a coupled impedance and mechanical test was devised. The results, depicted in Figure 8.3

show the mechanical response to the sinusoidal potential sweep as a function of frequency at 25 and 75 °C. At 75 °C, the stress magnitude appears shifted from the data observed at room temperature, though the relation between stress and frequency holds as the slope is unchanged between  $10^{-2}$  and  $10^0$  Hz.

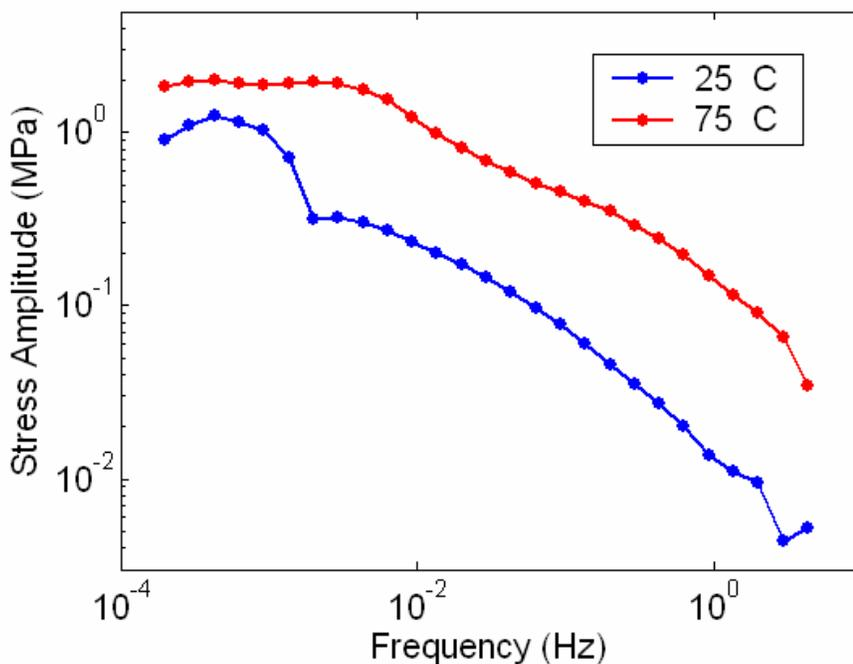


**Figure 8.3.** Isometric stress generation of PPy in BMIMPF<sub>6</sub> at 25 and 75 °C during 500 mV peak to peak sinusoidal frequency sweep.

The electrochemical impedance observed during this experiment is shown in Figure 8.4, with impedance magnitude and phase as function of frequency. At all frequencies the impedance is higher at 25 °C indicating a higher solution resistance. The onset of capacitive behavior as measured by the phase response also occurs at higher frequencies at 75 °C. These observations also corroborate the original data in Figure 8.1, though the relevance of the time constants and appropriate circuit models will be discussed in the next section.

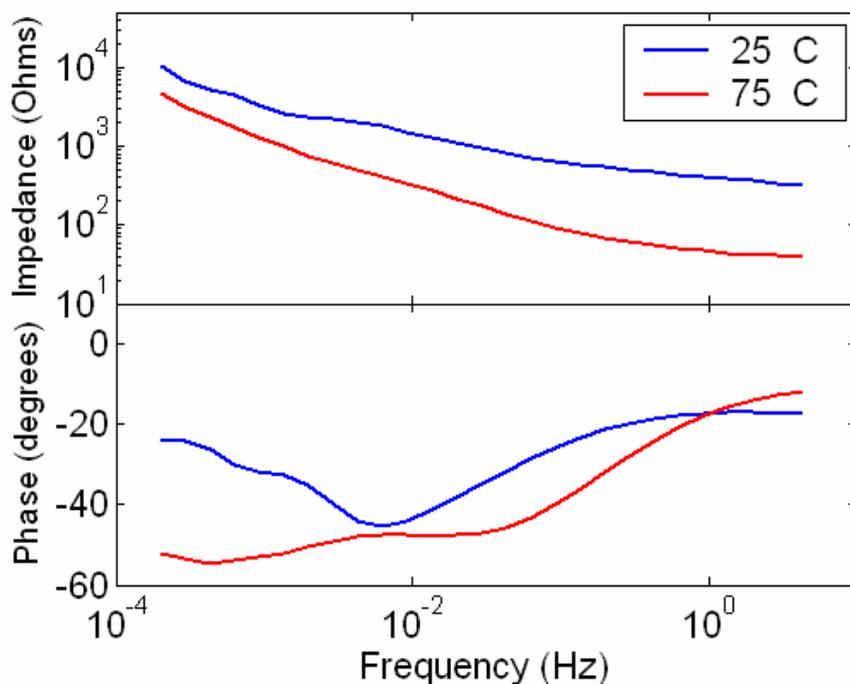


**Figure 8.4.** Electrochemical impedance of polypyrrole films at 25 and 75 °C. Potential sweep 500 mV peak to peak centered at 0.5 V versus Ag wire.

### 8.3 Equivalent Circuit Modeling

The square wave and frequency response experiments present two different opportunities to examine the mechanism of polypyrrole actuation and the effects of temperature. The potential square wave measurement replicates the application of an actuator and allows for direct time-based simulation of the results based on an equivalent circuit. A useful starting point for such an analysis is the Randle's circuit originally applied by Madden<sup>2</sup> and depicted in Figure 8.5.

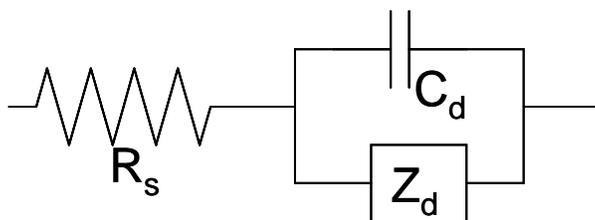


**Figure 8.5.** Randle's Circuit with solution resistance  $R_s$ , double layer capacitance  $C_d$  and polymer diffusion impedance  $Z_d$ .

It is possible to model diffusion with numerous electrical equivalents, including transmission lines and other distributed elements that have distributions of time constants. In response to a potential square wave, however, Figure 8.6 demonstrates that the response of the polymer can be adequately fit with two time constants. In the figure, the data from Figure 8.1 is plotted with the numerical fits superposed. Each fit is of the form

$$\sigma_1(1 - \exp(-t/\tau_1)) + \sigma_2(1 - \exp(-t/\tau_2)), \quad 3$$

with the values  $\sigma_1$ ,  $\sigma_2$ ,  $\tau_1$ , and  $\tau_2$  tabulated in Table 8.1. The fit was implemented by nonlinear least squares method in MATLAB.

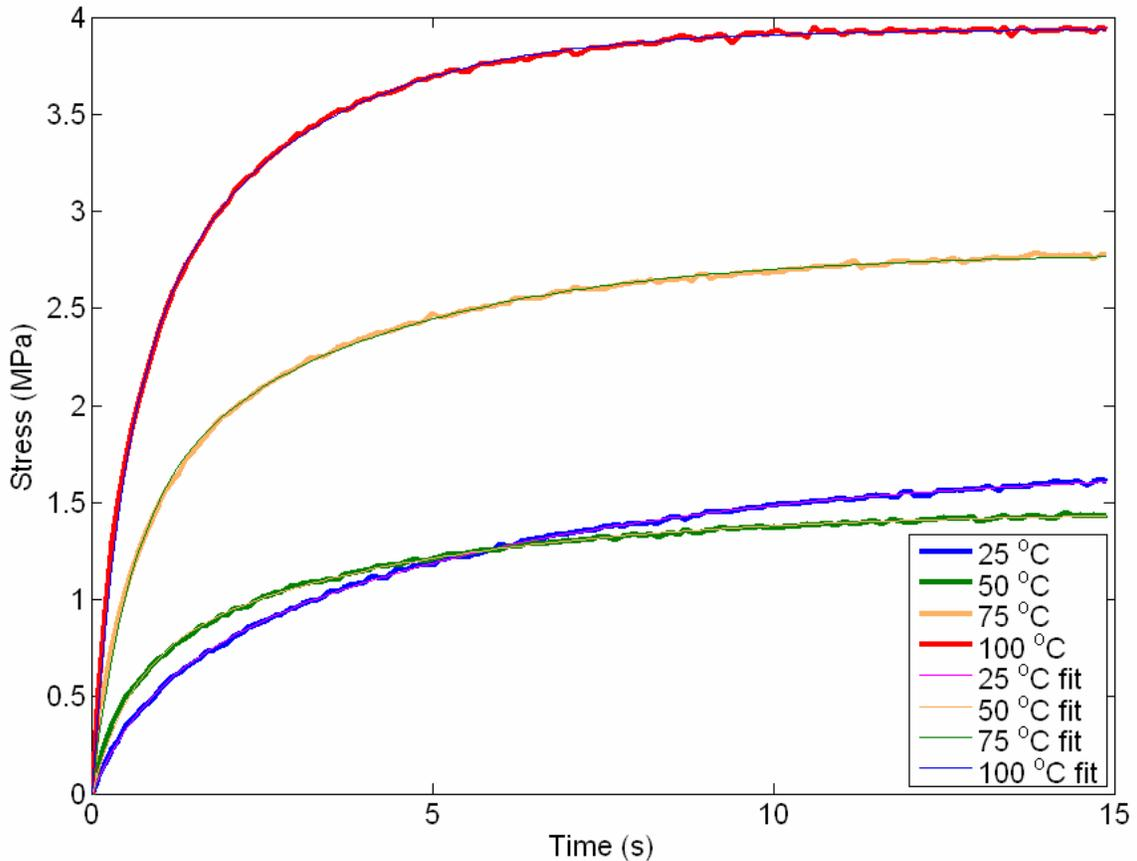


**Figure 8.6.** Isometric stress generation of PPy in BMIMPF<sub>6</sub> at 25, 50 75, and 100 °C with non-linear least squares fit superposed. Raw data identical to Figure 8.1.

<b>Temp (°C)</b>	<b><math>\sigma_1</math></b>	<b><math>\tau_1</math></b>	<b><math>\sigma_2</math></b>	<b><math>\tau_2</math></b>
<b>25</b>	<b>0.47</b>	<b>0.79</b>	<b>1.23</b>	<b>5.68</b>
<b>50</b>	<b>0.67</b>	<b>0.61</b>	<b>0.79</b>	<b>4.23</b>
<b>75</b>	<b>1.45</b>	<b>0.58</b>	<b>1.34</b>	<b>3.68</b>
<b>100</b>	<b>1.97</b>	<b>0.47</b>	<b>1.97</b>	<b>2.40</b>

**Table 8.1.** Fit parameters from isometric polypyrrole test at 25, 50, 75, and 100 °C.

Table 8.1 demonstrates that both time constants observed in the strain response decrease with increasing temperature. The stress magnitudes increase with temperature with the exception of the 50 °C test, already noted as an exception to this trend. The decrease in the time constants is expected from the resistance and diffusion effects discussed, though the agreement between the observed time constants and the proposed time constants requires further analysis. If the observed time constants are directly related to the charging and diffusion constants, the solution resistance and apparent diffusivity can be analyzed as a function of temperature. The thickness of the film tested was 18  $\mu\text{m}$  and it has been experimentally verified that the volumetric capacitance of polypyrrole is approximately  $0.2 \times 10^9 \text{ F/m}^3$ . Using these values and Equations 1 and 2, Table 8.2 depicts the values for diffusivity,  $D$ , and solution resistance,  $R$ , as a function of temperature.

<b>Temp (°C)</b>	<b>R (Ohms)</b>	<b>D (<math>\times 10^{-10} \text{ m}^2/\text{s}</math>)</b>
<b>25</b>	<b>53.1</b>	<b>1.03</b>
<b>50</b>	<b>39.5</b>	<b>1.33</b>
<b>75</b>	<b>34.4</b>	<b>1.40</b>
<b>100</b>	<b>22.4</b>	<b>1.72</b>

**Table 8.2.** Dependence of solution resistance and diffusivity as a function of temperature.

Theoretically the resistance should show an exponential dependence on the temperature and the diffusivity should show a linear dependence of the absolute temperature.<sup>1</sup> While the data trends in Table 8.2 are correct, the values at 50 °C and the limited quantity of data preclude an in depth analysis. The frequency response data depicted in Figures 8.3 and 8.4 offer an additional opportunity to verify the mechanism at elevated temperatures. This analysis is presented in the next section.

## 8.4 Frequency Response Analysis

Madden et al.<sup>3</sup> analyzed the frequency response data relating to the fundamental relation between strain and charge,  $\alpha$ . In the frequency domain, this equation is given by

$$\sigma(s) = E(s)\varepsilon(s) - E(s)\alpha(s)\rho(s), \quad 4$$

in which  $\sigma$ ,  $E$ ,  $\varepsilon$ ,  $\alpha$ , and  $\rho$  are all substituted by their complex representations. In the isometric configuration,  $\varepsilon(s)$  produces the zero frequency response and does not appear in the equation. Similarly if  $E$  and  $\alpha$  are considered to be constant, Equation 4 is reduced to

$$\sigma(s) = -E\alpha\rho(s). \quad 5$$

In the isometric impedance test configuration,  $\sigma$  and  $I = V/Z$  are measured. In the frequency domain the charge is given by

$$\rho = \frac{I}{Vs}, \quad 6$$

utilizing the integration of current,  $I$ , divided by the volume  $V$ . Substituting  $j\omega$  for  $s$  in the equation and solving for the stress magnitude divided by the current density,

$$\left| \frac{\sigma V}{I} \right| = -\frac{E\alpha}{2\pi f}, \quad 7$$

which in a log-log plot versus frequency will have a slope of -1 and an intercept that defines  $E\alpha$ . Taking the raw data from Figures 8.3 and 8.4, the log-log plot of stress magnitude divided by current density as a function of frequency is plotted in Figure 8.7.



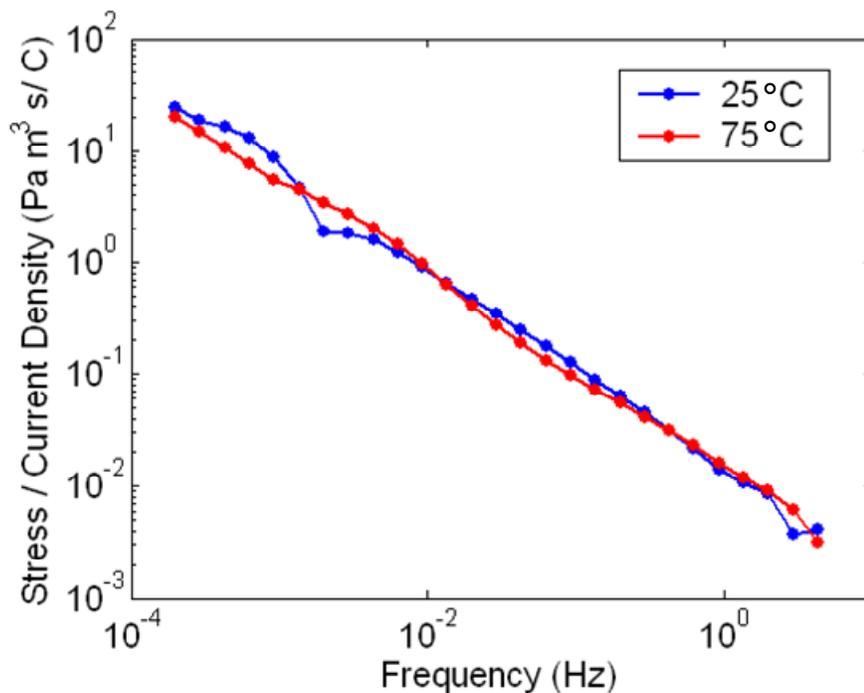


**Figure 8.7.** Isometric stress divided by the current density as a function of frequency at 25 and 75° C.

The data in Figure 8.7 both show the same slope and intercept behavior. This indicates that the product of  $E$  and  $\alpha$  is held constant as the temperature is increased, which indicates that the prediction of a relation between strain and charge holds at elevated temperatures, thereby validating the model presented by Madden.<sup>2</sup>

## 8.5 Summary

Polypyrrole actuation was measured at 25, 50, 75, and 100 °C. As the temperature was increased, the magnitude and rate of the response increased indicating decreases in the fundamental time constants identified by Madden.<sup>2</sup> This dependence is predicted by the effects of temperature on solution resistance and diffusivity, as identified by the Randle's circuit. The increased temperature, however, did lead to faster degradation of the actuation properties. Further evaluation of the frequency dependence of the isometric response at 25 and 75 °C demonstrated that the strain to charge ratio,  $\alpha$ , also holds at elevated temperatures. This data corroborates the model presented by Madden and demonstrates improved actuation at elevated temperatures.

## 8.6 References

1. Chen, A. Large Displacement Fast Conducting Polymer Actuators. M.S. Thesis. Massachusetts Institute of Technology, Cambridge, MA, 2006.
2. Madden, J. D. W. Conducting Polymer Actuators. Ph.D. Thesis, Massachusetts Institute of Technology, Cambridge, MA, 2000.
3. Madden, J. D. W.; Madden, P. G. A.; Hunter, I. W. Polypyrrole actuators: modeling and performance. *Proc. SPIE Int Soc. Opt. Eng.* **2001**, *4329*, 72-83.
4. Del Zio, M. Conducting Polymer Actuators: Temperature Effects. M.S. Thesis. Massachusetts Institute of Technology, Cambridge, MA, 2006.
5. Ding, J.; Zhou, D.; Spinks, G.; Wallace, G.; Forsyth, S.; Forsyth, M.; MacFarlane, D. Use of ionic liquids as electrolytes in electromechanical actuator systems based on inherently conducting polymers. *Chem. Mater.* **2003**, *15*, 2392-2398.

## 9. Conclusions

Conducting polymers demonstrate actuation capabilities, performing work against an applied load and mechanically responding to electrochemical stimuli. The mechanisms that are understood in this relationship include the ionic ingress and egress that occurs in polypyrrole and poly(3,4-ethylenedioxythiophene), or PEDOT. Other, more profound mechanisms, have been proposed,<sup>1</sup> and, in some cases, modeled with small molecules.<sup>2</sup> Still other actuation results have been observed without a precise understanding of the underlying mechanisms, as in poly(3-hexylthiophene), or P3HT. In each case, the objectives of the research remain the same: to achieve muscle-like behavior in a synthetic material.

The task of creating such materials logically spans a wide range of scientific disciplines, from organic synthesis to mechanical characterization, and requires good collaboration between experts in each of the related fields. The work presented here consists of elements in the progression from concept to verification. In doing so it takes both a forward look, asking what can be done with new materials, and a backward look, asking what materials would achieve the research goals. In this final summary, the achievements presented and the opportunities for further work will be highlighted. In addition, an examination on the state of the research will be presented in each of the areas covered in this document.

### 9.1 The Design Cycle

The steps involved in creating new conducting polymer actuators start with the design phase in which an observed change in a small molecule, such as the oxidative bending of a thiophene ring, is identified. The next step begins the synthetic process toward achieving a material that will exhibit this small characteristic on a bulk scale. To do so, the small molecule must be made into a monomer, conjugated for electrical conductivity, and modified to enable polymerization. The polymerization may proceed chemically or electrochemically, as long as the material obtained is robust enough to be characterized. The characterization of the material includes the passive and active properties, though the

insolubility of most conducting polymers limits the available techniques. If actuation is observed, it is studied and modeled. A material that is fully characterized must demonstrate sufficient capabilities to be implemented as a success.

Along the way, numerous opportunities exist for returning to any of the steps as needed. Monomers that cannot be polymerized may be modified, or the polymerization techniques may be modified directly. Other techniques, such as blending with a stabilizing material, like carbon nanotubes, may enter into the process to achieve the goals of individual steps. Characterization successes and failures lead to new design ideas and new materials to be synthesized. Modeling helps predict the effect of changes in the material and identify important metrics, such as the strain to charge ratio. The combined work takes the shape of a cycle, with the forward progression of ideas and feedback between each step.

### **9.1.1 Synthesis**

Conducting polymers are typically synthesized by oxidative coupling. Chemically or electrochemically a monomer is oxidized to produce a cation radical. Two oxidized monomers react to form a new carbon-carbon bond which returns to its  $sp^2$  hybridized state upon the elimination of the protons that were initially at the position of the radical formation. The  $sp^2$  carbons maintain the alternating double bond structure required for electrical conductivity along the backbone of the polymer. In this manner, monomers couple to become dimers, tetramers, and so on to high molecular weight polymer.

The monomers are synthesized by an array of means and many more monomers have been synthesized and tested than were presented here. The difficulty in obtaining new materials is not in monomer synthesis, but rather the polymerization. Most conducting polymer research focuses on thin polymer coatings as for electrochromic devices or sensors. These thin coatings do not require the robust conductivity of actuation, which requires the polymer to support the electrical transport used in the conversion to mechanical work. As such, many of the novel monomers developed lack

the conductivity as polymers for actuation. This is particularly true as the structural bulk of the monomer increases. The notable conductive polymers that possess high intrinsic conductivity, polyacetylene, polypyrrole, poly(3,4-ethylenedioxythiophene), and poly(3-hexylthiophene), all have compact molecular structure. The good electronic properties of these polymers compared to their bulkier relatives could be due to the interchain requirements on conductivity. This constitutes an optimization problem in creating novel conducting polymers. In order to make use of a novel mechanism, the target functional group must be appended with other groups that improve solubility for polymerization and enhance the electron density and conjugation. As these groups are included, however, the conductivity of the resulting polymer drops.

A similar problem is observed with mechanical stability. Novel monomer systems rarely polymerize well enough to obtain freestanding films. This shortcoming is likely due to the inability to polymerize the monomers to a molecular weight higher than the entanglement molecular weight. Polyelectrolyte counterions have been used to enhance the mechanical stability of such films,<sup>3</sup> though the non-conjugated nature of these systems reduces the conductivity. Similar results may be obtained by chemical cross-linking, though work in this direction was also limited by the low conductivity of the materials obtained.<sup>4</sup>

One solution to the conductivity problem is highlighted in Chapters 6 and 7. The addition of a conductive material, in this case carbon nanotubes, enhances the conductivity. Chapters 6 and 7 demonstrate this enhancement, particularly in the case of P3HT actuation which occurs in blended samples even without  $I_2$  doping. The carbon nanotubes also improve the mechanical robustness of films of novel monomers, though a suitable processing technique, such as the layer-by-layer approach used in Chapter 6 may be required for inclusion in insoluble systems. The price of improved mechanical stability is not yet known. In the case of polypyrrole and PEDOT, the relationships of between strain and stress as a function of the strain to charge ratio suggest that a stiffer material will generate more stress, though this may occur at the expense of the strain response. Chapter 6 demonstrated a PEDOT composite structure with a higher modulus

than the PEDOT control that exhibited similar strain magnitudes and less creep during isotonic testing. In this test system, all of the effects of the CNTs were positive including less creep, higher conductivity, and a faster response. It is unclear whether the volume fraction of CNTs in this case would be sufficient to lend suitable material properties to a novel monomer system, though the initial result is promising.

A different solution to the conductivity and mechanical stability problem is suggested by the results in Chapter 2. It has been shown that the conditions during electrochemical synthesis play an important role in the resulting films obtained. In the case of polypyrrole, highly conductive, smooth films are obtained when the deposition solution is cooled to  $-40\text{ }^{\circ}\text{C}$ .<sup>5</sup> The enormous parameter space available to electrochemical polymerizations suggest that further improvements could be made by technique alone. While potentiostatic and galvanostatic techniques work well with conventional conducting polymers such as polypyrrole and PEDOT, the complicated structure of many novel monomers may not be as electrochemically robust. From the work on thin films of novel conducting polymers it is clear that potentiodynamic conditions may be used to polymerize these species. The development of hybrid techniques, such as the galvanodynamic polymerization presented, may be required to obtain thick freestanding films of novel conducting polymers.

Thus, the area of conducting polymer synthesis presents numerous opportunities and challenges to the work of creating actuators. The allure of new monomers that have not yet been synthesized is compelling when addressing the failure of the current generation of monomers. It is useful, however, to continue study of these failed systems and develop new techniques from blending to electrochemistry.

### **9.1.2 Characterization**

The characterization of conducting polymers is a rich field, largely applied to thin coatings and small scale electrochemical measurements. The insolubility of films synthesized electrochemically further limits the characterization techniques commonly applied in polymer science. Standard questions as to the effects of molecular weight or

regioregularity cannot be answered. The exception to this observation is the scattering experiments used to study conducting polymer morphology and structure, which are accessible, though constitute an entire area of study to itself.

Furthermore, it is unclear whether results obtained for thin films will hold for thicker films used in actuation. For example, the use of EQCM is popular for monitoring the swelling of a polymer coated electrode, but the result may depend on the thickness of the film,<sup>6</sup> which negates the utility of applying the small scale test to a freestanding actuator. Thus, the characterization of conducting polymers focuses on properties of the freestanding films relevant to actuation, particularly the electrical and mechanical properties.

The electrical properties of freestanding films can be measured in numerous ways, highlighted in Chapter 3. The van der Pauw method is independent of the sample parameters except the thickness and, thus, reduces the experimental error. The in-situ conductivity technique is also useful, when applied correctly, to observe the effects of reduction and oxidation on the polymer conductivity. These effects can be measured on a mm scale sample used in actuation studies, as was done with the PEDOT composite samples presented in Chapter 6. The mechanical properties can be measured a number of ways, though the most useful method measures the effects of the electrolyte bath and the electrochemical state. The development of new characterization techniques as in the case of frequency dependent EQCM may also be useful for predicting actuation behavior, though any experimental techniques performed on coated electrodes may not scale to the full freestanding polymer response.

### **9.1.3 Actuation Testing**

The direct characterization of actuation behavior is the only way to measure the success of a conducting polymer actuator. No fully predictive, non-destructive alternative test has been developed. The proper characterization also requires instrumentation that is not commercially available. Numerous versions of electrochemical dynamic mechanical analyzers have been built, each with improved

performance or specialized function. As the instrumentation has been developed, additional relevant features have been added along with the overall flexibility of the testing capabilities. Ideally, an actuation testing instrument would allow for any combination of potential, current, stress, and strain waveform to be controlled or measured. Other considerations include the ease of use of the instrument especially in the area of sample loading and manipulation. Further care should be taken in providing a useful progression of relevant tests from passive mechanical characterization to isotonic and isometric testing.

In practice, conducting polymer actuator characterization is challenging because the experimenter must decide the test protocol. The viscoelasticity and volumetric capacitance of the polymer contribute to the effects of the test on the test results. In the case of the viscoelasticity, each mechanical loading is accompanied by a creep or stress relaxation response. In the case of the volumetric capacitance, each electrochemical cycle applied changes the doped state of the polymer, possibly in a non-uniform fashion through the thickness of the film. Thus, for a short isotonic test, for example, the polymer will start and end at two different mechanical and electrochemical states. Each subsequent test carries the effects of the previous tests. Obtaining a direct comparison between films of different composition under these circumstances is difficult unless a strict protocol is followed for each series of tests.

For conducting polymers that actuate via ion ingress and egress, such as polypyrrole and PEDOT, a few generalizations can be made. Potential control in these systems determines the equilibrium result if sufficient time is allowed for the response of the polymer. Current control determines the rate of charge and subsequently the rate of the response of the polymer. Increasing the current magnitude will increase the rate of response until the polymer degrades. The degradation is controlled by potential, so it can be avoided if potential limits are placed on a current controlled experiment. The strain to charge ratio can be measured by plotting the strain or stress response versus the charge. If two ions are mobile in the polymer, this plot will show two independent slopes as in Figure 5.4. Two complimentary experiments are the slow potential scan, as in cyclic



voltammetry, and the potential square wave. The slow scan will allow for the measurement of the ultimate properties while the square wave will demonstrate the speed of the response.

The characterization of new conducting polymer actuation mechanisms such as the potential-dependent mechanism discussed in Chapter 7 will not respond to the inputs in the same way. Further techniques need to be developed to measure the ultimate properties and speed of response in these materials. Frequency modulation techniques, such as the combined impedance and isometric test used in the measurement of the polypyrrole response at different temperatures in Chapter 8, may provide for better understanding of the underlying actuation mechanisms. For the purpose of application, however, there will be no substitute to the isotonic or isometric test corresponding to a real situation for conducting polymer actuation.

## 9.2 Contributions

The work presented has demonstrated the interdisciplinary nature of the research on conducting polymer actuation. From initial discussions of proposed mechanisms and ideas in conducting polymer actuation, a thorough review of synthesis and characterization techniques was presented. In Chapters 2 and 3, the use of the galvanodynamic polymerization technique as well as the in-situ conductivity and modulus tests were developed. In Chapter 4, the electrochemical dynamic mechanical analyzer was introduced, reflecting several generations of instrument built for that purpose.

Chapter 5 introduced PEDOT actuation, unstudied despite initial observations of bending actuation in coated electrodes. PEDOT was studied in several electrolytes, finally observing single strain to charge dependence in the ionic liquids BMIMPF<sub>6</sub> and BMIMB<sub>4</sub>. In these electrolytes, PEDOT exhibited strains of 4.5 % and strain rates of 1 % per second while maintaining a ratio between strain and charge density of  $-2.1 \times 10^{-10} \text{ m}^3/\text{C}$ . The unusual character of actuation in ionic liquids was also studied in mixtures of BMIMPF<sub>6</sub> with propylene carbonate. In these studies it was observed that the magnitude

of the actuation response depended on the concentration of ionic liquid and that the selectivity toward cation ingress was only observed in the neat ionic liquid. One possible mechanism based on the surface interaction in the absence of solvent was proposed.

Chapter 6 highlighted the effects of adding CNTs to PEDOT. The layered composite structure demonstrated a higher conductivity and modulus than the control PEDOT only film prepared in the same manner. The isotonic actuation response to potential triangle waves was similar in magnitude and shape in both films. The composite film did not creep as much as the control during the test, suggesting further improvement in a potential application. The isometric and isotonic responses to a potential square wave also demonstrated that the addition of the CNTs improved the speed of the response of PEDOT in the ionic liquid BMIMBF<sub>4</sub>. An in-situ conductivity also demonstrated that the addition of the CNTs enabled faster oxidation in the vicinity of the film contacts, though the CNT loading was not high enough to ensure conductivity in the sample independent of potential.

The actuation of P3HT was presented in Chapter 7, in which the strain and stress response depended on the applied potential rather than the charge in the electrochemical system. This response also showed a threshold behavior in which no response was detected at potentials below 1.25 V versus Ag wire. At higher potentials, the strain and stress both responded to potential, independent of potential scan rate at 5 and 10 mV/s. The isotonic tests also revealed that the film could remain in tension during the test, showing an upper limit to the potential-dependent mechanism. This mechanism was observed in I<sub>2</sub>-doped and undoped P3HT blended with CNTs proving that the I<sub>2</sub> was not critical to the mechanism. It was also observed in I<sub>2</sub> doped, unblended P3HT, proving that the CNTs were not critical to the mechanism. Several possibilities for the origin of the actuation mechanism in P3HT was discussed, though this remains an interesting area for further research.

In Chapter 8, the study of polypyrrole actuation between 25 and 100 °C was presented. In this data it was observed that increasing the temperature of the bath

improved the rate of the polypyrrole response as well as the ultimate magnitude of the response. This effect was attributed to the combined decrease of both the charging and diffusion time constants. Further study of the response of the polymer to a sinusoidal potential input of varying frequency revealed that the strain to charge ratio remained constant as the temperature was increased, further validating the work of Madden<sup>7</sup> and Madden.<sup>8</sup>

### **9.3 Recommendations for Further Research**

I started by noting the interdisciplinary and slow nature of this research, with a nod to the overall motivation that it can be done and we are proof. The work presented reflects the optimism of synthesis with the pragmatism of characterization. When “the next best thing” fails, it must be decided how long to continue trying it. The hardest part of such work is continuing to be optimistic about the new things. Nevertheless, it is important to realize the small gains and remember the failures that they may be tried again when a better approach has been identified.

With that in mind, the possibilities for future research in conducting polymer actuators are broad. The largest pressing need remains the transition from interesting monomer to useful polymer. Continued work with novel electrochemical systems and carbon nanotube blending will enable more materials to surpass this hurdle. The successful demonstration of CNTs as a passive enhancement in PEDOT, that does not hinder actuation, is particularly encouraging. Ideally, a template for mechanically testing the proposed mechanisms for actuation will be developed.

Once these issues have been addressed, greater attention must be paid to the microstructure of the materials. Further investigations into structure-property relationships will help to focus the synthetic efforts toward crystalline or amorphous materials. Ultimately, however, the proposed mechanisms all demonstrate anisotropy at the molecular scale. The bending and interchain interactions all have a direction which would ideally be aligned to achieve actuation in a bulk material. A logical first step in this direction is the further study of actuation in poly(3-hexylthiophene). Recent studies

of oriented polypyrrole has demonstrated differences in actuation<sup>9</sup> and similar work may enable greater understanding of the mechanism in P3HT.

The topic of actuation of P3HT is also a rich area for further research. Once the actuation is optimized, numerous applications would be possible, since the solution processable P3HT can be delivered directly to the point of implementation rather than clamped in place. P3HT can also be structured at micrometer length scales,<sup>10</sup> suggesting further work in microactuators and study of the effect of surface morphology. P3HT actuation also opens the area of characterization, relating traditional polymer properties such as molecular weight and tacticity to the actuation properties. Finally, the ongoing work of P3HT stabilized dispersions of nanotubes will enable improved blending with CNTs and characterization of novel monomers.

The actuation of PEDOT has not presented significant opportunities in conducting polymer actuation beyond those already addressed with polypyrrole. In principle, PEDOT is more electrochemically stable, so it can be used at higher and lower potentials without degradation, though the measured performance has not demonstrated a significant improvement. The synthesis of PEDOT is not yet optimized for actuation, however, and the monomer is easier to work with than pyrrole, suggesting that it be brought into the polypyrrole community as a useful partner.

Finally, the development of additional characterization techniques and instrumentation is paramount to the success of conducting polymer actuator research. Tests implementing frequency sweeps are useful and should be considered as an alternative to the ad hoc methodology often employed in general characterization. Improvements in data acquisition and computer control should continue to be used to upgrade characterization equipment.

More than any individual research opportunity, the key to realizing successful muscle-like behavior is the continuation of the collaboration between synthesis and characterization research.

## 9.4 References

1. a) Anquetil, P. A. Large contraction conducting polymer molecular actuators. Ph.D. Thesis, Massachusetts Institute of Technology, Cambridge, MA, 2005. b) Yu, H.-H. Molecular Actuators: Design, Syntheses and Applications toward Actuation and Sensory Materials. Ph.D. Thesis, Massachusetts Institute of Technology, Cambridge, MA, 2003.
2. Kingsborough, R. P.; Swager, T. M. Polythiophene hybrids of transition-metal bis(salicylideneimine)s: Correlation between structure and electronic properties. *J. Am. Chem. Soc.* **1999**, *121*, 8825-8834.
3. Anquetil, P. A.; Yu, H.-H.; Madden, J. D.; Madden, P. G.; Swager, T. M.; Hunter, I. W. Thiophene-based conducting polymer molecular actuators. *Proc. SPIE Int Soc. Opt. Eng.* **200**, *4695*, 424-434.
4. Vandesteeg, N. Massachusetts Institute of Technology. Unpublished results, 2004.
5. Yamaura, M.; Hagiwara, T.; Iwata, K. Enhancement of Electrical-Conductivity of Polypyrrole Film by Stretching - Counter Ion Effect. *Synth. Met.* **1988**, *26*, 209-224.
6. Inzelt, G.; Kertesz, V.; Nyback, A. S. Electrochemical quartz crystal microbalance study of ion transport accompanying charging-discharging of poly(pyrrole) films. *J. Solid State Electrochem.* **1999**, *3*, 251-257.
7. Madden, J. D. W. Conducting Polymer Actuators. Ph.D. Thesis, Massachusetts Institute of Technology, Cambridge, MA, 2000.
8. Madden, P. G. A. Development and Modeling of Conducting Polymer Actuators and the Fabrication of a Conducting Polymer Based Feedback Loop. Ph.D. Thesis, Massachusetts Institute of Technology, Cambridge, MA, 2003.
9. Pytel, R. Massachusetts Institute of Technology. Unpublished results, 2005.
10. Song, L.; Bly, R. K.; Wilson, J. N.; Bakbak, S.; Park, J. O.; Srinivasarao, M.; Bunz, U. H. F. Facile Microstructuring of Organic Semiconducting Polymers by the Breath Figure Method: Hexagonally Ordered Bubble Arrays in Rigid-Rod Polymers. *Adv. Mater.* **2004**, *16*, 115-118.

## Appendix A

The following MATLAB code was used for measuring van der Pauw conductivities.

```
%take initial data
data=input('Please input matrix [R1 R2 t] \nResistances in Ohms and thickness in m \n');

R1 = data(1)           %parse user inputed data
R2 = data(2)
t = data(3)

count = 0;             %set initial count

Rnew = pi*(R1+R2)/(2*log(2)); %initial guess is solution if R1=R2

R = 2*Rnew             %defaults condition too high for tolerance

while abs((Rnew-R)/R) > 0.00001 %sets tolerance condition

    R=Rnew;             %iteration

    Rnew = R-(exp(-R1*pi/R)+exp(-R2*pi/R)-1)/((pi/R^2)*(R1*exp(-R1*pi/R)+R2*exp(-R2*pi/R)));
    %implementation of Newton's method
    count = count+1;    %keep track of loop

    if count>20         %catch error
        sprintf('WHOA, you screwed something up')
        return
    end

end

count                  %prints the number of iterations

sigma = 1/(Rnew*t);    %conductivity

sprintf('Conductivity (S/m): %d',sigma) %output results
```